The Salmon Disturbance Regime: Effects on Biofilm, Sediment and Water

by

Sam J. Albers

BSc. University of Victoria, 2006

THESIS SUBMITTED IN PARTIAL FULFILLMENT OF
THE REQUIREMENTS FOR THE DEGREE OF
MASTER OF SCIENCE (ENVIRONMENTAL SCIENCE)
IN
NATURAL RESOURCES AND ENVIRONMENTAL STUDIES

UNIVERSITY OF NORTHERN BRITISH COLUMBIA

December 2010

Abstract

Recent work in salmon spawning streams has shown that sediment resuspended during nest construction aggregates with salmon organic matter to form suspended particles called flocs. These nutrient-rich flocs interact with streambed biofilms suggesting a potential floc trapping mechanism that drives biofilm growth. Using the Horsefly spawning channel, the role of biofilms in trapping fine sediment was evaluated as a mechanism of salmon-derived nutrient processing. In the active spawn period, biofilm was reduced in abundance while the streambed sediment infiltration was at its highest level. During salmon die-off, downstream biofilm abundance recovered to pre-spawn values indicating a nutrient pulse over a small scale. With the re-established biofilm layer, sediment was increasingly trapped at the streambed surface by biofilms. This increase in biofilm abundance will likely influence the nutrient dynamics at all levels of the stream foodweb. Biofilms transfer increases in productivity to higher trophic levels. This transfer has a positive effect on the next generation of juvenile salmon growth and survivorship.

Contents

List of Tables

List of Figures

Acronyms

AFDM ash-free dry mass

ANOVA analysis of variance

CLSM confocal laser scanning microscopy

DFO Department of Fisheries and Oceans

DIN dissolved inorganic nitrogen

DO dissolved oxygen

DOC dissolved organic carbon

DON dissolved organic nitrogen

EPS extracellular polymeric substances

GFF glass fiber filter

HFC Horsefly River spawning channel

KJN Kjeldahl nitrogen

LISST laser in-situ scattering and transmissometry

MAM minimum adequate model

MDN marine derived nutrient

OMR organic matter ratio

SA surface area

SEM standard error of the mean

SRP soluble reactive phosphorus

TDP total dissolved phosphorus

TIN total inorganic nitrogen

TN total nitrogen

TP total phosphorus

TSP total soluble phosphorus

UNBC University of Northern British Columbia

Preface

This thesis is divided into four chapters. Chapter 1 provides an overview on the relationship between biofilms and aquatic environments. Specifically, Chapter 1 reviews the ecological impacts of salmon spawning and die-off as a mechanism which structures biofilm growth. Results presented in Chapter 2 test the hypothesis that biofilm abundance is driven by in-stream flocculation and resultant streambed salmon nutrient delivery. This salmon nutrient delivery is in turn driven by the overlap between salmon spawning activity and salmon die-off. A portion of Chapter 2 first appeared as Petticrew and Albers (2010). Chapter 3 is the first known attempt to characterize changes biofilm components driven by salmon die-off using confocal laser scanning microscopy. Chapter 4 provides several conclusions based on the data presented in Chapters 2 and 3 in addition to placing these findings in a broader context.

Acknowledgements

I have many individuals to thank without whom, this project would have never succeeded. First and foremost, I thank my supervisor Ellen Petticrew for her guidance, mentorship, support and willingness to literally get her feet wet in a stream filled with salmon. Ellen, your calm during some difficult days of my field season was an example to be followed, and an anchor to prevent complete panic. I have benefitted greatly from your experience and intelligence and I sincerely thank you for this opportunity.

I would like to thank my committee of Dr. Joselito Arocena, Dr. Ian Droppo, Dr. John Rex and the external reviewer Dr. Mark Wipfli. Each of you have provided significant contributions throughout the course of this project. Special thanks goes to John Rex for patiently passing on technical knowledge and developing a significant portion of the conceptual basis upon which this thesis rests.

This project would have not been possible without all the help I received in the field and the lab. Special thanks goes to Rob Little for his enormous efforts in the field. Rob, I appreciate that snow and ice couldn't keep you away from rotten fish. Thanks to DFO staff Roy Argue, Doug Turvey and Jason Hwang for support with the channel. Thanks to Jordan Holmes for assistance and channel-side chats. Thanks to the community of Horsefly for a wide range of support and interest. Thanks to Rick Holmes and Bill Best of the QRRC. Thanks to George Swerhone and John Lawrence at Environment Canada for taking the time to teach me confocal techniques. Thanks to Tom Johnston for help with modelling salmon decay products. I gratefully acknowledge financial assistance from Peace/Williston Aquatic Research Award.

Many thanks to my family and friends who are a continuous source of inspiration. Thanks to my parents: John and Leslie Albers, my sister: Jane Albers, my brother's family: Jesse, Heather and Ella Albers and my Nana: Patricia Taylor. Thanks to old buddies: Mike, Brooke, Leslie, Morgan, Dave, Ben, Quinn, Simon and John. Thanks to everyone at UNBC. Thanks to COL buddies: Jack, Katrina, Ty, Eric, Becky, Jordie and Lesley. Our economics discussions provided stimulation and welcome relief from thesis topics.

Finally, I wish to thank Brooke Wilken. Thank you Brooke for agreeing to begin our life together in Northern BC. Thank you for spending long hours listening about sediment and biofilm. All this is simply an elaborate attempt to impress you.

This entire document was written using freely available open-source software. I gratefully acknowledge the developers and programmers who have freely given their time to produce such high quality software such as LaTeX, Emacs, R and ImageJ.

Chapter 1

Salmon and Biofilm: A Literature Review

1.1 Introduction

Anadromous fishes are important nutrient vectors that can substantially alter their natal habitats through yearly nutrient pulses (Naiman et al., 2002) and substantial physical disturbance (Rex and Petticrew, 2006; Moore, 2006). Each year millions of anadromous Pacific salmon (*Oncorhynchus spp.*) return from the ocean to their natal freshwater streams to spawn and die (Quinn, 2005). Salmon biomass, accumulated primarily at sea, is transported to upstream freshwater spawning grounds (Naiman et al., 2002). This marine derived nutrient (MDN) pulse is atypical of most rivers. Globally, nutrient and energy flow in rivers usually proceeds downstream, eventually ending up in the sea (Vannote et al., 1980). These types of ecosystem linkages are increasingly being seen as crucial components of a healthy ecosystem (Lamberti et al., 2010). This is particularly true with a culturally and commercially valuable species such as Pacific salmon.

Pacific salmon migrate against the typical nutrient and energy river gradient, impacting terrestrial and aquatic ecosystems (Quinn, 2005) that are sometimes considerably inland from the marine environment (e.g. Johnston et al., 2004). In the terrestrial landscape, bears and other large mammals will carry salmon carcasses up to 20-m away from the river bank, fertilizing the surrounding system with unused portions of salmon flesh (Cederholm et al., 1989) as well as fecal material (Reimchen, 2000). This nutrient input is a significant driver of primary and secondary productivity in the terrestrial ecosystems of the Pacific Northwest (Naiman et al., 2002; Drake et al., 2002; Hocking and Reimchen, 2002).

Similarly, spawning salmon enrich aquatic systems with MDNs via indirect trophic pathways and direct consumption pathways (Bilby et al. 1996; Wipfli et al. 1998; Figure 1.1). Nowlin et al. (2008) report that nutrient pulses travel more quickly through aquatic systems than terrestrial systems. This nutrient pulse also tends to be more persistent in terrestrial systems suggesting that yearly variability in salmon numbers has a large effect on salmon spawning river systems. Large gaps, however, remain in understanding the mechanisms by which MDNs enter these aquatic system (Janetski et al., 2009).

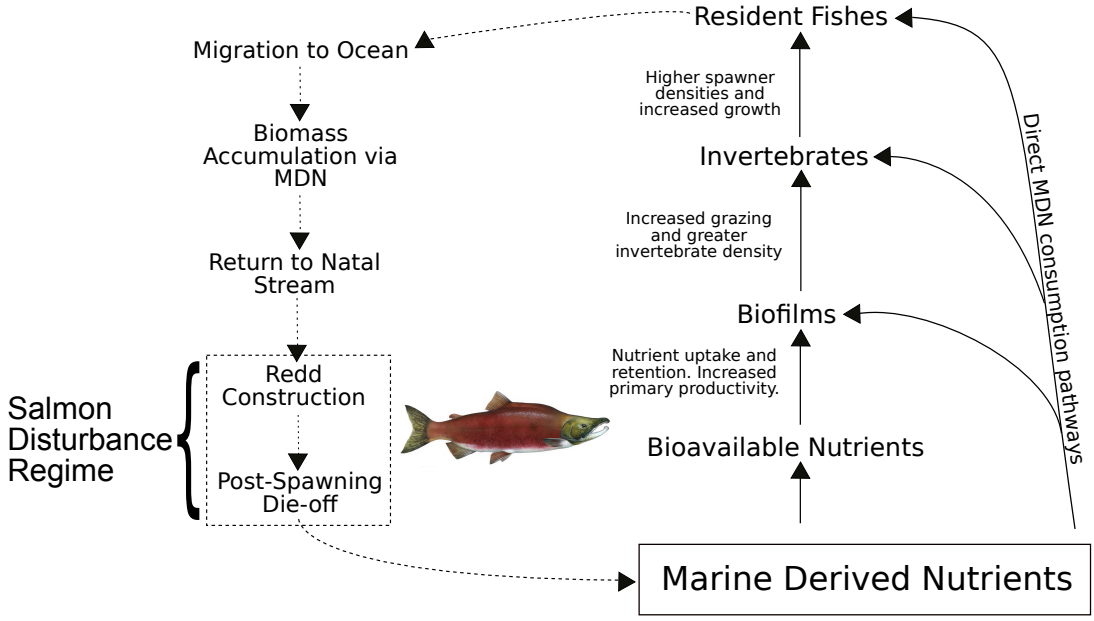

Figure 1.1: Trophic linkages in salmon spawning system and the general life cycle of anadromous salmon. The salmon disturbance regime encompasses both the redd construction and the post-spawn die-off phases of the salmon life cycle. Energy and nutrient transfers within the river are indicated by solid lines. Dashed lines refer to the marine component of the salmon life cycle. Modified from Wipfli et al. 1998.

Depending on the time period and spatial scale examined, salmon can be either a positive material subsidy from carcass nutrient release or a negative process subsidy via nest (redd) construction (Winemiller et al., 2010). Characterizing the effects and the interaction of redd construction and subsequent *in-situ* salmon die-off is a crucial step towards re-

solving the complexities of the salmon ecological picture (Rex and Petticrew, 2008; Moore and Schindler, 2008). Taken together, these two processes represents a salmon disturbance regime that structures both the biological and physical characteristics of a salmon bearing stream (Figure 1.1). The simultaneous disturbance and fertilization from salmon represents a complex and unique ecological process (Moore and Schindler, 2008). The end result of this salmon disturbance regime on aquatic spawning systems has not been completely assessed.

Coastal nutrient limited streams receiving inputs of MDNs generally experience a boost in primary and secondary productivity (Bilby et al., 1996; Quinn, 2005). This trend also seems to hold true for interior streams although these systems are much less well studied. Regardless of habitat, the post-spawn die-off leaves many salmon to rot on the river bed (Quinn, 2005). This rotting salmon flesh can be metabolized into the aquatic system in several ways. Nutrients are either consumed directly by invertebrates (Minakawa and Gara, 1999) or fish (Wipfli et al., 1998) or are taken up by benthic biofilms (Schindler et al., 2003).

Regardless of the pathway, this nutrient pulse is usually felt at all trophic levels as grazers consuming basal components of the food web (biofilms) transfer increases in productivity to higher trophic levels (Bilby et al., 1996). This transfer has a positive effect on juvenile salmonid growth and survivorship (Wipfli et al., 1999, 2003). This suggests a positive feedback loop whereby more salmon returning to their natal streams will result in an positive benefit to the next generation of juvenile salmon populations (Figure 1.1, Schindler et al. 2003).

In many cases these systems have evolved over thousands of years with an expectation of a reliable MDN pulse. A more complete ecological picture of salmon streams will aid restoration, management and maintenance of this habitat and the salmon themselves. Accurate prediction of the response of spawning stream ecosystems to the influx of MDNs will enable a more realistic ecological approach to the management of salmon as

a resource (Pauly et al., 1998). Underlying this need for a better understanding of salmon habitat is the knowledge that many salmon stocks are under significant threat (Table 1.1). Diminished salmon runs mean fewer spawning salmon and a consequently smaller nutrient input to the stream. This reduction may have large consequences for conservation and management goals; fewer nutrients retained within the river systems may inhibit the ability of the system itself to sustain future salmon populations (Bilby et al., 1996).

Table 1.1: Estimated salmon abundance by region. Values are percentages of the total number of populations in each category. After Quinn (2005); Scheuerell et al. (2005).

Region	Healthy	In jeopardy	Extinct	Unknown	Total # of Distinct Genetic Pop$^{\underline{n}}$'s
Southeast Alaska	10.0	0.1	<0.1	89.9	9228
British Columbia	48.3	9.7	1.3	40.7	9038
Washington	37.5	22.2	16.1	24.2	248
Coastal Oregon	32.6	49.7	6.4	11.3	141

1.2 Benthic Response

In river ecosystems, the benthic community is the main processor of organic material (Romaní et al., 2004). Benthic communities can consist of invertebrates, colonial algae, fishes and biofilm structures. This community forms the basal portions of the river food chain and is an important component of river productivity (Wipfli et al., 1998). Biofilms, a mixed autotrophic and heterotrophic community fixed in a polysaccharide material, are the primary producers in benthic communities (Costerton et al., 1995). Biofilms[1] remove nutrients from a river primarily through uptake and retention (Sabater et al., 2002).

The ecological response of the benthos in a natural system is likely dependent on the number of salmon spawners, the location of the run, the species examined and the phase of the salmon run examined. Moore and Schindler (2008) found that at densities of 0.1

[1]Biofilms are known by various names within the salmon ecology literature. In the context of this study, I interpret epilithon and periphyton to equally refer to the material that I call biofilms. Therefore here, biofilms refer to the biological material growing on gravels in the benthic habitats of salmon spawning streams.

salmon m^{-2}, active salmon spawning reduces both biofilm and invertebrate abundance by 75–85%. This density dependent response has implications for interspecific variation as coho salmon (*O. kisutch*) often spawn at lower densities than sockeye (*O. nerka*) or chum (*O. keta*) (Bilby et al., 1996). Later in the spawning cycle, during the die-off period, there is often an increase in biofilm abundance sometimes equalling or exceeding pre-spawn levels (*cf.* Johnston et al., 2004). This response may also be density dependent as smaller runs equate to small MDN additions to spawning grounds. Nevertheless, given that most salmon spawning streams are oligotrophic (Naiman et al., 2002) even small MDN additions may constitute important nutrient sources (Bilby et al., 1996).

Table 1.2 summarizes the major findings of several previous biofilm-salmon studies. Although there is a wide range in biofilm response to MDNs, there is an equally large range of parameters measured in an attempt to characterize biofilm activity. Of particular importance to this study are the prior attempts to measure the response of benthic communities to an influx of MDNs. Biofilm growth is usually measured by chlorophyll *a* and ash-free dry mass (AFDM) while MDN uptake is measured by δ^{13}C and δ^{15}N isotopic signatures.

1.2.1 Biofilms

The biofilm growth response to the salmon disturbance regime is spatially and temporally variable and MDN uptake in particular δ^{13}C tends to be variable as well (Claeson et al., 2006). This variable response can be attributed to hydrodynamic conditions (Stoodley et al., 1999), light, nutrients (Moore and Schindler, 2008), and redd construction (Mitchell and Lamberti, 2005; Hassan et al., 2008) as well as inadequate characterization of biofilms (Sabater et al., 2002). Part of this variable response is a temporal issue and can best be assessed by examining the benthic response during both the active-spawn and post-spawn period (Janetski et al., 2009). This approach to characterize gross effects allows for assessing stream resistance, the ability of the stream to oppose the effects of redd construction,

Table 1.2: Summary of major biofilm studies in relation to salmon spawning. Unless otherwise indicated responses are either from a salmon presence/absence study or a before, during and after assessment of relevant variables or both.[a]

	Study Characteristics				**Biofilm Characteristics**			
Study	System/Location	Time of Year	Salmon Density/m^2	Salmon Species	AFDM (mg/cm^2)	Chl *a* ($\mu g/cm^2$)	$\delta^{15}N$ (‰)	$\delta^{13}C$ (‰)
Wipfli et al. (1998)	River/Alaska	Aug-Oct	80 kg/L	pink	↑	–	–	–
Peterson and Foote (2000)[b]	River/Wash.	July-Aug	–	sockeye	–	↓	–	–
Johnston et al. (2004)	River/Interior BC	July-Oct	0.8	sockeye	–	↑	–	–
Mitchell and Lamberti (2005)	River/Alaska	July-Sept	0.07	mix	NSD	↑	–	–
Moore and Schindler (2008)[b]	River/Alaska	Multi-year	0.54	sockeye	–	↓	–	–
Tiegs et al. (2008)	River/Alaska	July-Oct	–	mix	NSD	↑	–	–
Cak et al. (2008)	Estuary/Alaska	July-Sept	0.57	mix	↑	↑	–	–
Wipfli et al. (1998)	Mesocosm/Alaska	Aug-Oct	3.6-4.7	pink	NSD	–	–	–
Chaloner et al. (2002)	Mesocosm/Alaska	Aug-Oct	4	mix	–	–	NSD	↑
Mitchell and Lamberti (2005)	Mesocosm/Alaska	July-Sept	1.5	mix	↑	↑	–	–
Claeson et al. (2006)	River/Wash.	July-Oct	0.8	chinook	NSD	NSD	↑	NSD
Kline et al. (1990)	River/Alaska	July-April	25	sockeye	–	–	↑	NSD
Bilby et al. (1996)	River/Wash.	Whole Year	0.36	coho	–	–	↑	↑
Chaloner et al. (2002)	River/Alaska	Aug-Oct	–	mix	–	–	↑ no test	↑ no test
McConnachie and Petticrew (2006)	River/Interior BC	June-Aug	0.7	sockeye	–	–	↑	↑
Kline et al. (1993)	Lake/Alaska	Multi-year	–	sockeye	–	–	↑	↑
Chaloner et al. (2007)	River/Alaska	6 years	2.1 kg/m^2	pink, chum	↑	↑	–	–

[a]NSD: no significant difference; –: not measured; ↑: increased after salmon run; ↓: decrease after salmon run

[b]Samples were collected during the active spawn period

and stream resilience, the ability of the system to process the post-spawn MDN pulse (Biggs et al., 1999).

1.2.1.1 Active-Spawn

Recent work in spawning salmon streams has identified the role salmon play in enriching and disturbing the quality of their natal habitats (Naiman et al., 2002; Hassan et al., 2008; Rex and Petticrew, 2008). During active-spawning salmon can excavate redds that are 10-35 cm deep, considerably disturbing streambed biofilms (Schindler et al., 2003). During this process clay, silt and sand is resuspended into the water column. The ecological importance of redd construction is highlighted by reduced fine sediment in the gravelbed (Hassan et al., 2008), subsequent nutrient delivery to the gravelbed (Rex and Petticrew, 2008), and increased egg survival due to scour resistance (Montgomery et al., 1996).

Many studies have reported significant decreases in benthic biofilm abundance during active spawning (Table 1.2). In one example, Moore and Schindler (2008) found no benefit of MDN to the stream ecosystem as redd construction reduced biofilm abundance below critical levels suggesting that the system may be unable to recover after the redd construction disturbance. This result, however, is likely dependent on context and on many factors including spawners densities, light availability, hydrologic variables, bed characteristics, background nutrient levels and the timing and species of the run (Moore and Schindler, 2008). Table 1.2 highlights both the varied biofilm response to a salmon run and the fact that the full ecological ramifications of this habitat modification are still unclear. For example, during redd excavation, biofilms are resuspended into the water column along with sediment. The fate of this biofilm remains unclear. It could either be transported downstream to receiving lake systems or retained in the stream. The reduction in biofilm abundance due to redd construction, however, may reduce the ability of the system to process the subsequent nutrient pulse from the post-spawn dead salmon (Romaní et al., 2004).

1.2.1.2 Post-Spawn

Material from the post-spawn carcass decay is the most substantial nutrient subsidy to salmon bearing streams particularly in oligotrophic streams (Naiman et al., 2002). Many studies have reported increases in biofilm density after redd construction sometimes equalling or exceeding pre-spawn densities (Table 1.2). For example, after the active-spawn decrease in biofilm abundance, Moore and Schindler (2008) reported a post-spawn increase in biofilm abundance that exceeded pre-disturbance levels but only in some years. The post-spawn MDN pulse may have a longer-lasting effect than active-spawn disturbance as the in-stream carcass decay can last well after all fish have died (See Johnston et al., 2004). This post-spawn increase, however, is not always found suggesting that MDNs are not always incorporated into the ecosystem via biofilms.

1.2.1.3 MDN contribution

MDNs have a higher isotopic signature (e.g. δ^{15}N and δ^{13}C) that allows for accurate tracing of nutrient pathways (Bilby et al., 1996). Because salmon gain most of their biomass at sea, they tend have marine carbon and nitrogen isotopic ratios. Convergence to this marine isotopic signature by freshwater organisms implies utilization of MDNs (Kline et al., 1993). In particular δ^{15}N is a good indicator of marine nutrient origin (Kline et al., 1990). For example, Bilby et al. (1996) found that all trophic levels in streams were enriched in both δ^{15}N and δ^{13}C after a salmon run. However, many geographic, analytical, spatial, and temporal issues still plague the interpretation of MDN uptake and have not been resolved (Staal et al., 2007). Hence, other studies on the effect of MDNs have yielded varying results (Table 1.2).

The overall response of biofilms to MDNs has not been conclusively shown to be unidirectionally positive. Claeson et al. (2006) found no increase in δ^{13}C values from sampled biofilms after salmon die-off over a period of eight weeks. In contrast, δ^{15}N levels were significantly higher over the same period. Chaloner et al. (2002) found that biofilms

grown in a natural salmon-bearing creek exhibited lower MDN incorporation of carbon than nitrogen. In another part of the same study, biofilms in a mesocosm channel exhibited lower δ^{15}N values than δ^{13}C than a non-salmon carcass control (Chaloner et al., 2002).

Potentially, increased algal growth rates due to MDNs, a factor unaccounted for in that study, may have been altered via reduced δ^{13}C discrimination during photosynthesis (Chaloner et al., 2002). Using only isotopes and biomass estimates to characterize biofilm function is a useful but limited approach to identify MDN uptake as the algal-bacterial and carbon-nitrogen ratio are also critical measures of biofilm activity (Romaní and Sabater, 2000). However, to the detriment of a clearer ecological picture, many studies have ignored the more general biofilm literature.

1.2.1.4 Biofilm Composition

Sabater et al. (2002) state that the function of biofilms is intimately tied both to its components and structure. Biofilm composition and structure are in turn determined by a combination of physical, chemical and biological factors. Biologically, biofilms are comprised of autotrophic and heterotrophic organisms. The ratio of these two biotic components determines the ability of a biofilm to process organic matter. Predominantly autotrophic biofilms tend to absorb fewer nutrients because of high internal nutrient cycling (Romaní et al., 2004). Conversely, more heterotrophic biofilms tend to absorb more nutrients due to diminished nutrient release by algae available for internal cycling (Romaní et al., 2004). This biofilm behaviour has important consequences for MDN uptake within a salmon spawning river. Most studies characterize some combination of these factors but rarely is biological composition taken into account. Often, this is a practical consideration as the analytical and microscopic tools needed to properly characterize biofilms are unavailable to ecologists either due to a lack of specific knowledge or field sampling constraints.

Yoder et al. (2006), one of only a few salmon-biofilm studies that include a measure

of biofilm composition, suggested a nutrient incorporation model whereby heterotrophic bacteria are the initial streambed colonizers; autotrophic algae lag in response until they are able to establish populations over microbial mats. This suggests a differential response of autotrophs to heterotrophs to a salmon nutrient pulse and may explain variable patterns of δ^{13}C and δ^{15}N uptake by biofilms (Table 1.2). As stated above, to characterize this process, the full salmon disturbance regime needs to be sampled. It can be expected that an increase in algae abundance, as seen by Yoder et al. (2006), will result in a second bacterial population spike as heterotrophic bacteria use nutritive products exuded by algae (Romaní and Sabater, 2000). This suggests a composition-based model to explain how salmon nutrients are processed within a stream.

1.2.2 Particle Aggregation

The flocculation feedback loop proposed by Rex (2009) elucidated that the temporal overlap between redd construction with increased suspended sediment levels and salmon die-off with increased salmon decay products in the water column provided ideal conditions for flocculation. The formation of flocs within salmon-bearing streams due to salmon redd construction is well documented (Petticrew and Arocena, 2003; Petticrew and Rex, 2006). Rex and Petticrew (2008) demonstrated the trapping and deposition into the gravelbed of suspended microbial MDN flocs. These suspended microbial flocs or aggregates consist of organic and inorganic components and can be considered as suspended biofilms (Droppo, 2001). Flocs differ from their constituent particle in size, shape and most importantly in a MDN delivery context, settling velocity (Droppo et al., 1997). Observed flocculated particles laden with MDNs may deliver nutrients over short riverine distances by increased floc settling rates (Figure 1.2; Rex and Petticrew 2008).

The structure of flocs may interact with the structure of biofilms providing a potential mechanism for biofilm MDN mineralization. External structures called extracellular polymeric substances (EPS) on both biofilms and floc provide a chemical 'stickiness' that may

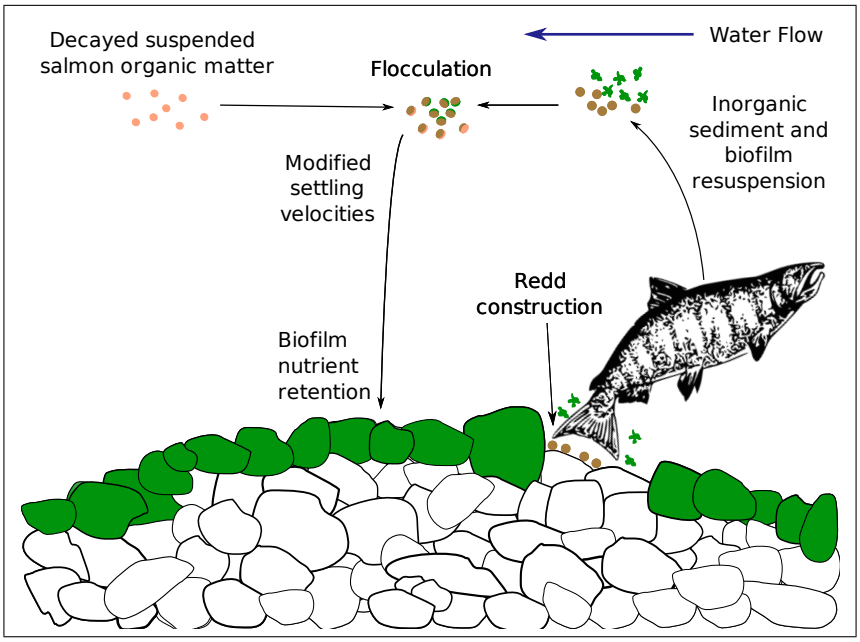

Figure 1.2: Diagram of a salmon spawning stream illustrating the relationship between redd construction, biofilm resuspension and flocculation (Rex and Petticrew, 2008)

aid in particle trapping (Sutherland, 2001). EPS is a comprehensive term for the organic matrix that house biofilms and flocs composed of polysaccharides, proteins and nucleic acids (Wingender et al., 1999). The interactions between these two EPS sources may play an important role in particle trapping and subsequent MDN absorption (Droppo, 2001) particularly in the context of increased biofilm growth (Battin et al., 2003b) after salmon die-off (Johnston et al., 2004).

1.2.3 Invertebrates

The effect of salmon spawning and die-off on benthic invertebrate communities is an area of active research and ongoing debate as to whether salmon positively or negatively impact these communities. Some studies have reported reduced invertebrate densities and altered community structure in streams with actively spawning salmon (Minakawa and Gara, 2003). Peterson and Foote (2000) found that redd construction caused a significant increase in invertebrate drift in the water column and reduced invertebrate densities. Ad-

ditionally, Moore and Schindler (2008) found a significant decrease in invertebrate densities above a threshold salmon density of 0.1 salmon per m^2.

In contrast, salmon carcasses experimentally added to an artificial flume increased invertebrate density by 8 to 25 times (Wipfli et al., 1998). Over a 50-m reach Claeson et al. (2006) measured an increase in invertebrate density due to MDNs. Both Claeson et al. (2006) and Bilby et al. (1996) reported δ^{15}N and δ^{13}C enrichment of invertebrates indicating uptake of MDNs in secondary production in response to salmon die-off.

Moore et al. (2004) found that different taxa of invertebrates responded differently to MDNs. The ability of invertebrates to transfer energy and nutrients gained from biofilms to higher trophic levels is a crucial link in understanding the effect of MDNs on salmon productivity. Studies that have found an increase in invertebrate densities tend to explicitly account for spatial variability within streams, especially downstream linkages of invertebrates to an MDN pulse. Although the exact nutrient pathways have not been determined, the increase in productivity seen in biofilm does seem to transfer upwards to resident fishes (Wipfli et al., 2003).

1.2.4 Resident & Juvenile Anadromous Fishes

In contrast to the disparate response of invertebrates, resident fishes seem to exhibit a clear trend of increased growth in the presence of MDNs. This response manifests itself in several ways. Resident and juvenile anadromous fishes become enriched with δ^{15}N and δ^{13}C (Wipfli et al., 2003) indicating incorporation of MDNs (Bilby et al., 1996; Claeson et al., 2006). Moreover, increased growth rates of cutthroat trout (*O. clarki*), Dolly Varden (*Salvelinus malma*) and anadromous salmon (*Oncorhynchus spp.*) suggest a trophic transfer of energy and nutrients from decaying salmon to subsequent fish populations (Wipfli et al., 2003). Finally, salmon flesh and eggs provide a rich food source for resident fishes (Schindler et al., 2003).

1.2.5 Water Chemistry

Table 1.3 summarizes the response of common aquatic nutrient measures to salmon spawning. Consistently, NH_4^+ and soluble reactive phosphorus (SRP) levels are significantly elevated in the active-spawn period due to waste products (McIntyre et al., 2008) and during the post-spawn period *in-situ* carcass decay (Hood et al., 2007). The consistent pattern of NH_4^+ and SRP levels may be due to their prominence in the chemical makeup of fish excretion (Moore and Schindler, 2008) and decay (Cak et al., 2008) products. Modelling of nutrient dynamics, however, by Johnston et al. (2004) suggests that the decay products are primarily responsible for this increase in NH_4^+ and SRP. Given the ephemeral nature of NH_4^+ as a nitrogen form, large fluctuations in NH_4^+ levels would indicate that fast microbial metabolic pathways are the main processors of organic material (Johnston et al., 2004). The increase in flocculated material in the water column reported by Rex and Petticrew (2008) and the concomitant increase in suspended bacterial matter (in the form of flocs) (Droppo, 2001) suggests one potential mechanism for this processing. Most studies, however, have only been reproduced in coastal areas which contrast greatly with interior systems in terms of nutrient availability and demand.

Additionally, Table 1.3 highlights the range of measures used to characterize the water column during salmon spawning. Often, NO_3^- and dissolved organic carbon (DOC) are observed to increase. These NO_3^- and DOC fluxes, however, are often not correlated to any point of the salmon spawning cycle (Cak et al., 2008).

Table 1.3: Summary of water chemistry responses to salmon spawning. NH_4^+ and SRP generally increase in response to salmon run. NO_3^- values generally increase in a salmon spawning stream but the increase is not correlated with the arrival of salmon. All nutrient measures are presented as comparison of concentrations (e.g. mg/l). Note that most studies on biofilm and salmon have been conducted in coastal areas rather than interior ecosystem.[b]

Study	Type of Control	Study Location	NH_4^+	NO_3^-	DOC	SRP	TN	NO_2^-	TDN	TSP	KJN
Bilby et al. (1996)	Experimental	Wash	↑	nsd	–	–	–	–	–	↑	nsd
Chaloner et al. (2004)	Spatial	Alaska	↑40 ×	nsd	nsd	↑4 ×	–	–	–	–	–
Johnston et al. (2004)	None	Interior BC	↑	↑(nc)	–	↑40 ×	nc	–	–	–	used for TN
Claeson et al. (2006)	Spatial	Wash	↑	nsd	nsd	nsd	–	nsd	nsd	–	–
Mitchell and Lamberti (2005)	Spatial	Alaska	↑10 ×	↑(nc)	↑(nc)	↑4 ×	–	–	–	–	–
Hood et al. (2007)	Spatial	Alaska	↑100 ×	↑(nc)	↑(nc)	↑10 ×	–	–	–	–	–
Cak et al. (2008)	Spatial	Alaska	↑40 ×	↑(nc)	↑(nc)	↑6 ×	–	–	–	–	–
Tiegs et al. (2008)	None	Alaska	↑	nsd	–	↑	–	–	–	–	–
Tiegs et al. (2009)	Cage Exclusion	Alaska	↑	↑	–	↑	–	–	–	–	–
Chaloner et al. (2007)	Spatial	Alaska	↑	nsd	nsd	↑	–	–	–	–	–
Wipfli et al. (2010)	Experimental	Alaska	↑	–	–	↑	–	–	–	–	–

[b]nsd, no significant difference; –, not measured; ↑, increased in the spawning stream; ↓, decrease in the salmon spawning stream; nc, not correlated with the salmon run

Chapter 2

Sediment and Biofilm Interactions in a Salmon Spawning Stream: Aspects of Marine-Derived Nutrient Infiltration and Trapping

2.1 Introduction

Biofilms remain an understudied component of the nutrient cycling pathways in rivers (Battin, 2000). Similarly, interior salmon spawning streams remain understudied habitats compared to coastal systems (See Tables 1.2 & 1.3). Interior systems differ considerably from coastal systems. The longer distances from the ocean (Quinn, 2005) to the interior habitats diminish the marine connectivity as the downstream nutrient sinks are often rearing lakes rather than the ocean. This connectivity between rearing habitat and spawning grounds in interior systems has considerable implications for the spatial component of nutrient retention. The life history of interior salmon stocks reflects this different habitat as juvenile fish often spend a year in the rearing lake prior to proceeding out to sea.

Considerable information has been gained on salmon spawning ecology (Schindler et al., 2003; Janetski et al., 2009) from using both artificial stream-based studies (Claeson et al., 2006; Rex and Petticrew, 2008) as well as field observations (Moore and Schindler, 2008). The Horsefly River spawning channel (HFC) represents a unique environment that spans the manipulability of an artificial stream with the realism of a natural habitat. For example, hydrodynamic conditions can be kept constant while salmon activity still closely mimics that of a typical stream. This type of ecological realism has been previously highlighted as vitally important for making consistent observations (Janetski et al., 2009).

The objective of this study is to examine the significance of biofilm uptake and retention of MDNs as related to salmon spawning and die-off in an interior British Columbia

river. The interaction between sediment and biofilms is examined in the context of a salmon spawning event (i.e. the salmon disturbance regime). This research explored two broad themes as they relate to salmon spawning and biofilm ecology.

2.1.1 Theme One

How does biofilm biomass change in response to the salmon disturbance regime? Changes in biofilm biomass and isotopic signature have been observed to reflect nutrient uptake by biofilms in other freshwater systems (Bilby et al., 1996; Sabater et al., 2002; Yoder et al., 2006). What effect does redd construction have on biofilm abundance? Does a reduction of biofilm during the active-spawn period inhibit growth of biofilms during the post-spawn phase? Is there a spatial component to this growth? Do downstream biofilms become enriched with MDNs from upstream salmon carcass decay? Chlorophyll *a* and AFDM will be used as indicators of change in biofilm biomass and isotopic signatures will be used to infer MDN addition.

2.1.2 Theme Two

What effect does salmon redd construction have on biofilm and sediment resuspension and subsequent nutrient delivery to downstream streambeds? Salmon resuspend biofilm and sediment when cleaning gravels during redd construction (Figure 1.2). Resuspension of these materials into the water column via redd construction has an unknown impact on the overall nutrient retention capacity of streambeds both spatially and temporally. The fate of these reworked biofilms may represent an important in-stream nutrient vector, if they are deposited within the channel. The fate of resuspended sediment may be a key indicator of mechanisms transferring MDNs to the streambed (Rex and Petticrew, 2008).

2.2 Methods

2.2.1 Study Site

The Horsefly watershed (52° 19'N/121° 1'W) is located within the Cariboo region of British Columbia. The Horsefly River is the largest tributary of Quesnel Lake. Historically, the Horsefly River supports a large sockeye escapement although recent years have seen steep declines. The Horsefly river escapement is often more than the combined total of all other Quesnel River tributaries (Lawrence, 2004).

2.2.1.1 Horsefly Spawning Channel

The Horsefly River spawning channel (HFC) is an artificial salmon stock enhancement stream constructed by the Department of Fisheries and Oceans (DFO) (Figure 2.1). The channel is 1600-m in length and approximately 10-m in width with a slope of 1%. Water flow into the channel is controlled by a large siphon supplying water from a settling pond which is directly connected to the Horsefly River. The mouth of the channel flows into the Horsefly River (Figure 2.1). Sockeye salmon (*Oncorhynchus nerka*) enter the HFC via the Horsefly River. Upstream access to the Horsefly River for the salmon is restricted within the HFC by a permanent gate at the upper portion of the channel. Confined salmon then spawn inside the channel.

In summer and fall of 2009, in addition to regular DFO enhancement activities, a portion of the HFC was converted into an experimental reach (Figure 2.1). Sampling began on August 28^{th}, 2009 and lasted until October 26^{th}, 2009. Prior to the start of the sampling period (August 26^{th}, 2009), the channel bed was cleaned of sediment and biofilms using a rake with 30-cm teeth mounted on a bulldozer. The rake resuspended material from the streambed, which was then flushed out of the channel to a downstream settling pond via artificially-generated high discharge.

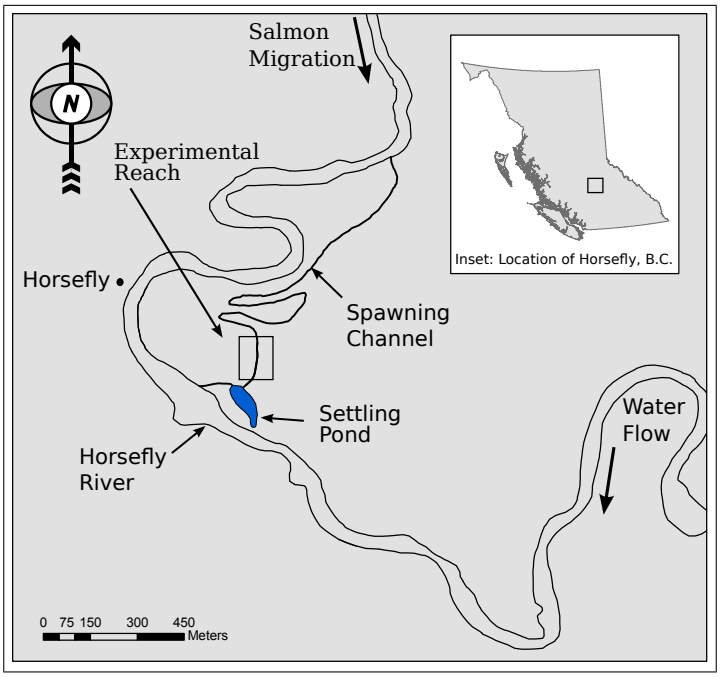

Figure 2.1: Location of the Horsefly River spawning channel (HFC) and position of the experimental reach.

2.2.1.2 Measurement of Site Characteristics

Discharge in the HFC was monitored through a combination of staff gauge readings and a pressure transducer (Unidata 8007 WPD) and applied to a calibrated rating curve. The rating curve was estimated by measuring flow velocity at 0.6 of the depth at 1-m intervals across the channel and at a range of representative stage heights (n=4). Stage height was an excellent predictor of discharge (r^2=0.997). Precipitation was measured using three anchored buckets located in three open fields near the study site. Precipitation was calculated by averaging the volume of water in each bucket and normalizing it per unit area.

Water temperature was continuously recorded in each section using calibrated Tidbit Temp Loggers (Onset Corp.). Tidbits were calibrated by placing them in a bucket of water at a known temperature and establishing a correction term for each Tidbit based on the difference between the measured and known temperatures. Conductivity and pH were recorded using a Combo Multiparameter Meter with two-point calibration (Geo Scientific, Ltd.). Average grain size was determined by measuring the three major axes of

gravels (n=100) randomly selected from each section. Other resident fishes observed in the channel during the experimental period were a small number of Rainbow trout (*O. mykiss*), Kokanee (*O. nerka*) and Chinook Salmon (*O. tshawytscha*). Light levels were similar across the entire experimental reach of the HFC. The west side of the channel was devoid of tree cover. The east side of the channel had a 3-m strip of deciduous trees that provided uniform shade over the length of the experimental reach.

2.2.2 Study Design

2.2.2.1 Spatial and Temporal Controls

The study site was located in the upper portion of the spawning channel (Figure 2.1). A 60-m section of the channel was divided into three sections using steel fences which limited salmon entry into a particular section. Channel sections will be henceforth referred to as 'Upstream' for the spatial control, 'Middle' for the middle section with the most active salmon spawning area and 'Downstream' as the downstream deposition area (Figure 2.2). A 1-m buffer around each fence was excluded from sampling and used for movement through the channel.

Sampling was divided into three spawning periods. All samples collected prior to salmon arrival were defined as 'Pre-Spawn'. Samples collected during the most active spawning period were termed 'Active-Spawn' and the die-off period was termed 'Post-Spawn'. Collectively these temporal divisions of the salmon spawning cycle are referred to as 'Period'.

2.2.3 Salmon

Salmon densities were enumerated visually and with a digital camera. The salmon were visually counted by two individuals. In instances where the counts differed greatly (>10 salmon), the salmon were recounted until a similar count was reached. Where live salmon

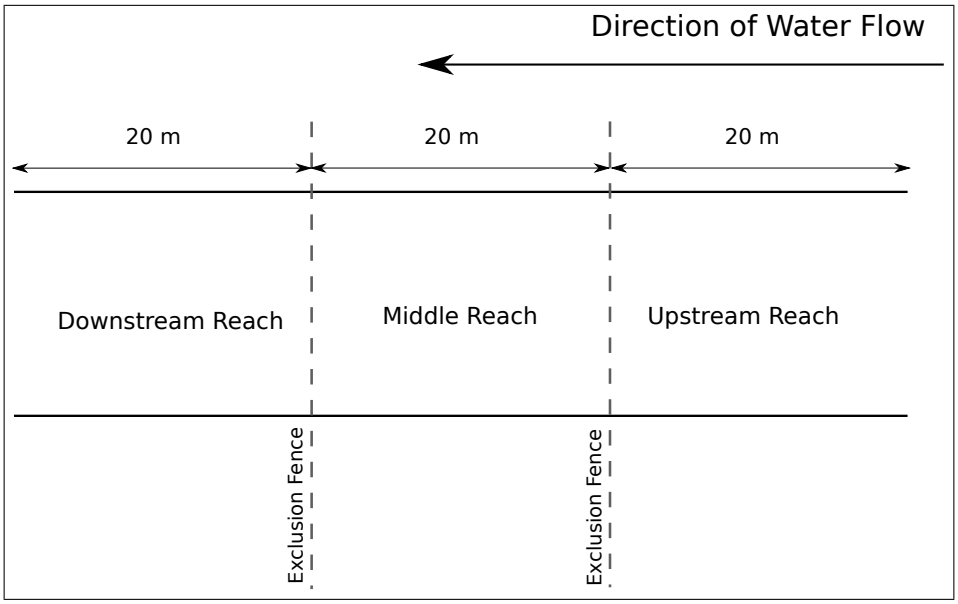

Figure 2.2: Division of the HFC into experimental sections. Downstream spawning salmon not part of the experiment were excluded from the experimental section at the lower portion of the downstream reach by an additional steel fence.

densities were too active to be counted visually (September 12^{th}-28^{th}), a digital photograph was taken of the reach and salmon were counted at a later date. Freshly dead salmon[1] flesh (n=4) was sampled and analyzed for δ^{15}N , δ^{13}C and %C and %N.

A range of salmon numbers were loaded into each section. The downstream and middle sections were used as areas to assess the effect of active salmon spawning and die-off. The upstream section was intended to remain free of fish as the spatial control on salmon redd construction and die-off. A small number of salmon, however, escaped into the upstream section diminishing the spatial control. Live salmon were removed from the upstream section when possible, minimizing spawning activity. Dead salmon were also immediately taken out of the upstream section removing any potential die-off effects from the upstream control.

[1]Salmon were sampled within an 1h of dying. In each case, the fish was observed to cease swimming and sampled once it had completely stopped moving

2.2.4 Biofilms

2.2.4.1 Biofilm Collection

Streambed biofilms were collected in each section from randomly sampled gravels during the pre-spawn, active-spawn and post-spawn periods. On every sample date, five rocks were randomly collected at each of three streambed depths from the three section sections. Five samples have been previously identified as an appropriate sample size to characterize the spatial variability of biofilm within a reach of similar size (see Chaloner et al., 2004). Measurements taken from these five rocks were averaged to generate a mean data point for each sampling day. The three sampling depths were streambed surface, 5-cm below the streambed ($\approx d_{50}$) and 10-cm below the streambed ($\approx 2 \times d_{50}$). Because of a small number of escapees into the upstream section, rocks were collected in this section where there had clearly been no redd building activity. Rock surface area (SA) was determined using the method of Graham et al. (1988). A second surface biofilm sample was collected on each sampling date in triplicate from each section for stable isotope analysis.

2.2.4.2 Biofilm Characterization

Immediately after collection, gravels were scrapped with a toothbrush and rinsed with distilled water to remove all biofilm and inorganic sediment. The resultant slurry was filtered onto a pre-ashed, pre-weighed GFF, protected from light and frozen at -20°C until further analysis (Mitchell and Lamberti, 2005). Chlorophyll *a* was extracted from the slurry in 25 ml of 90% buffered acetone for 24h at 4°C and the extract was centrifuged at 3100 rpm for 20 min. Extracted chlorophyll *a* was analyzed spectrophotometrically correcting for phaeophytins by acidification with HCl (APHA, 1995; Steinman and Lamberti, 1996; Mitchell and Lamberti, 2005). Any material left on the GFF after extraction and material centrifuged into a plug in the above centrifugation step was combined, dried at 60°C for 12h, weighed, ashed at 550°C for 2h and weighed again. The mass lost during

the ashing step was defined as ash-free dry mass (AFDM) and the material left on the GFF was the amount of inorganic sediment trapped by the biofilm.

Biofilms for stable isotopes analysis were scraped from each gravel in the same manner as described above except the biofilm slurry was frozen in a microcentrifuge tube. Upon returning to the lab, samples were freeze-dried and analyzed for δ^{13}C , δ^{15}N and total C and N (Pacific Centre for Isotopic and Geochemical Research, University of British Columbia). Isotope enrichment was determined as follows (Kline et al., 1993):

$$‰\ \delta^{13}C\ or\ \delta^{15}N = \frac{R_{sample} - R_{standard}}{R_{standard}} \times 1000 \tag{2.1}$$

where R is the ratio of the heavy isotope to the light isotope. The standard for C is Peedee Belemnite and for N is air (Bilby et al., 1996).

2.2.5 Infiltration Bags

Sediment and nutrient infiltration in the streambed was assessed using modified infiltration bags which allow for vertical and horizontal sediment delivery to a sample column of gravel (Rex and Petticrew, 2006). Prior to sampling, three 0.35-m holes were dug in each section. Plastic bucket frames covered with galvanized steel mesh (aperture 0.025-m) were placed in each hole. The plastic frames prevented outside gravels from filling the hole, while the steel mesh allowed for normal water flow through the gravels. Additionally, the plastic frames allowed for periodic removal of the sample column and replacement with clean gravel in the same unaltered position within the streambed. In each experimental section, infiltration bags were placed at the base of three buckets and covered with gravel cleaned of sediment <2-mm. Bags were removed weekly, and replaced with new bags and cleaned gravel. For each weekly sampling date, gravels were rinsed through a 2-mm sieve to remove all <2-mm sediment into a volumetrically calibrated bucket.

2.2.5.1 Sediment Characterization

Fine sediment was sampled by resuspending all the material collected from infiltration bags in a sample bucket, waiting 10-s and sub-sampling the top portion of water. This method allows for larger particles to settle out and ensures that only fine sediment (<70-µm) is sampled (Rex and Petticrew, 2006; Petticrew and Albers, 2010). Samples were taken for particle size analysis and for AFDM and inorganic sediment characterization. Fine sediment from the infiltration bags was filtered onto GFF, dried at 60°C for 12h, weighed, ashed at 550°C for 2h and weighed again. Response variables derived from this process were AFDM and inorganic sediment. Sediment <2-mm subsamples were also analyzed for δ^{15}N , δ^{13}C and total N and C in the same manner as biofilms as described above (Section 2.2.4.2).

2.2.5.2 Particle Size

Particle size distributions were determined using laser in-situ scattering and transmissometry (LISST) (Sequoia Scientific, Inc.). A LISST probe measures the degree of diffraction when a laser is passed through a 60-ml sample to determine a distribution of 32 size classes of particles ranging from 2µm to 460µm (Agrawal and Pottsmith, 2000). The LISST protocol was adapted from Rex (2009, Appendix 1). Samples (60-ml) were analyzed with the LISST within 5 days of sampling. Samples were gently mixed and poured into the LISST sample chamber to prevent the formation of air bubbles. Rex (2009) identified that bulk samples of sediments are more easily collected than water column aggregates and can reflect particle sizes distribution shifts in the water column. Three subsamples from each infiltration bag were collected and averaged to account for any potential variability associated with LISST sampling (Williams et al., 2007). LISST data were processed using a semi-automated macro with MS Excel (Microsoft, Inc.) that calculated cumulative distributions, measures of central tendency as well as diagnostic parameters. Standard error bar plots of d_{16}, d_{50} and d_{84} values as per Kondolf (2000) and cumulative distribution plots

were used to qualitatively compare changing particle size during the salmon spawning cycle.

2.2.6 Suspended Sediment

ISCO automatic water samplers (Teledyne ISCO, Inc.) were placed streamside with the sampling tube located in the thalweg of the HFC near the rear of each section to sample for suspended sediment. Water was sampled every 3 hours 8 times per day to form one daily composite sample. ISCO water samples were also filtered with GFF, dried at 60°C for 12h, weighed, ashed at 550°C for 2h and weighed again. The ratio of the material lost during the ashing step to the material that remained was used as a response variable for the ISCO water samples. This variable was defined as the organic matter ratio (OMR) and used to assess the nutrient quality of suspended sediment in the HFC as it reflects the organic and inorganic components of the sediment. The total mass of sediment (inorganic or organic fractions) in the water column was determined by multiplying the sediment concentration by the discharge to estimate the total daily suspended sediment load.

Particle size of suspended sediment was examined using the LISST on September 24^{th}, 2009 and July 14^{14}, 2010. A particle size measurement with the LISST was taken on July 14^{th}, 2010 in the HFC to determine background or pre-spawn particle size distribution. Measurements taken on July 14^{14}, 2010 were conducted under similar channel conditions and it is assumed that measurements taken on this day are representative of pre-spawn conditions in 2009. On both sample dates, the LISST was placed in the rear portion of the middle section to measure the size of suspended particles passing through the instrument aperture. The LISST was programmed to sample particles every 15-s. The LISST was left in the channel to sample for approximately 15-min. Data was processed in a similar manner to section 2.2.5.2. Post-processing included averaging every three observations to calculate a single point. A Kolmorov-Smirnov test (Siegel, 1957) was used to compare mean background and active-spawn distributions and cumulative distribution plots were

used to examining grain coarsening patterns.

2.2.7 Piezometers

To monitor intergravel DO, three piezometers constructed of plastic tubing were buried in each section at a depth of 28-cm in the bed prior to beginning the experiment. Piezometers were sampled daily, and analyzed for DO following an evacuation of the tubing to ensure residual water was not sampled. The oxygen meter was calibrated for each sampling date by determining the saturation point of oxygen corrected for temperature and elevation.

2.2.8 Statistical Analysis

All biofilm, piezometer and infiltration bag response variables were analyzed with a two-way ANOVA using period and section as fixed effects. Reaches were considered to be adequately independent to merit an ANOVA approach although I acknowledge that some temporal dependence may exist (Cak et al., 2008). The minimum adequate model (MAM) for each parameter was determined by comparing the F-ratio of a full and reduced ANOVA model (Whittingham et al., 2006; Crawley, 2007). Replicate biofilm, infiltration bag and piezometers measurements for each sampling day were averaged. These single data points from each sampling day served as replicates for the period of salmon activity factor. A significant period $\times$ section interaction indicated that a particular reach demonstrated a different temporal trend as the salmon run progressed. Linear contrasts of means were used to test specific hypotheses if a significant interaction was determined (*sensu* Mills and Bever, 1998). Each contrast was compared both to its temporal and spatial controls. Contrasts were chosen to determine the effect of the salmon disturbance regime on biofilm abundance. To confirm similar starting conditions in each section, the contrasts tested for differences in the means at the outset of the experiment. Contrasts were coded according to the conditions for linear contrasts set out by Fox (1997).

Models without a significant interaction term had to be interpreted solely on their main effects. In this case an effect of salmon was still inferred. However, the causality of this effect is less clear although significant trends may still be assessed. In the absence of a significant interaction term, pairwise multiple t-test's with Holm's p-value correction was used to compare mean differences for the main effects (Fox, 1997). Other mean comparisons test all possible combination of factors leading to overly conservative estimates (Quinn and Keough, 2002). Response variables were log and square-root transformed as necessary to meet the assumptions of parametric tests. Null hypotheses were rejected at an α level of 0.05. All statistical analysis were conducted using R 2.11.1 (2010). All graphics were created using R 2.11.1 (2010) with the *memisc* (Elff, 2010), *ggplot2*, (Wickham, 2009) and *lattice* (Sarkar, 2008) packages.

2.2.8.1 Correlations

All correlations were analyzed using Pearson's product moment correlation (Quinn and Keough, 2002). The relationship between AFDM and chlorophyll *a* of biofilms was analyzed using individual surface rock values. The relationship between inorganic sediment and chlorophyll *a* was limited to post-spawn downstream surface biofilms to examine deposition characteristics. The correlation between infiltration bag sediment and surface chlorophyll *a* from biofilms was a comparison between the weekly values of both parameters from all sections.

2.3 Results

Any study that attempts to demonstrate the net impact of salmon on their natal stream should ideally sample to characterize all stages of salmon activity, while maintaining concurrent spatial controls to assess how a system responds in the absence of salmon (Janetski et al., 2009). This type of study design would provide a means to test the interaction be-

tween spatial and temporal controls and assess the resistance and resiliency of the stream ecosystem in its totality (Biggs et al., 1999). In this way the entire salmon disturbance regime can be assessed and the stability of the system can be accurately measured (Biggs et al., 1999).

In this study, many of the parameters measured did not yield a significant interaction term but rather significant main effects. These models are no less significant or important than those with a significant interaction term. However, interpreting these main effects is more difficult as the hypothesis tested only allows for the comparisons of the marginal means[2]. Therefore, statistical evidence of differences in cell means is only present in cases where there is significant interaction term. This statistical framework provides the context in which to view the patterns seen in the response variables.

Table 2.1: HFC Site Characteristics. Values represent mean values over the sampling period. Unless otherwise indicated, values in parentheses are the standard deviation of that parameter. Grain size measurements are from the B axis of gravels collected in each experimental section.

Section	Water Temperature (°C; max/min)	Conductivity (µS)	pH	Grain Size (cm)
Upstream	12.33 (-0.04; 21.67)	126 (44)	7.56 (0.43)	4.11 (1.19)
Middle	12.41 (0.05; 21.86)	133 (45)	7.51 (0.46)	4.22 (1.11)
Downstream	Equipment Failure	120 (39)	7.77 (0.54)	4.24 (1.17)

2.3.1 HFC Characteristics

Site characteristics of the HFC remained relatively constant across stream sections and varied in a similar manner over the course of the study (Table 2.1). Sections experienced similar maxima and minima in the physical parameters tested. These differences across sections were relatively minor compared to differences in biofilm, sediment and intergravel DO.

[2]Marginal means are defined as the mean of one factor averaged over all the levels of the other factor (Quinn and Keough, 2002). Thus, in the context of this study, an example of a marginal mean is the value of a parameter in the post-spawn period averaged over all sections.

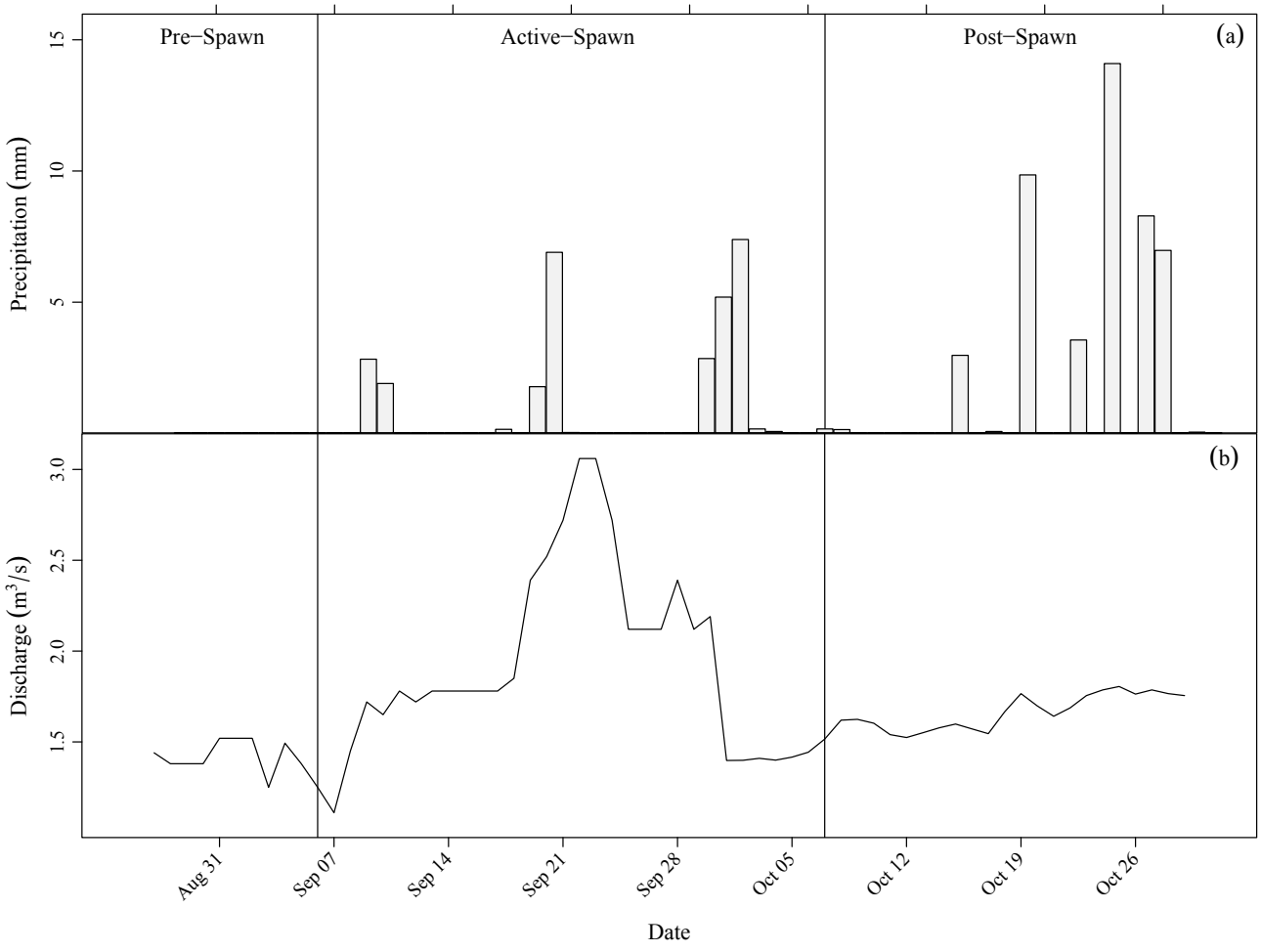

Figure 2.3: Characterization of stream conditions at the HFC. (a) Precipitation; (b) Discharge measurements. Vertical solid lines divide sampling periods defined by salmon activity.

In the summer and fall of 2009, the Horsefly region experienced relatively little precipitation (Figure 2.3a). Excluding one observation (October 7^{th}; snow), all precipitation fell as rain. The frequency of rain events increased during the active-spawn and post-spawn periods although these were still relatively small storms that were experienced equally by all three sections. Aside from one period, discharge remained stable over the course of the sampling period (Figure 2.3b). For a brief period, discharge increased by ≈50% (≈ September 19^{th}-28^{th}). The high discharge reading was likely caused by the daily build-up of salmon carcasses at a separation fence downstream of the study site rather than an a 50% increase in discharge. The build-up caused an increase in water depth at the staff gauge as water backed-up which may have resulted in overestimated discharge values.

2.3.2 Salmon Numbers

Discharge, the number of salmon loaded into the channel, and fish densities reflected natural spawning conditions and historical usage of the HFC. Salmon arrived in small numbers inside the experimental area on September 2^{nd} (Figure 2.4). However these fish were not actively spawning and present in such small numbers that I still considered this period as pre-spawn. Salmon numbers peaked on September 12^{th} in both the middle and downstream sections. Peak die-off in the middle section occurred on October 7^{th} and this date was defined as the beginning of the post-spawn period.

On September 25^{th} dead salmon were removed from the middle and downstream sections. Removal of dead fish from the HFC by black bears (*Ursus americanus*) occurred on several occasions and is accounted for by daily counts of dead salmon numbers. There was no indication that black bears were removing any live fish from the channel. As a result of escaped salmon from the enhancement section into the experimental section of the HFC, salmon numbers exceeded target densities although they were still within a natural range (See Table 1.2 & 2.2). Sockeye also typically spawn at extremely high densities for salmon (Bilby et al., 1996).

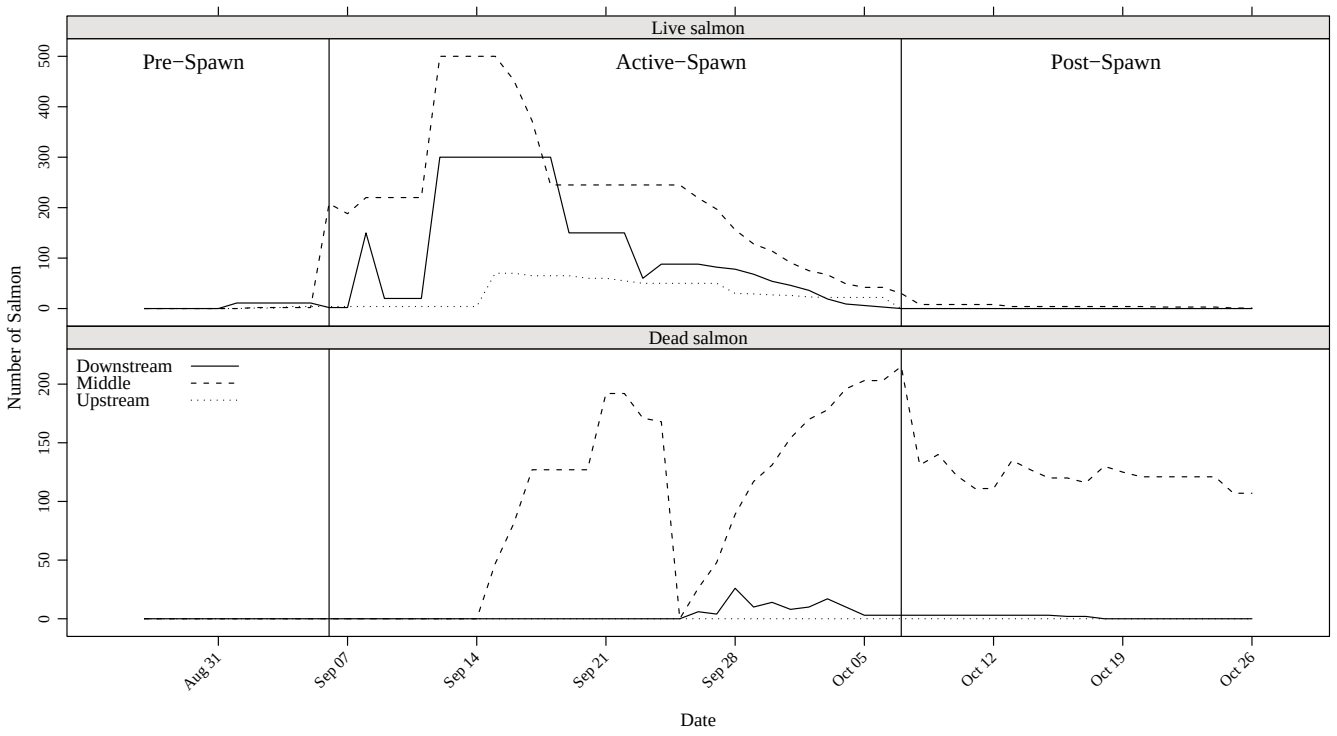

Figure 2.4: Live and dead salmon counts by section. Vertical solid lines indicate divisions of the salmon period.

Table 2.2: Salmon densities for historical usage of the HFC and the densities loaded into the experimental sections for this study. Densities used for the HFC study were slightly higher than historical usage but there are examples of studies using similar densities (Table 1.2; Chaloner et al. (2002))

Year/Section	Density (Fish/m^2)
Middle	**2.5**
Downstream	**1.5**
1989	1.7
1990	2.1
1991	1.3
1992	0.3
1993	1.3
1994	1.4
1995	1.2
1996	0.8
1998	1.8
1999	0.9
2000	0.2
2003	1.6
2006	1.4
2007	0.5
2009	0.6

2.3.3 Biofilms

2.3.3.1 Surface Biofilms

The section × period interaction was significant for surface chlorophyll *a*, AFDM and inorganic sediment (Table 2.3). Pre-spawn conditions in each section were not different enough to reject the null hypothesis that there was no difference in all biofilm parameters at the outset of the experiment (Figure 2.5, 2.6 & 2.7). Mean chlorophyll *a* values during the active-spawn period were significantly different from spatial and temporal controls. During the active spawning period mean chlorophyll *a* values in the middle section were significantly reduced by 4.2× from the upstream control over the same time period and by 1.5× from the pre-spawn values from the same section (Figure 2.5-Surface). Downstream surface biofilms were 2.7× higher in chlorophyll *a* than the active-spawn period in the same reach and 1.4× than the upstream control during the same period. Post-spawn chlorophyll *a* in the middle section was not significantly different from the active-spawn

period in the same reach and the upstream section for the same period.

Table 2.3: Results from a two-way ANOVA of spatial (section) and temporal (period) salmon treatments on surface chlorophyll *a*, AFDM or inorganic sediment. Interaction contrasts are separated by a |. Contrasts are labelled by the first letter of the corresponding section and the spawning period (U:Upstream; M:Middle; D:Downstream).

		Chlorophyll *a*		AFDM		Inorganic Sediment	
Source of Variation	Df	Sum Sq	Pr(>F)	Sum Sq	Pr(>F)	Sum Sq	Pr(>F)
Section	2	2.288	0.009	1.779	0.008	0.338	<0.000
Period	2	3.309	0.002	4.060	0.000	0.866	<0.000
Section × Period	4	3.297	0.011	2.009	0.024	0.281	0.001
M:Active|U:Active & M:Pre	1	2.424	0.002	1.337	0.006	0.212	<0.000
D:Post|D:Active & U:Post	1	0.868	0.044	0.663	0.042	0.001	0.819
M:Post|M:Active & U:Post	1	0.000	0.965	0.008	0.812	0.057	0.029
Starting Conditions	1	0.005	0.878	0.002	0.916	0.011	0.300
Residuals	18	3.342		2.483		0.181	

Surface mean ash-free dry mass (AFDM) values demonstrated a similar pattern as the chlorophyll *a* values described above. AFDM was significantly reduced during the active spawning period by 3.2× compared to the upstream section during the same period and 1.4× times compared to pre-spawn values in the same reach. Post-spawn values in the downstream reach were significantly higher (3.0×) than the active-spawn period in the same reach. Similar to the chlorophyll *a* values, no significant difference was found in the middle section in the post-spawn period contrasted to the appropriate controls (Figure 2.6-Surface).

Inorganic sediment found in the biofilm samples followed a slightly different pattern than the two parameters described above. Like chlorophyll *a* and AFDM, inorganic sediment trapped by biofilms in the middle reach during active spawning was reduced compared to the pre-spawn values in the same reach (3.0×) and the upstream section during the same period (3.4×; Figure 2.7-Surface). In contrast to measurements on the other two biofilm parameters, inorganic sediment was not significantly different in the downstream section in the post-spawn period but was significant in the middle section during the post-spawn period. Inorganic sediment was higher when compared to active

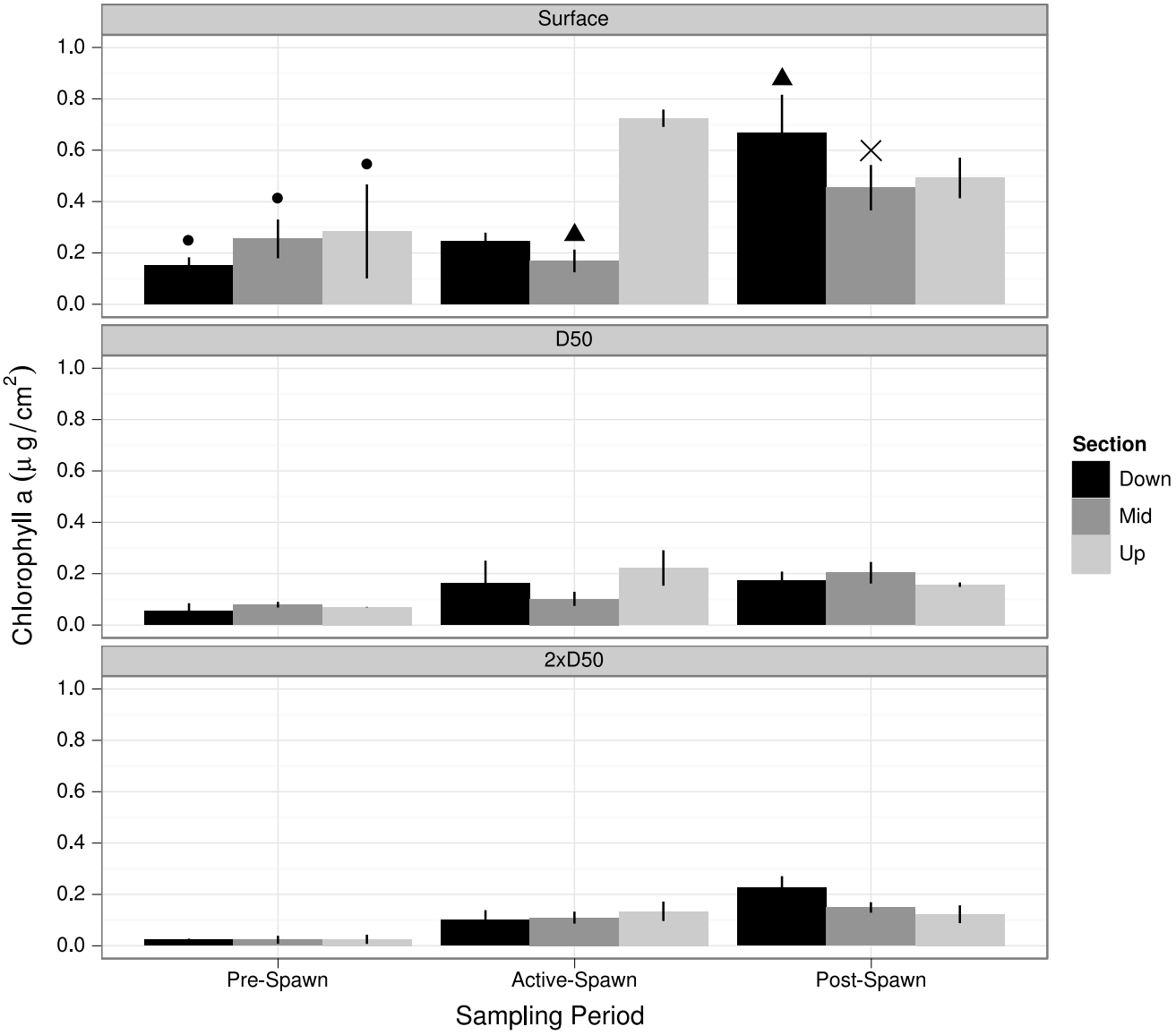

Figure 2.5: Chlorophyll *a* from gravels sampled in the HFC over the course of a salmon spawning event. Bar heights are mean values with error bars representing $\pm$ 1 SEM. Gravels were sampled at three depths which are indicated by the panel heading. An ▲ indicates a significant difference in the contrast test. A $\times$ symbol indicates a non-significant contrast. The • symbol is an indicator of a non-significant differences in the starting conditions. All surface means were contrasted according to Table 2.3.

spawning period in the middle section (3.7×) but lower when compared to the upstream control during the same period (1.6×). Both values were contrasted in the same manner as above (See Table 2.3).

2.3.3.2 Sub-surface Biofilms

The mean chlorophyll *a*, AFDM and inorganic sediment from biofilms sampled below the surface at 5 and 10 cm demonstrated no statistically significant difference with respect to spawning period and experimental section (all $p>0.05$). The lower two panels of Figures 2.5, 2.6 & 2.7 demonstrate the muted response seen at depth over the course of the salmon disturbance regime. The pattern of reduced chlorophyll *a* and AFDM in the middle section during the active spawn period appeared to only extend to the 5 cm depth although this result is not significant.

2.3.3.3 Stable Isotopes

Across all three parameters tested, there was a significant effect of sample period (Table 2.4). Additionally, section was a significant factor for δ^{15}N values. All post-hoc tests were pairwise comparisons used t-tests with Holm's correction. Levels of δ^{15}N were significantly higher during the active-spawn ($p<0.000$) and post-spawn ($p<0.000$) periods than the pre-spawn temporal control. Post-hoc comparisons revealed no significant differences in the mean amount of δ^{15}N across sections. Levels of δ^{13}C were significantly greater during the active spawn period than the post-spawn period ($p=0.019$). However, there was no significant difference in the remaining period comparisons for δ^{13}C (See Figure 2.8). All pairwise comparisons of period means of C:N ratios were significantly different from each other (all $p<0.05$).

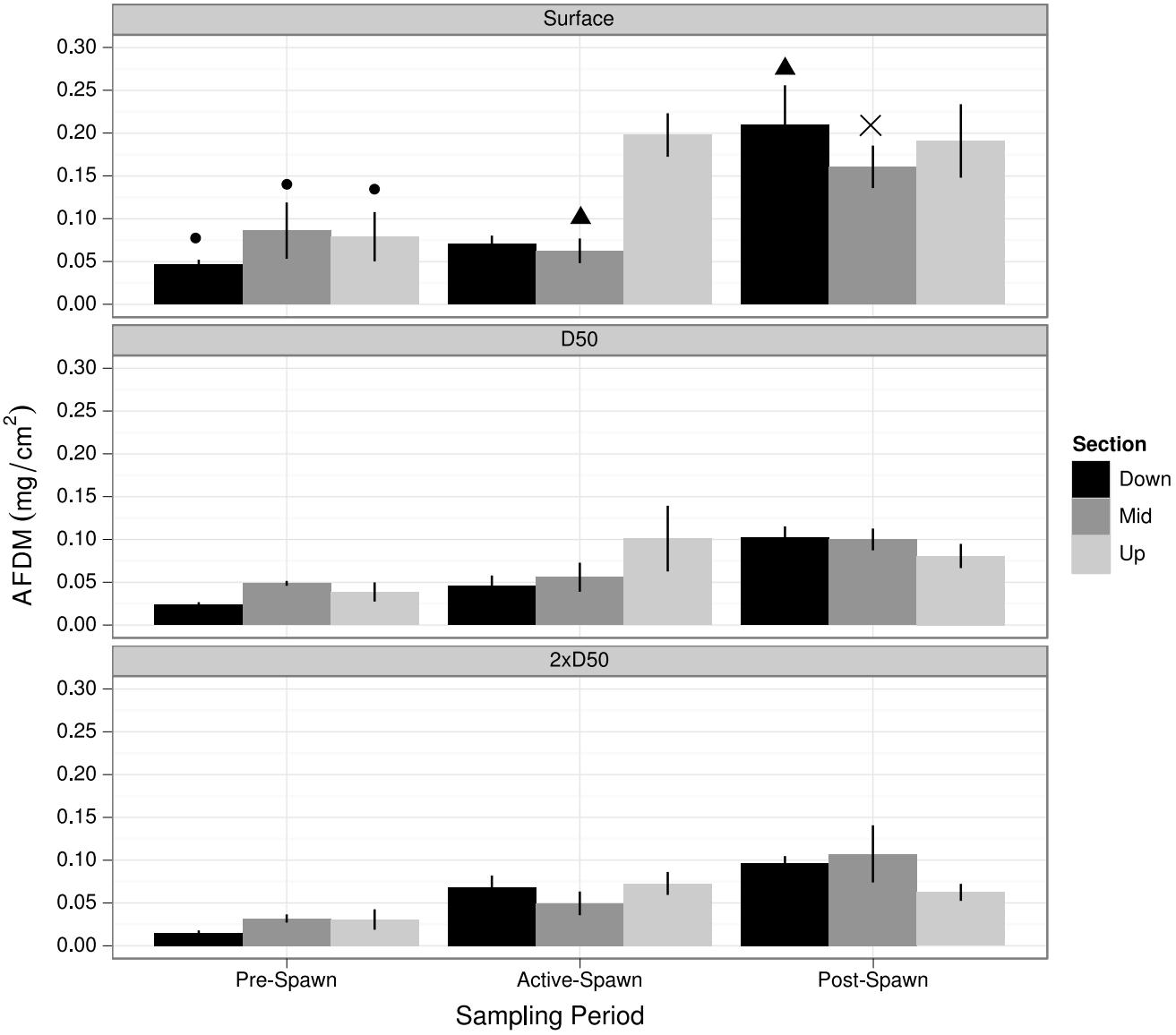

Figure 2.6: AFDM values from gravels sampled in the HFC over the course of a salmon spawning event. AFDM was determined by ashing GFF filters. Bar heights are mean values with error bars representing $\pm$ 1 SEM. Gravels were sampled at three depths which are indicated by the panel heading. An ▲ indicates a significant difference in the contrast test. A $\times$ symbol indicates a non-significant contrast. The • symbol is an indicator of a non-significant differences in the starting conditions. All surface means were contrasted according to Table 2.3.

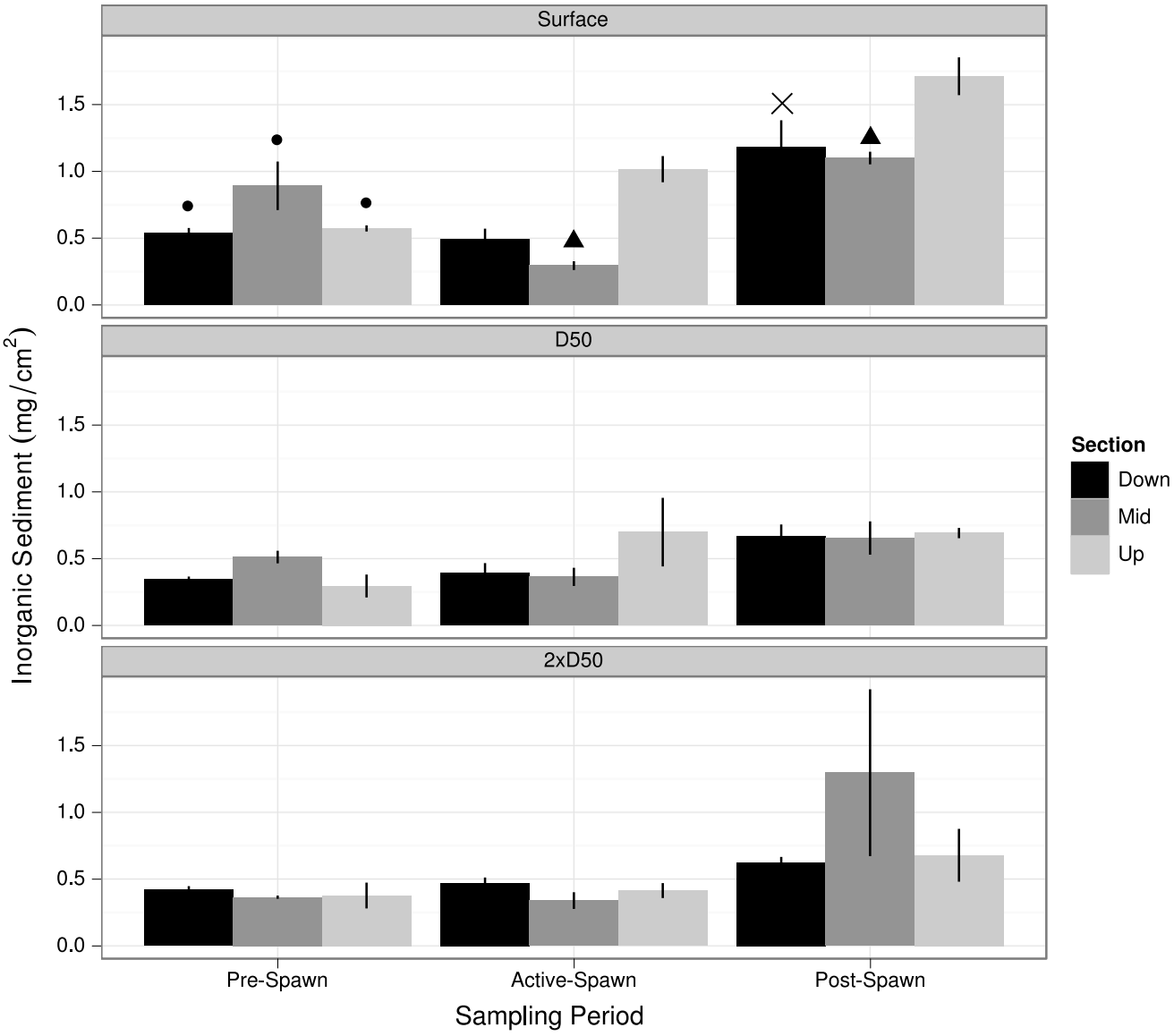

Figure 2.7: Inorganic sediment values from gravels sampled in the HFC over the course of a salmon spawning event. Inorganic was determined by ashing GFF filters. Bar heights are mean values with error bars representing $\pm$ 1 SEM. Gravels were sampled at three depths which are indicated by the panel heading. An ▲ indicates a significant difference in the contrast test. A $\times$ symbol indicates a non-significant contrast. The • symbol is an indicator of a non-significant differences in the starting conditions. All surface means were contrasted according to Table 2.3.

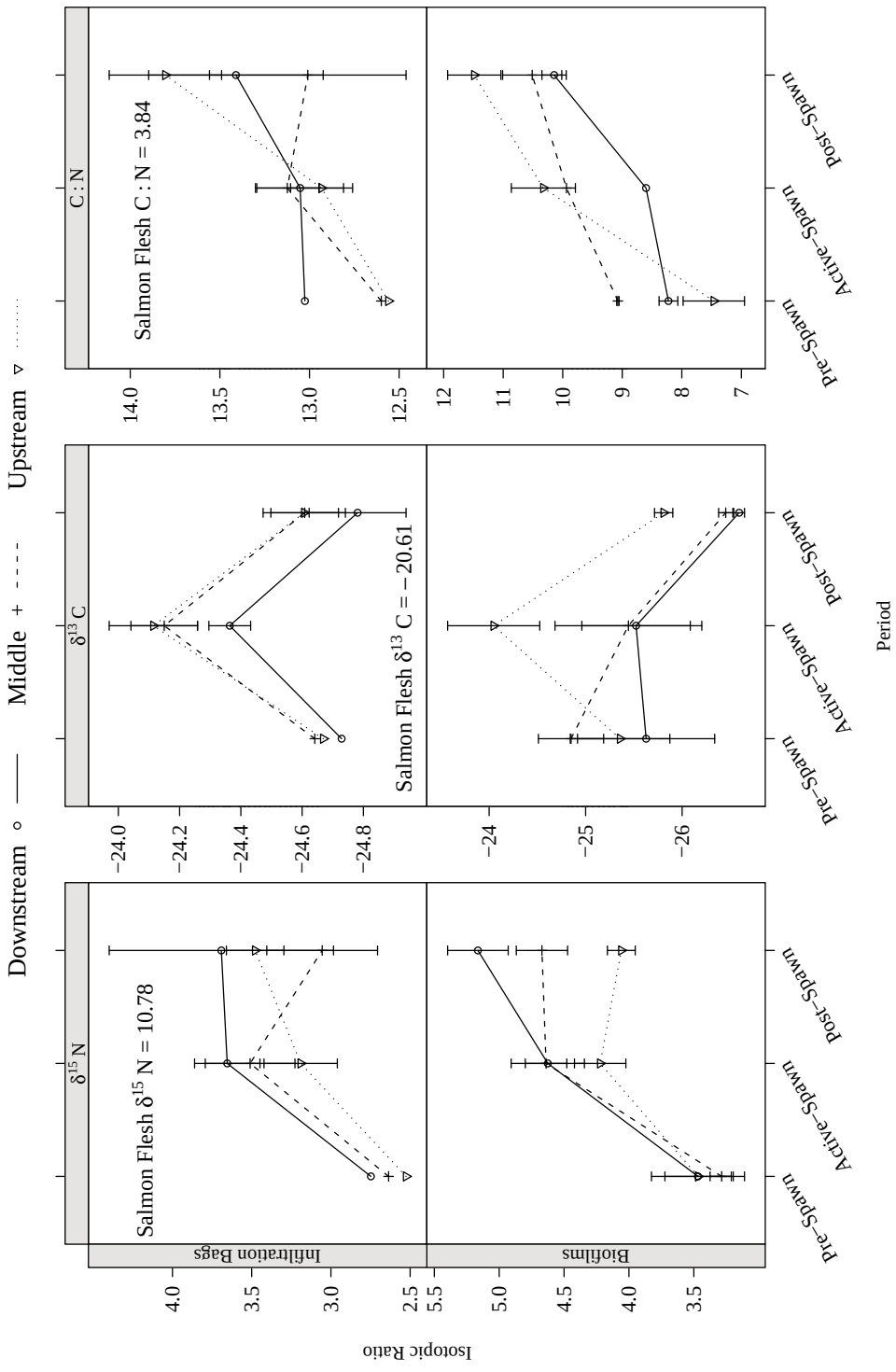

Figure 2.8: Isotopic ratio of benthic biofilms and infiltrated sediment. Ratios moving towards salmon flesh values indicate a marine nutrient source although δ^{13}C values can be confounded by photosynthetic processes (Staal et al., 2007). Isotopic ratios were calculated as per equation 2.1. The far right panel shows the carbon to nitrogen ratio of both biofilms and sediment. Salmon flesh values were sampled from fresh salmon carcasses (n=4). Points are mean values $\pm$ 1 SEM.

Table 2.4: Results from a two-way ANOVA of spatial (section) and temporal (period) salmon treatments on surface δ^{15}N , δ^{13}C and the carbon:nitrogen molar ratio from benthic biofilms. The minimum adequate model (MAM) only included an interaction term for C:N ratio. This interaction term was non-significant so only the main effects were tested for all models.

		δ^{15}N		δ^{13}C		C:N		
Source of Variation	Df	Sum Sq	Pr(>F)	Sum Sq	Pr(>F)	Df	Sum Sq	Pr(>F)
Period	2	0.351	0.001	8.769	0.012	2	3.677	<0.000
Section	2	0.066	0.041	4.618	0.080	2	21.807	0.063
Section × Period	–	–	–	–	–	4	5.837	0.074
Residuals	22	0.196		17.897		14	7.570	

2.3.4 Infiltration Bags

2.3.4.1 Stable Isotopes

Table 2.5: Results from a two-way ANOVA of spatial (section) and temporal (period) salmon treatments on δ^{15}N and δ^{13}C from infiltrated sediment. The minimum adequate model (MAM) included only the residual term for C:N ratio indicating that neither spawning nor die-off had any effect on intergravel C:N ratios. Therefore, the C:N model summary is not included here. Dashes (–) indicate a dropped parameter in the MAM.

	δ^{15}N			δ^{13}C		
Source of Variation	Df	Sum Sq	Pr(>F)	Df	Sum Sq	Pr(>F)
Period	2	0.166	0.128	2	1.405	<0.000
Section	–	–	–	2	0.213	0.148
Residuals	24	0.887		22	1.127	

Only δ^{13}C of intergravel sediment was affected by the presence of salmon (Table 2.5). A significant period term in the ANOVA model and significant post-hoc comparisons indicate a large spike in δ^{13}C levels during the active-spawn period and a subsequent decrease in the post-spawn period (All $p<0.01$) although this trend is consistent across across all sections and is small in magnitude (Figure 2.8).

2.3.4.2 Particle Size

The lower end of the particle size distribution (d_{16}) remained relatively stable in each section. Similarly, the pre-spawn and active-spawn d_{84} remain stable across all sections (Figure 2.9a). The most notable change in particle size is seen in the post-spawn period in the downstream section. Post-spawn values in this section were higher than similar particle sizes in the middle and upstream section. There was, however, a general trend of increasing particle size in the post-spawn period but this result is not significant ($p>0.20$). Figure 2.9b supports a general coarsening trend of material being deposited in infiltration bags corresponding to salmon activity. This result, however, was not statistically tested due to a lack of rigourous multi-sample distribution tests. Furthermore, distribution comparisons, like the Kolmogorov-Smirnov test, only test for difference and not location of difference reducing their usefulness in this particular context (Quinn and Keough 2002; But see section 2.3.5). A qualitative assessment of particle size via Figure 2.9 indicated that during the post-spawn period, downstream particle size was bigger with approximately 35% of particles greater than 200 µm.

2.3.5 Suspended Sediment

Table 2.6 summarizes the results of an ANOVA on three suspended sediment variables. The MAM with the organic response variable only included a period term, which was significant. Pairwise comparisons, however, were not significantly different for any section making interpretation of the organic variable ambiguous. Both period and section had a significant effect on inorganic suspended sediment. Pre-spawn inorganic sediment was significantly lower than both the active-spawn ($p=0.0076$) and the post-spawn periods ($p=0.0183$). Upstream inorganic suspended sediment was significantly higher than sediment collected from the middle section ($p=0.0026$) and the downstream section ($p=0.0012$).

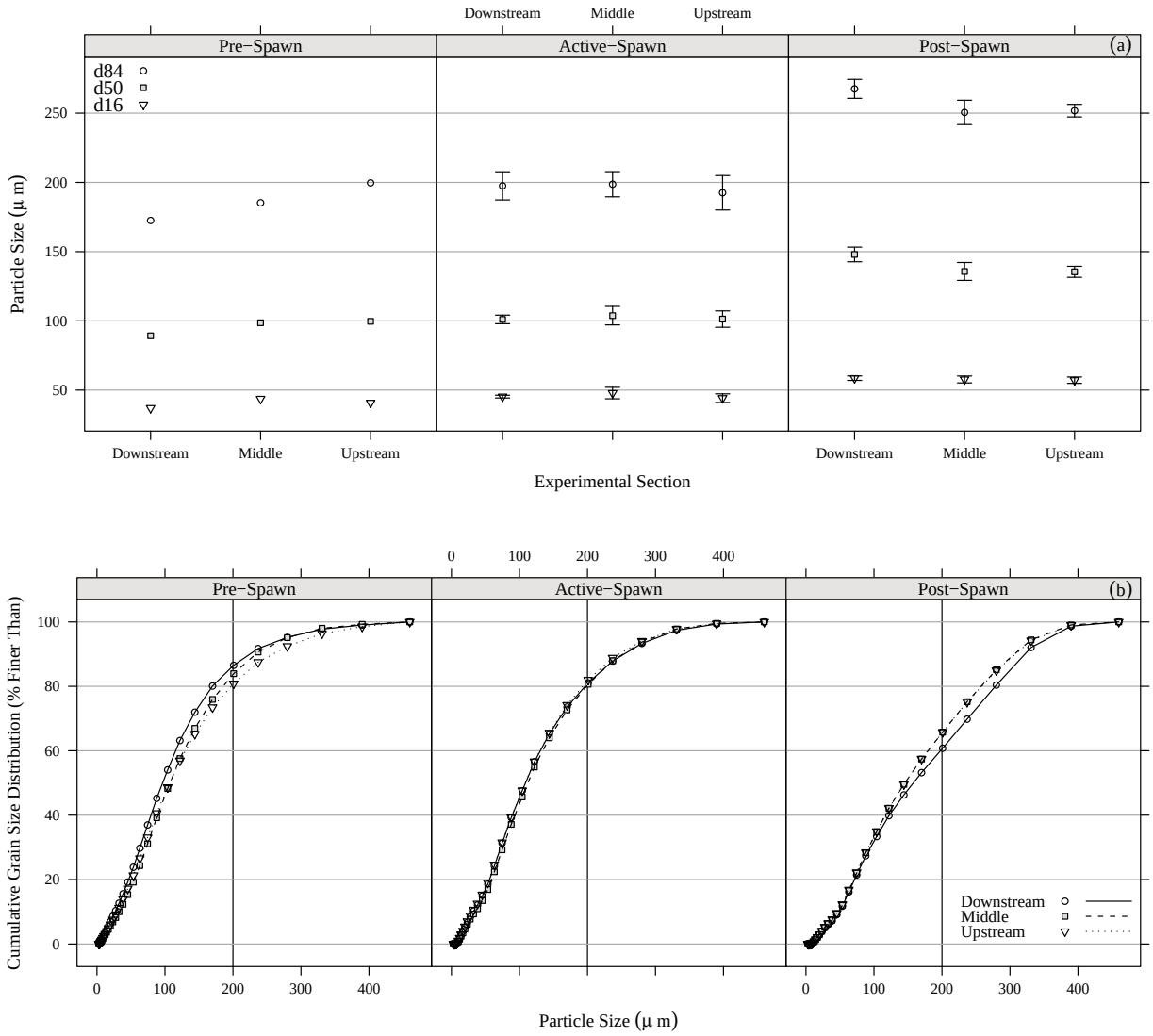

Figure 2.9: Range of particle sizes deposited on the stream bed into infiltration bags as measured by laser in-situ scattering and transmissometry (LISST). Top panel (a) data points are the mean values $\pm$ 1 SEM. Lower panel (b) is the cumulative distribution of particle size. Both figures are different visual representations of the same data.

Table 2.6: Results from a two-way ANOVA of spatial (section) and temporal (period) salmon treatments on suspended sediment variables. All models were determined using a minimum adequate model (MAM) (Crawley, 2007). OMR refers to the organic matter ratio of suspended sediment. See section 2.2.6 for details.

		Organic			Inorganic		OMR	
Source of Variation	Df	Sum Sq	Pr(>F)	Df	Sum Sq	Pr(>F)	Sum Sq	Pr(>F)
Period	2	0.919	0.044	2	2.791	0.004	0.601	0.229
Section	–	–	–	2	4.037	<0.000	2.347	0.004
Residuals	137	19.698		135	33.055		27.205	

There was a significant effect of section on the suspended sediment quality (OMR; Table 2.6). Pairwise comparisons indicated that upstream OMR was significantly lower than both the downstream (p=0.0083) and middle (p=0.0080) sections. All sections experienced a decrease in the ratio during the active-spawn period although this drop was most pronounced in the middle and downstream sections (Figure 2.10).

Suspended sediment particle size comparisons between July 14^{th}, 2010 (proxy background/ pre-spawn conditions) and September 24^{th} were significantly different (K-S test: D=5312, p-value<0.000). The K-S test was conducted on the mean distributions of each sampling date (Figure 2.11). The background proxy sample exhibited greater variability in particle size and a greater percentage of smaller particles in the system. In contrast, the particle size characterization taken during the active-spawn period exhibited less variation in particle size and a greater percentage of larger particles.

2.3.6 Intergravel Oxygen

Intergravel DO measured using piezometers was significantly affected by the presence and arrival of salmon into the HFC (Table 2.7). Post-hoc comparisons are summarized in Table 2.8. Pre-spawn and active-spawn intergravel DO measurements did not significantly differ. However all other pairwise comparisons for period were significantly different ($p<0.05$). The mean post-spawn oxygen level was significantly higher than the

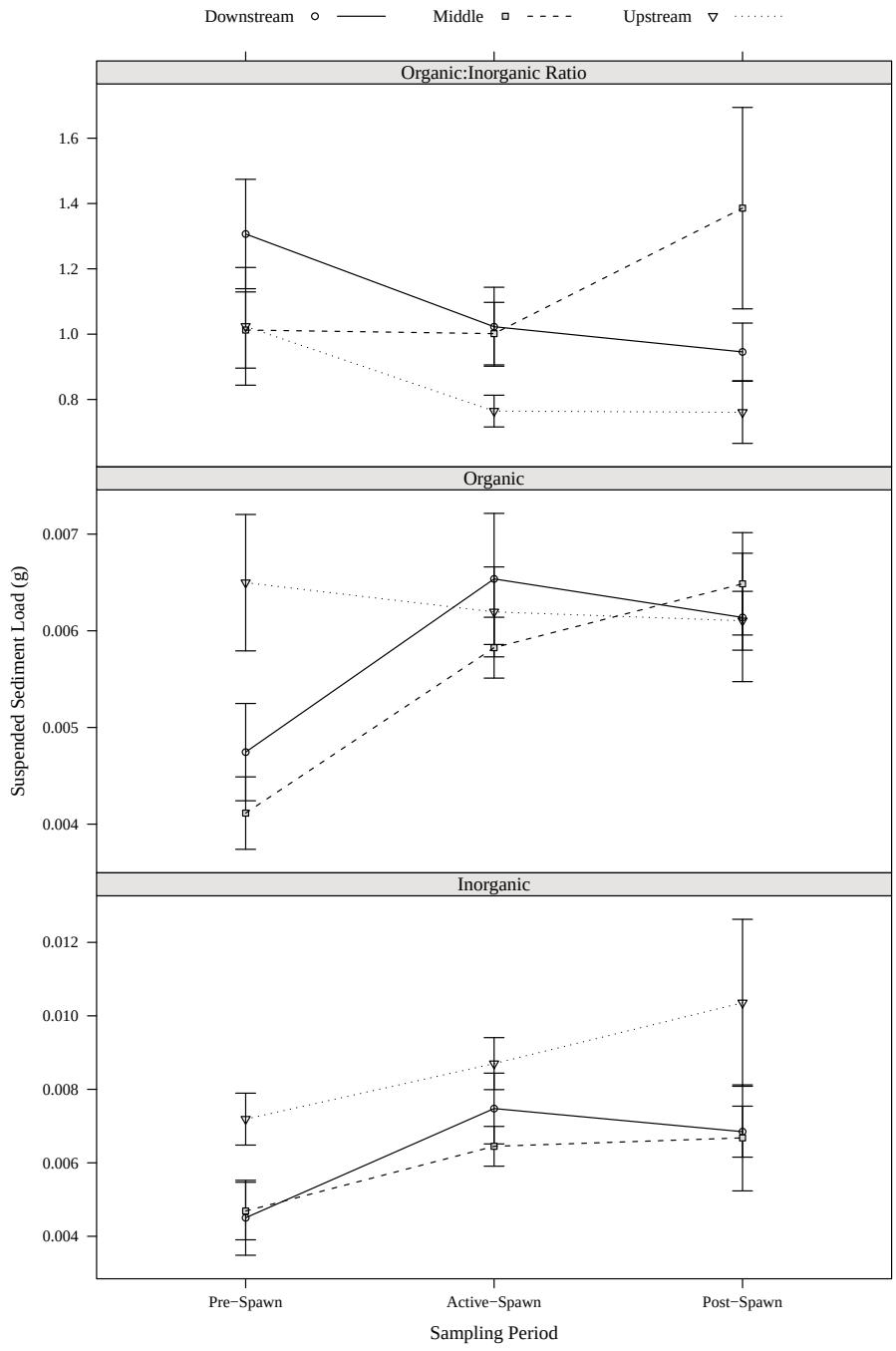

Figure 2.10: Suspended sediment loads and sediment ratios. Suspended sediment was sampled by an automatic ISCO water sampler placed in the rear portion of each section. Loads were calculated by multiplying the concentration of sediment by the discharge to get a total load. Mean values $\pm$ SEM.

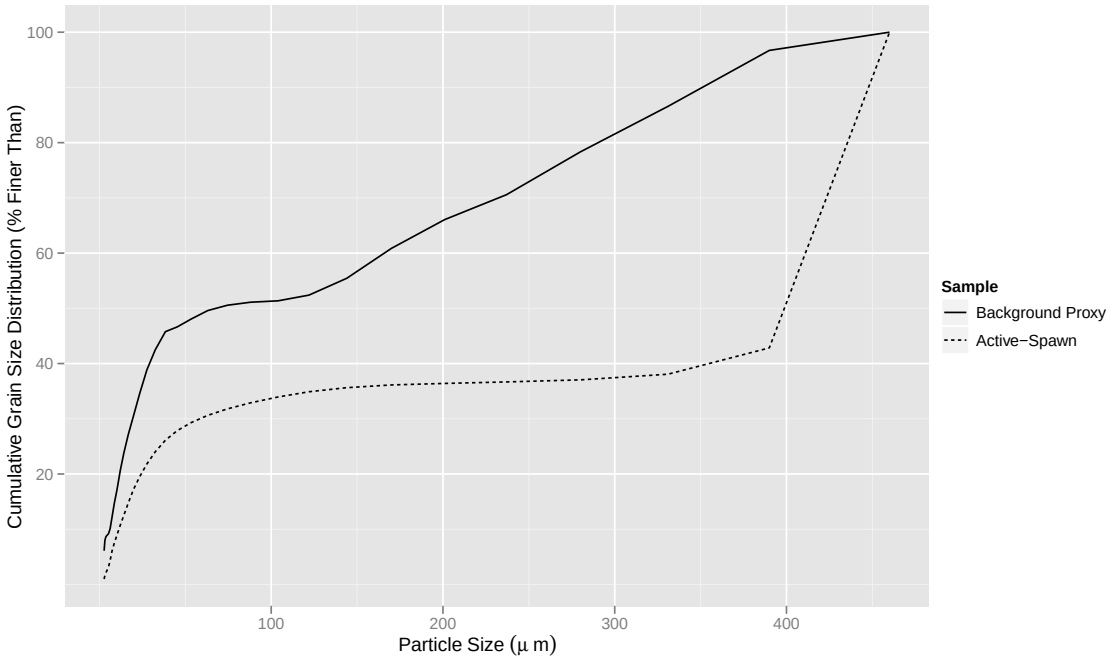

Figure 2.11: Particle size distributions of suspended sediment in the HFC. Background suspended sediment particle sizes were sampled on July 14^{th}, 2010 while the active-spawn particle size was taken during the HFC study on September 24^{th}, 2009.

other two periods (Table 2.8). All spatial section pairwise comparisons were significantly different. The downstream oxygen values were the highest while the middle section had significantly lower DO levels.

Table 2.7: ANOVA table of spatial and temporal responses of intergravel dissolved oxygen (DO) from piezometers.

Source of Variation	Df	Sum Sq	Pr(>F)
Section	2	47.768	<0.000
Period	2	83.000	<0.000
Residuals	166	187.664	

2.3.7 Correlations

Downstream surface biofilm chlorophyll *a* was significantly and highly correlated to downstream surface biofilm inorganic sediment (p-value<0.000, r=0.815) and ash-free dry mass

Table 2.8: Means and marginal means of intergravel DO. Bold font indicates the grand mean of the model (Table 2.7). Common letters indicate non-significance in pairwise t-test's with Holm's correction. All values are mg l^{-1}.

Variable	Downstream	Middle	Upstream	Period
Pre-Spawn	8.3	8.0	8.2	8.2^{a}
Active-Spawn	9.0	7.4	8.4	8.3^{ab}
Post-Spawn	10.4	9.4	9.4	9.7^{c}
Section	9.4^{x}	8.1^{y}	8.7^{z}	**8.8**

(AFDM) (p-value$<$0.000, r=0.926). Intergravel sediment (the mass of inorganic material collected from the infiltration bags) and chlorophyll *a* were significantly negatively correlated (p-value$<$0.006, r=-0.509)

2.4 Discussion

The results presented here correspond well with other studies that have reported decreases in biofilm abundance during active salmon spawning followed by a post-spawn increase in biofilm abundance (See Table 1.2; e.g. Moore and Schindler, 2008). Factors that influence biofilm abundance include the supply of light and nutrients in addition to hydrologic and physical disturbances (Biggs et al., 1999; Sabater et al., 2006). All biofilms in each section received approximately the same level of light because of similar tree cover and were subject to the same experimental flow conditions (Table 2.1). Thus, temporal and spatial biofilm abundance patterns were primarily driven by disturbance from salmon redd construction and nutrients from salmon carcass decay. Taken together, these two processes can be called the salmon disturbance regime. Patterns seen in chlorophyll *a*, AFDM and inorganic sediment provide strong evidence that the system is unable to *resist* the disturbance of redd creation while the system is ultimately *resilient* evidenced by its ability to process nutrients from the salmon die-off.

Similar to other studies, the salmon disturbance regime was characterized by two main periods (active- and post-spawn). The middle section during the active-spawn pe-

riod was meant to simulate a natural spawning ground. The downstream section during the post-spawn period was intended to simulate a nearfield habitat downstream of salmon carcass decay. The middle section, during active-spawning was evidenced by lower biofilm abundance, increased sediment infiltration into the bed, decreased levels of intergravel DO and a lower OMR. The post-spawn period in the downstream section was characterized by higher biofilm abundance, lower sediment infiltration, increased levels of intergravel DO and a higher OMR.

2.4.1 Streambed Benthic Response

Initial low pre-spawn biofilm abundance can be attributed to the preparatory channel cleaning and suggests young immature biofilms. Chlorophyll *a*, AFDM and inorganic sediment patterns in upstream biofilms, therefore, reflect natural biofilm growth in the absence of salmon. During the active-spawn period, salmon disturbed the streambed by creating redds to the extent that areas of disturbance were visibly reduced in biofilm abundance. In contrast, biofilms growing in the absence of salmon (upstream section) were noticeably thicker and uniformly spread out throughout the reach (*Pers. Obs.*; Figure 2.12). This pattern is supported by chlorophyll *a* and AFDM measurements in the upstream section. The standing stock of surface chlorophyll *a* and AFDM was significantly reduced in the middle section during the active-spawning period (Figure 2.5 & 2.6-Surface). This decrease in biofilm biomass during active spawning has been previously reported and is usually attributed to the physical reworking of gravels by salmon (e.g. Moore and Schindler, 2008). Other major biofilm disturbance forces like light and hydrologic conditions (Peterson, 1996) were kept constant across sections, indicating that the reduction in biofilm abundance is primarily due to salmon redd construction.

Post-spawn downstream chlorophyll *a* and AFDM increases suggest a salmon carcass decay influence on biofilm growth (Figure 2.5 & 2.6-Surface). Over the same time period, biofilms in the middle section did not experience the same level of growth. Com-

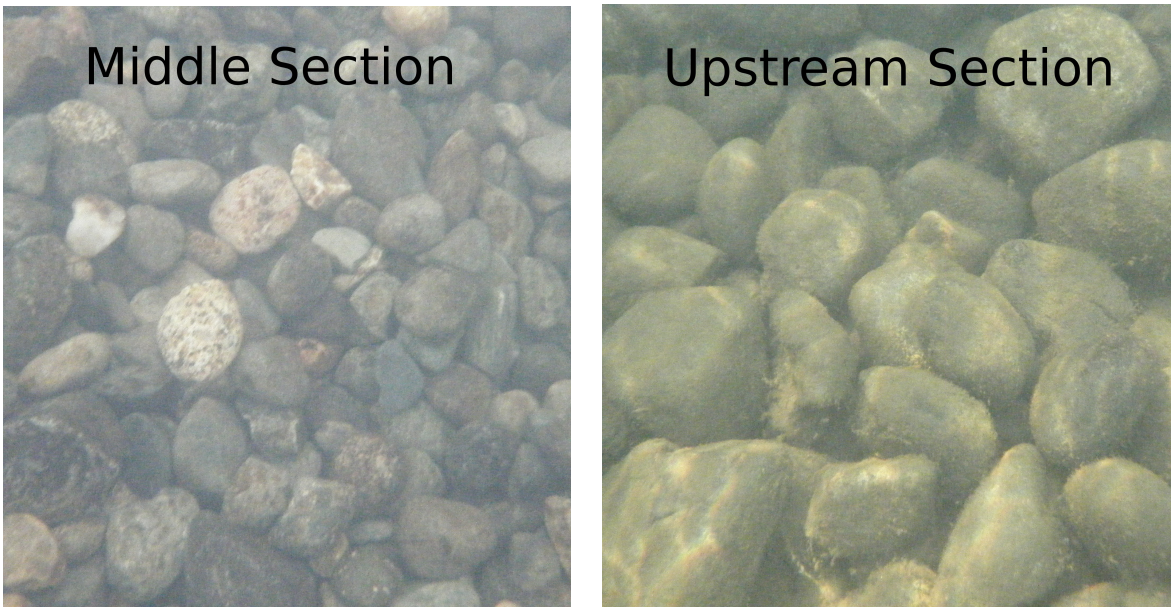

Figure 2.12: Visual difference in the biofilm abundance present on gravels in the upstream and middle sections. Gravels in the middle section are visibly reduced in biofilms and sediment while gravels in the upstream section, grown in the absence of salmon, are noticeably thicker with biofilm and sediment. Both images were taken on the same date during the active-spawn period.

parisons with spatial and temporal controls suggest that the increase is not simply due to natural biofilm succession and growth (Vannote et al., 1980; Peterson, 1996, Figure 2.5-Surface). Rather differences in post-spawn middle and downstream biofilm growth can be explained by the position of decaying salmon. During the post-spawn period, in contrast to the middle section, the downstream section had a large upstream source of decaying salmon (Figure 2.4). Biofilms in the middle section, recovered from the salmon disturbance primarily via natural succession while the downstream section had the added nutrient pulse of decaying salmon. Hunt and Perry (1999) found that a strong correlation between AFDM and chlorophyll *a* levels suggests an in-stream nutrient source. Thus, Figure 2.13b provides further evidence that decaying upstream salmon are the source of the biofilm abundance increase.

An alternative explanation may be that downstream biofilms experienced an "immigration effect" where resuspended biofilm from the middle section acted as a nutrient

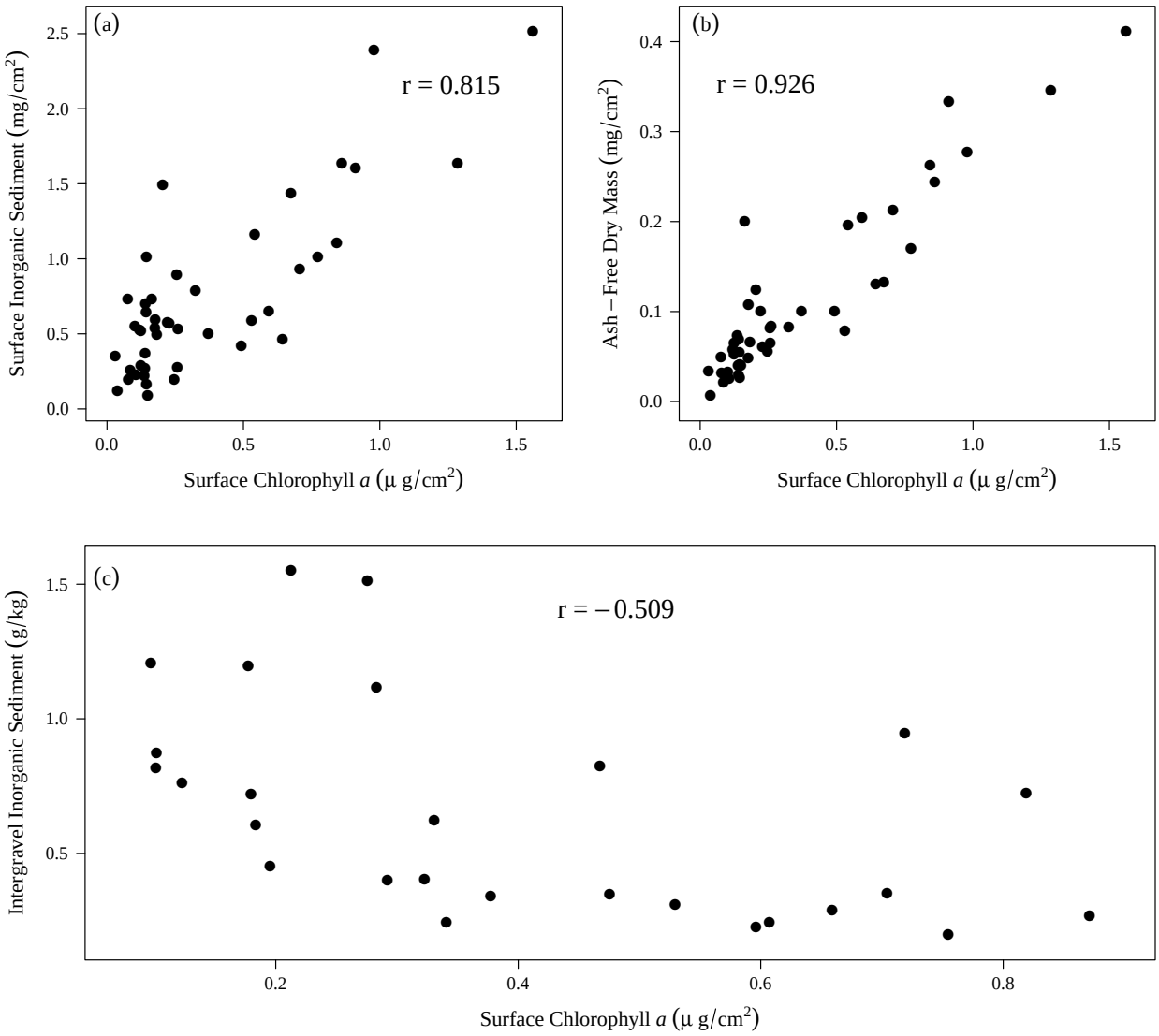

Figure 2.13: Relationship between inorganic sediment and biofilms indicators. (a) Relationship between biofilm growth (chlorophyll *a*) and inorganic sediment trapped by the biofilm from gravels sampled in the downstream surface section. (b) Strong correlation between two measures of biofilm growth suggest an in-stream nutrient source (Hunt and Perry, 1999). (c) Chlorophyll *a* versus intergravel inorganic sediment collected from infiltration bags that has deposited into the streambed. Decreased surface biofilm abundance results in larger masses of fine sediment infiltrating into the gravelbed (Bag depth=0.30-m). All p-values <0.05.

source for the downstream biofilm growth (Peterson, 1996). This explanation, however, is not supported by either the timing of salmon redd building activity (Figure 2.4) or isotope data (See Section 2.4.2). Moreover, the ultimate source of the nutrients would still be salmon. Instead the difference in post-spawn biofilms sampled from the downstream and middle sections is attributed to MDNs.

It should be noted that chlorophyll *a* values are very similar to values reported in the literature. In particular, the timing and magnitude of chlorophyll *a* increases and decreases reported by Moore and Schindler (2008) is very similar to Figure 2.5-Surface. Post-spawn increases in chlorophyll *a* are also very comparable to values reported by Cak et al. (2008). Both of these studies were conducted in coastal environments suggesting a common response across a range of habitats.

2.4.2 Stable Isotope Analysis

Table 2.9: Summary of literature stable isotope values and C:N of salmon flesh and values from this study. All values are from adult salmon flesh.

Study	Type of Study	Species	δ^{13}C (‰)	δ^{15}N (‰)	C:N Ratios
HFC Study	**Interior**	**sockeye**	**-20.6**	**10.8**	**3.9**
McConnachie and Petticrew (2006)	Interior	sockeye	-21.2	10.9	3.41
Johnston et al. (1997)	Interior	sockeye	-20.6	10.6	–
Claeson et al. (2006)	Flume	chinook	-17.1	15.9	–
Bilby et al. (1996)	Coastal	coho	-17.9	14.2	–
Chaloner et al. (2002)	Coastal	pink	-20.6	12.7	–
Kline et al. (1993)	Coastal	sockeye	-19.6	12.3	–
Hilderbrand et al. (1996)	Coastal	chinook	-20.1	11.2	–

Salmon carcass tissue sampled from the HFC was within the range of other reported values both for sockeye and other species of salmon (Table 2.9). Salmon δ^{15}N was in the lower end of the range of the examined values although comparable to studies conducted at similar latitudes and distances from the ocean (Johnston et al., 1997; McConnachie and Petticrew, 2006). Convergence to the salmon isotopic signature can usually be attributed to utilization of that nutrient source for growth and development and suggests processing

of MDNs (Kline et al., 1990) although this is sometimes problematic with δ^{13}C (See below).

2.4.2.1 Biofilms

Middle and downstream biofilm δ^{15}N isotope ratios increased compared to the upstream control over the course of the salmon spawning event (Figure 2.8). Low source δ^{15}N, as shown in Table 2.9, may account for observed low biofilm δ^{15}N values (3.1–5.6‰) as reported values are generally higher (e.g. Bilby et al., 1996, δ^{15}N = 7.1‰). Isotopic values from biofilms collected from the HFC were highest in the post-spawn period suggesting progressively greater MDN enrichment (Kline et al. 1990; Figure 2.8). These results are typical of other studies that have found increases in δ^{15}N values and indicate salmon nutrient sequestration by biofilms. The increase in δ^{15}N also corresponds to increases in biofilm abundance (Figure 2.5 & 2.6-Surface) suggesting that the abundance increase is due to a MDN source (Bilby et al., 1996). The increase of δ^{15}N is statistically significant indicating that the rapid growth of biofilm following the active-spawn decrease is primarily driven by marine-derived nitrogen.

The patterns of biofilm δ^{13}C isotopic enrichment are not typical of previous reports that use δ^{13}C as a tracer for MDNs (e.g. Kline et al., 1990; Bilby et al., 1996). The least negative (i.e. higher) δ^{13}C value in this study (-24.0‰) corresponded to the active spawn period in the upstream section where there were few salmon present (Figure 2.4). Interpretation of biofilm δ^{13}C values, therefore, is confounded by several processes that prevents establishing a clear relationship between MDNs and δ^{13}C ratios.

Firstly, variable discrimination of isotopes by biofilms at different stages of development tends to confound isotopic ratios (Kline et al., 1990; Peterson and Fry, 1987). Older, thicker, more mature biofilms, for example, tend to have higher (less negative) δ^{13}C isotopic ratios because of well developed internal carbon cycling processes (Staal et al., 2007). Carbon isotopic ratios were higher in the upstream section both in the active and post-spawn period. Biofilms growing in that area remained undisturbed by salmon and as a

result were visibly thicker and more mature than disturbed biofilms growing in the middle and downstream sections. Furthermore, elevated δ^{13}C levels in mature biofilms may have been exacerbated by relatively low δ^{13}C values of salmon flesh (Table 2.9) which may have been masked by internal cycling processes.

Second, typically in studies that use the prevalence of marine isotopes to infer a salmon nutrient source, the degree of δ^{13}C fractionation is usually assumed to be small. This assumption, however, may not be warranted. Some fractionation usually occurs in the uptake of C by algal-dominated biofilms, resulting in elevated δ^{13}C biofilm values (Peterson and Fry, 1987; Bilby et al., 1996; Schindler et al., 1997). Surface chlorophyll *a* values (Figure 2.5) suggest algal-mediated isotopic fractionation may have occurred (Peterson and Fry, 1987) and may further explain variation in δ^{13}C that does not correspond to the presence of salmon.

Thirdly, there is considerable natural variability associated with δ^{13}C values (France, 1995; Johnston et al., 1997). Three pseudoreplicates per day and replications within each sample period may have not been sufficient to characterized patterns of δ^{13}C enrichment through natural variability. This variability is in contrast to δ^{15}N values (Figure 2.14) and potentially limits the usefulness of δ^{13}C as a nutrient tracer in this type of study design.

Lastly, the patterns of δ^{13}C may suggest alternative sources of carbon for biofilms. In particular, nutrient leaching from upstream macrophytes may have contributed to an isotopic signature that did not directly represent salmon influence. Isotopic carbon decreased during the post-spawn period. The decrease coupled with the rapid biofilm growth during the same period suggest that biofilms were not limited by a carbon source and may have been using other sources of carbon.

2.4.2.2 Infiltration Bags

Isotopic ratios of infiltrated sediment follow similar patterns in terms of δ^{15}N during the active spawn period. During the post-spawn period, however, there was no difference

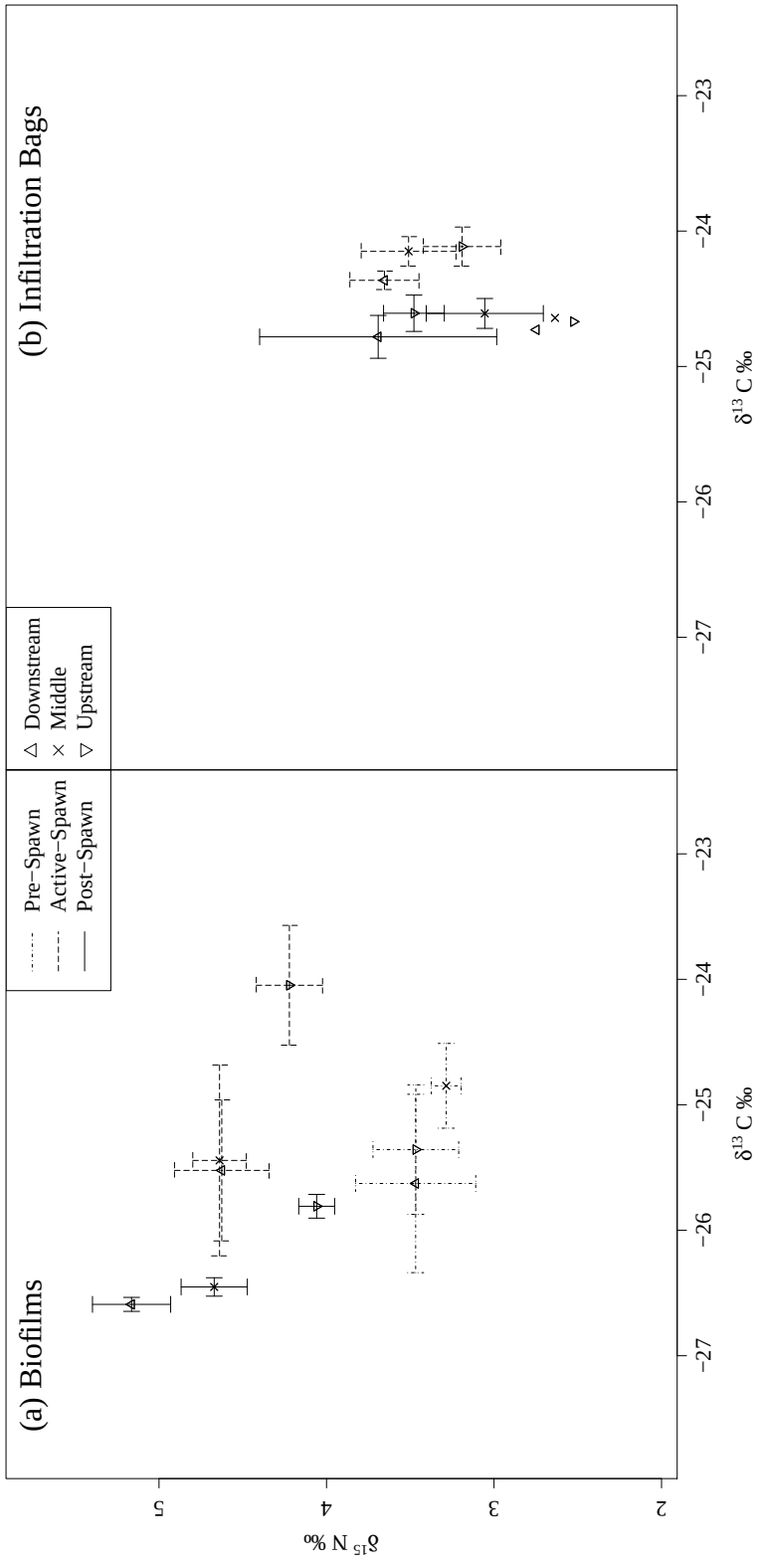

Figure 2.14: Dual plots of biofilm (a) and infiltration bag (b) isotopic ratios. Section is represented using different symbols while the sampling period representative by different error bars line styles. Means $\pm$ 1 SEM.

when comparing downstream and middle section δ^{15}N values with upstream δ^{15}N values. This pattern corresponds to the re-establishment of the biofilm layer and suggests that surface biofilms are sequestering most of the MDNs being released into the system by decaying salmon. Infiltrated values of δ^{13}C , while statistically significant, may not be biologically significant as the range of values are not sufficient to imply incorporation of salmon organic matter (Figure 2.8). Active-spawn isotope values may be from salmon waste products (McIntyre et al., 2008) although these products should have been absent from the upstream section.

2.4.3 Infiltration and Trapping

Sediment is often ignored in discussions of biofilm and salmon. This omission is usually attributed to the fact that the relevant studies use a fisheries rather than a geomorphological approach (Kondolf, 2000; But see McConnachie and Petticrew, 2006). The results of this experiment indicate that sediment plays a crucial role in two ecological processes outlined below, highlighting the importance of abiotic factors on benthic stability and on the salmon disturbance regime. Furthermore, the inorganic sediment component of biofilm analysis is rarely reported alongside measures like chlorophyll *a* and AFDM. These findings highlight important insights that can be gained from using this information.

A persistently high level of suspended inorganic sediment in the upstream section (Figure 2.10) can be attributed to the structure of the HFC. Most spawning channels in British Columbia are built with a 2% grade. The HFC, however, was built with a 1% grade and is annually cleaned to prevent sediment build-up (See section 2.2.1.1). A similar pattern of high background inorganic sediment was also found in the HFC in 2007 (Hulsman and Wubben, 2008) supporting the assertion that background sediment levels are indicative of regular channel conditions.

Biofilm inorganic sediment levels generally followed the same temporal and spatial patterns as biofilm abundance (Figure 2.7). During the active-spawn period, surface grav-

els were significantly cleaned of sediment in the middle and downstream section. Similar to the decrease in biofilm abundance, this decrease is attributed to physical reworking of gravel by salmon and implies salmon-mediated addition of inorganic sediment to the water column. One potential concern is that the biofilm communities may have been diatom-dominated causing an overestimation in the inorganic sediment values (Conover, 1966). Microscopic visualization of biofilms, however, suggest that this is not the case although this is only a qualitative assessment (See Chapter 3).

Salmon-mediated inorganic sediment resuspension to the water column is supported by suspended sediment values (Figure 2.10). Inorganic sediment load increased in the water column during the active-spawn period in both the middle and downstream section presumably via redd construction. Surface gravel reaccumulation of sediment then occurred during the post-spawn period when salmon activity decreased evidenced by inorganic sediment values in biofilms (Figure 2.7-Surface). Increased sedimentation has been demonstrated to reduce biofilm growth by shading the algal component (Power, 1990) and inhibit stream restoration (Moerke and Lamberti, 2003). Sediment shading, however, appears to have not influenced biofilms growing in the HFC. In most cases, greater sediment deposition accompanied increases in AFDM and chlorophyll *a* (Figure 2.13a-b). Instead of shading, the increase in inorganic sediment trapped by biofilms suggests a mechanism by which MDNs are delivered to biofilms.

Redd construction resuspends a broad range of particle sizes of sediment some of which deposits onto the streambed (Rex and Petticrew, 2006). This resuspended sediment, which includes gravel bed aggregated particles, has been demonstrated to form in-stream flocculated particles when exposed to MDNs (Rex, 2009). Coarsening of suspended sediment suggest the presence of either flocculated particles or aggregates in the water column (Figure 2.11). Increases in downstream surface inorganic sediment are closely related to increases in biofilm abundance (Figure 2.13a) which suggests two mechanisms operating in concert.

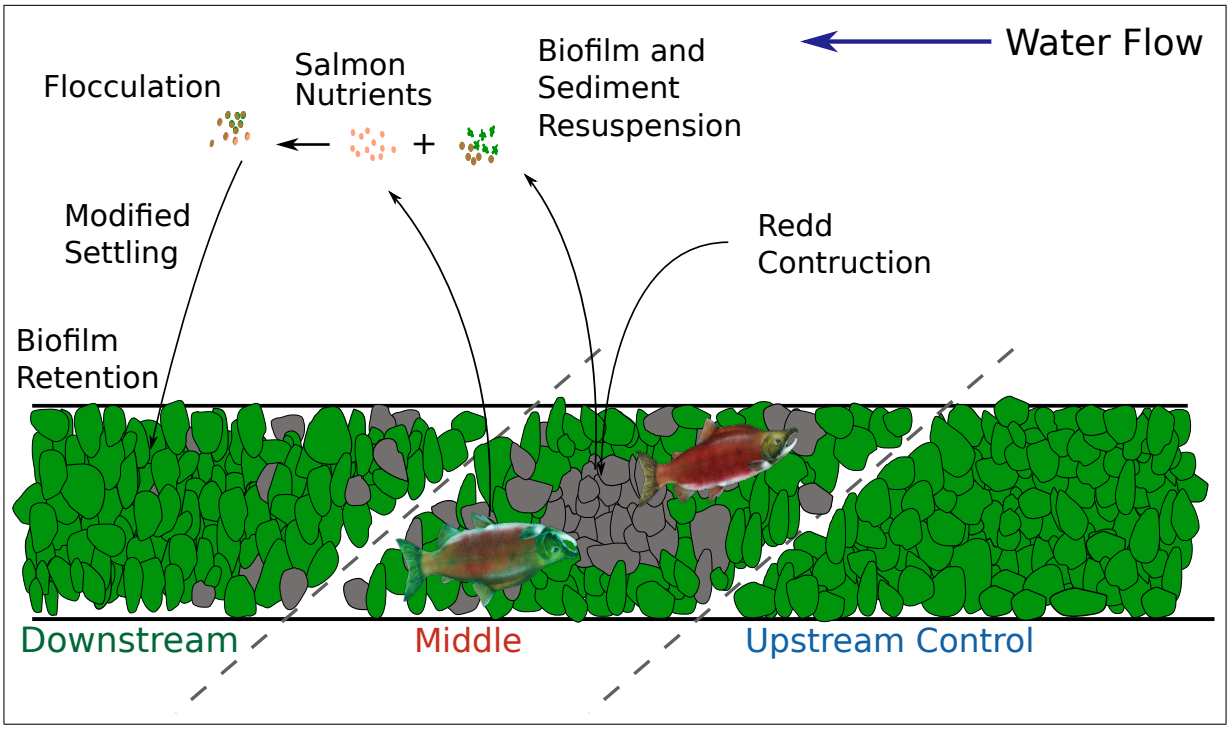

Figure 2.15: Schematic of a potential mechanism of MDN enrichment of the downstream section via the flocculation feedback loop (Rex, 2009).

Firstly, it seem clear that flocs are forming in the middle section and settling over a small spatial scale in the downstream section (Figure 2.15). Secondly, increased biofilm growth may be facilitating particle trapping via EPS and fine sediment trapping interactions (Romaní and Sabater, 2000). The biofilm abundance increase is likely being driven by MDNs (Section 2.4.2) which suggest a positive feedback loop whereby biofilm biomass increase allows for greater subsequent nutrient enrichment. Rather than shading biofilms, flocs and particle aggregates appear to the source of inorganic sediment and salmon nutrients, aiding in streambed nutrient delivery. Biofilm abundance increases and δ^{15}N values suggest these are then rapidly processed by downstream biofilms.

The presence of flocs during the post-spawn period is also supported by increases in the OMR of suspended sediment (Figure 2.10). Since the ISCOs were placed in the rear of each section, each value is an indication of the suspended sediment being delivered to the next section. For example, a high middle section value during the post-spawn

period is the material being delivered to the downstream section in that same period. This increase provides evidence that flocs are forming as flocs tend to have a higher organic matter content. The timing of this increase when salmon are actively decaying in the water column suggests that the organic matter enrichment is due to salmon. More organic material present in the water column provide ideal conditions for flocculation (Droppo et al., 1997).

This floc settling mechanism is also supported by an increase in the size of particles deposited on the streambed in the post-spawn downstream section (Figure 2.9) as well as the size of particles present in the water column during active-spawn (Figure 2.11). Increased settling rates of MDN particles from the middle section as a result of flocculation would explain the nearfield biofilm response (Droppo et al., 1997, Figure 2.15). Additionally, this result provides further evidence in support of the flocculation feedback loop proposed by Rex and Petticrew (2008).

This work also identifies a previously unreported effect of salmon redd construction. Rapid growth of biofilms after redd construction appears to aid surface sequestration of MDNs. A significant negative relationship between intergravel sediment as measured by infiltration bags and biofilm growth indicates that greater biofilm abundance in the post-spawn period decreases infiltration of sediment into the streambed (Figure 2.13c). Similarly, low biofilm abundance during redd construction (Figure 2.5 & 2.6-Surface) is accompanied by higher sediment infiltration (Figure 2.13c). This suggests intergravel storage of MDNs during the active-spawn periods when biofilm abundance is low and streambed surface storage when biofilm abundance is high. A growing surface biofilm layer may facilitate rapid MDN uptake as photosynthetic activity is diminished deeper in the streambed (Gibert and Deharveng, 2002; Also see sub-surface panels in Figures 2.5, 2.6 & 2.7). This idea corresponds well with a subsurface increase in bacterial abundance as seen by Rex and Petticrew (2008) in an artificial flume in response to MDNs and suggests that bacteria are processing sediment stored during active-spawn (Petticrew and Albers,

2010).

Surface processing of MDNs is indirectly supported by post-spawn intergravel DO patterns (Table 2.8). Processing of MDNs by heterotrophically-dominated microbial communities (Yoder et al., 2006) would likely deplete oxygen levels (Horn and Hempel, 1997) and account for post-spawn decreases in intergravel DO. Reduced light penetration into the intergravel would have favoured heterotrophic microbes leading to the depletion of the DO pool (Bastviken et al., 2004). Conversely, during the post-spawn period in the downstream section, an increase in intergravel DO suggests a decrease in intergravel biological activity by decreased sediment infiltration into the bed (Figure 2.13c) and increased surface biofilm abundance (Figure 2.5). This drop in DO may have also been facilitated by nest digging of salmon. Salmon can construct redds 10-35 cm deep (Schindler et al., 2003) in the streambed which is approximately the piezometer depth that intergravel DO was sample from. The digging may have facilitated organic matter delivery further depleting DO levels.

Interpretation of the intergravel DO is complicated by patterns seen during the active-spawn period. Sections experiencing approximately the same level of salmon activity (Middle and Downstream) exhibit opposite patterns of intergravel DO (Table 2.8). From a management perspective, these differences are not biologically significant as they are still within the acceptable DO range for proper egg development (Cope and Macdonald, 1996). The difference, however, is persistence across replicates and is statistically significant (Table 2.7). For a brief period, during the active-spawn period in the middle section, the apparatus used to sample piezometer water was also sampling a small portion of surface water. This discrepancy, however, likely lead to higher levels of DO, not lower. This difference during the active-spawn period remains unexplained.

As mentioned above, high biofilm abundance during the post-spawn period was accompanied by low sediment infiltration rates (Figure 2.13c). During the post-spawn period in the downstream section biofilms likely trapped MDN laden flocs, preventing them

from penetrating further into the bed. The EPS of both biofilms and flocs are known to interact suggesting a possible mechanism for this trapping ability of biofilms (Sutherland, 2001). The biofilm layer at the surface thus can utilize nutrients and photosynthesize more readily allowing for quick uptake of MDNs. Furthermore, this biofilm layer acts as a barrier to subsurface storage. These results have implications for salmon as habitat regulators as the temporal and spatial conditions of spawning and die-off may dictate the degree in which MDNs are incorporated.

2.4.4 Implications

This pattern of biofilm abundance shifts in response to salmon spawning and die-off is indicative of the high benthic resiliency to the salmon disturbance regime as biofilm abundance rebounded from low active-spawn levels. Additionally this highlights the important role that biofilms play in trapping sediment. As a basal portion of benthic foodwebs, biofilms often structure benthic resilience and resistance ultimately determining overall system stability (DeAngelis et al., 1990; Stoodley et al., 2002). The interaction and thus the importance, however, between sediment and biofilms with respect to intergravel and streambed MDN storage patterns is also highlighted by these results.

Well oxygenated intergravel DO is crucial for proper egg development and is one of the primary goals of spawning channels (Toews and Brownlee, 1981). The establishment of the biofilm layer and the corresponding increase in DO suggest that the downstream areas in the post-spawn period are crucial both for nutrient retention and viable egg development. Active-spawn DO levels are well below saturated levels and sediment levels are also likely too high for proper egg development. In an example, however, of the resiliency of the total system, DO levels rebounded and sediment infiltration decreased, re-establishing saturated DO which are ideal conditions for egg development. Primary remineralization of MDNs has also been demonstrated to occur mostly via autochthonous production supporting the link between adult to juvenile sockeye via increased basal

component abundance (Kline et al., 1993). Thus nutrient retention at the surface provides both a spatially stable nutrient source for optimal incubation conditions and future salmon.

Chapter 3

Benthic Biofilm Composition in a Salmon Spawning Stream: A Microscopic Approach to Biofilm Characterization

3.1 Introduction

Improved experimental methods have reformed our perception of microorganisms beyond the single culture models into more complex biofilm frameworks. That is, there is now a recognition that most microorganisms reside within some biofilm matrix (Sutherland, 2001). With a greater knowledge of biofilm structure and function, it is now realized that biofilms represent complex microbial communities that display the same characteristics and properties as any other ecosystem (Battin et al., 2007).

Biofilms can be broadly defined as the accumulation of single-celled organisms (both prokaryotic and eukaryotic) and extracellular polymeric substances (EPS) (Costerton et al., 1995). In the context of aquatic systems and this study, biofilms are specifically defined as the autotrophic and heterotrophic microbial communities embedded in EPS that grow in the benthic zone. The morphology and amount of EPS associated with a biofilm growth is important for the nutrient trapping ability of biofilms (Neu and Lawrence, 1997). Thus changes in EPS structure and growth due to a MDN pulse may be important for the assimilation of suspended nutrients into biofilms. Inorganic sediment contributes to biofilm structure as a stabilizer. EPS binds sediment and cellular material together and this interaction between EPS and sediment confers a stability to the biofilm (Wolfaardt et al., 1999) enabling greater development.

The function of a biofilm matrix is intimately tied to its structure. Stoodley et al. (1999) found that biofilms grown under nutrient rich conditions developed significantly

different morphologies than biofilms grown under nutrient poor conditions. Specifically, biofilms in nutrient rich conditions respond with greater biomass, increased biofilm thickness, increased algal/bacterial ratio and greater SA coverage allowing for greater nutrient uptake (Stoodley et al., 1999; Sabater et al., 2002). This pattern, however, has not been tested in an MDN context. The presence of MDNs, particularly during the post-spawn period, would suggest elevated nutrient concentrations (e.g Tiegs et al., 2009) and a similar structure change as demonstrated by Stoodley et al. (1999).

In addition, biofilm morphologies adapted to changing nutrient conditions by developing 'streamers' and 'cell clusters'. Battin et al. (2003b) demonstrated the functional significance of this morphological change. Battin et al. (2003b) showed that streamers grown due to enriched nutrient conditions altered the hydrodynamic environment near the streambed interface. This change in microhydrodynamic conditions resulted in increased settling velocity of suspended organic particles. This suggests a positive feedback loop in biofilms whereby nutrient rich water set the conditions necessary for the optimal utilization of nutrients by biofilms.

3.1.1 Confocal Laser Scanning Microscopy

Since the first usage of confocal laser scanning microscopy (CLSM) for the analysis of river biofilms (Lawrence et al., 1991), it has become both a powerful and standard tool in biofilm research. The use of CLSM has significantly expanded our knowledge of biofilm structure (Neu et al., 2005; Battin et al., 2003a), composition (Lawrence et al., 1998; Neu et al., 2005), functioning (Neu et al., 2001) and development (Neu and Lawrence, 1997; Mohamed et al., 1998). Use of CLSM in biofilm research has become so pervasive that in many respects it now the *de facto* tool with regards to process-based biofilm research.

Conducting biofilm research using CLSM is advantageous over other microscopic methods (scanning electron or environmental-scanning electron microscopes) when the research questions being asked are biologically process-based. Numerous unique com-

pounds exist within the biofilm matrix, each contributing to the process and functioning of biofilms (Wingender et al., 1999). Traditional analytical methods require separation, purification and identification of unique biofilm components to infer function and address process-based questions (Neu et al., 2005). With CLSM, paired with fluorescent markers, biofilm components can be viewed in a fully hydrated and natural state. Samples can be non-destructively sampled by growing biofilms on a portable and removable medium (e.g. polycarbonate slides). Samples can be taken directly from a field site with little to no preservation. Other methods of visualizing biofilms do not always preserve the natural composition of the sample as sample preservation often disturbs these parameters (Neu and Lawrence, 2004). The need for sample preparation is also greatly reduced as compared to other microscopic methods (Lawrence and Neu, 1999).

The need for higher resolution biofilm research in all areas of river aquatic ecology is strong. The ecological importance of the biofilm layer is recognized (Battin et al., 2007) while information on attached bacterial and algal communities (biofilms) is lacking (Manz, 1999; Neu and Lawrence, 2004). Phenomenal progress has been made in terms of our understanding of biofilm and nutrient dynamics and much of this progress can be attributed to sophisticated CLSM techniques (See Battin et al., 2003a; Pauling and Wagner-Döbler, 2006). This progress, however, has not translated across all related fields and CLSM remains primarily a specialized microbiological tool rather than an broad ecological one.

3.1.2 Objective

Table 1.2 lists several important biofilm-based studies of salmon habitat and spawning. Although, ash-free dry mass (AFDM) and chlorophyll *a* remain important coarse measures of biofilm mass and composition, finer details of biofilm structure and function require higher resolution tools. CLSM characterization has been highlighted as a promising technique to aid research in nutrient dynamics within aquatic systems (Cross et al., 2005).

The Horsefly River spawning channel (HFC) and the controlled loading of salmon into the HFC served as an experimental environment to a) examine changes in biofilm composition in response to salmon carcass decay and b) test the feasibility of CLSM analysis in a remote field setting.

The goal of this research was to image two functional components of biofilms (bacteria and algae) growing in the HFC after a salmon spawning event. This was done via multiple parameter imaging to determine changes in abundance patterns of these components in response to salmon carcass decay which is hypothesized to affect biofilm community composition. Three research questions were addressed to accomplish this goal.

3.1.3 Research Questions

3.1.3.1 Question One

How do the bacterial and algal components of biofilms change in response to varying nutrient concentrations from marine derived nutrients (MDNs)? Rotting salmon release nutrients that are utilized by the benthic community and in particular biofilms (Johnston et al., 2004).

3.1.3.2 Question Two

What is the impact of these compositional changes in algae and bacteria on temporal and spatial patterns of MDN storage by biofilms?

3.1.3.3 Question Three

How do common destructive measurements of biofilm composition and biomass (chlorophyll *a* and AFDM) compare to CLSM measurements of these same parameters? Previous salmon-biofilm studies have not made use of CLSM to characterize the biofilm response to MDNs (Table 1.2). This study will relate these two types of measurements and explore

sources of variation.

3.1.4 Secondary Objectives

A secondary objective of this work was to establish a protocol for future users of the CLSM at University of Northern British Columbia (UNBC) to adapt to their own uses especially in a remote field setting.

3.2 Methods

3.2.1 Site Characteristics

Biofilms were sampled from the HFC in Horsefly, British Columbia. A more detailed description of site characteristics can be found in section 2.2. Briefly, experimental sections of the HFC (n=3) were characterized by two different densities of salmon spawners and a spatial control with no salmon (Figure 2.2). The upstream section served as a spatial control with little salmon influence while the middle and downstream sections received inputs of salmon organic matter.

3.2.2 Biofilm Growth

For the analysis of river biofilms, removable slides were attached to ceramic tiles that were placed directly on the streambed. The slides were made of polycarbonate strips, a suitable growth substrate for biofilms (Lawrence and Neu, 1999). For each sampling date, five slides (one stain control & four samples) were collected from each experimental section, immediately immersed in river water and placed in a sealed container. Samples were transported for three hours in a refrigeration unit and stained and viewed on the same day.

Five ceramic tiles were placed in each section of the HFC on September 25^{th}, 2009 and

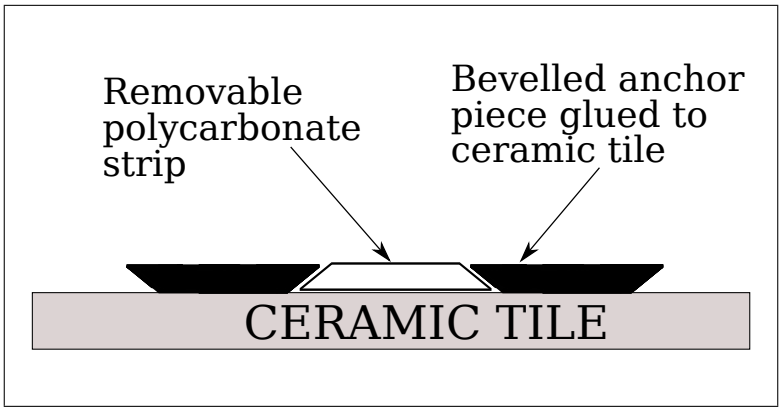

Figure 3.1: Schematic of the slide mounting system used in the HFC. Polycarbonate strips have been previously identified as suitable growth substrates for CLSM analysis of biofilms (Lawrence et al., 1998).

sampled weekly until October 27^{th}, 2009. Tiles were placed in the thalweg of the HFC. Because of reduced salmon activity, the slides were not physically disturbed during this period and any growth on the polycarbonate strips can be viewed can cumulative biofilm growth over the post-spawn period.

3.2.2.1 Confocal Specifications

An Olympus Fluoview 1000 with a multiline argon gas laser (458, 488 & 515 nm) and two independent Helium-Neon gas lasers (543 & 633 nm) mounted with an inverted Olympus microscope was used to image biofilms. Observations of biofilms grown on polycarbonate strips were made on a 60x water immersible lens, 1.2 numerical aperture. Scanning was done sequentially to minimize photobleaching (Pawley, 1995). Optimum settings for each sample period were determined so that all microscope parameters were kept constant with a minimum number of saturated pixels (i.e. white value of 255) to ensure intercomparability between samples. Five fields of view from each sample were taken to account for biofilm spatial variability (Neu et al., 2005). These five fields of view were averaged to form a composite sample.

3.2.2.2 Stains and Fluorescent Markers

All staining protocol was derived chiefly from Lawrence et al. (1998), Strathmann et al. (2002) and Neu and Lawrence (2004). Bacteria nucleic acids were stained with the nucleic acid stain, SYTO9 (ex=488 nm, em=522/32 nm; Molecular Probes, Inc.). For each staining period 1 µl of SYTO 9 and 1 ml of distilled water were mixed to form a stock staining solution. Two to three drops of this stock solution were added to a fresh biofilm sample under subdued light and incubated at room temperature for 15 minutes (Neu and Lawrence, 2004). A washing step is not necessary with SYTO9 (Lawrence et al., 1998).

Autofluorescence in the far red channel was used as a measure of algal abundance. Lawrence et al. (1998) found that algal cells fluorescence brightly at a excitation wavelength of 647 nm and a detection of emission of 680/32 nm. The Olympus Fluoview technical specification required a slight modification to the laser parameters used to detect algal autofluorescence which was deemed acceptable (ex=633, em=647nm; *John Lawrence pers. comm.*). Algal abundance was corrected for cyanobacteria autofluorescent interference by subtracting any autofluorescence in the red channel (ex=543nm, em=578nm) from algal autofluorescence in the far red channel (ex=633, em=647nm).

3.2.2.3 Image Analysis

Image analysis was conducted by the same person using the same computer monitor using the same brightness and contrast settings. This consistent approach to image analysis ensures that any potential biases or errors are kept constant throughout the experiment (Neu, 2000). Image J (Rasband and ImageJ, 2009) was used to convert the Olympus file formats to 24-bit RGB stacked TIFF files with a semi-automated macros. These files were sufficiently high in contrast to justify any loss in dynamic range by the conversion to a 24-bit TIFF file. Images collected from each field of view were 512 pixels by 512 pixels.

The TIFF files were then loaded into Scion Image for subsequent image analysis. Images from each CLSM channel were thresholded to define the boundary of the objects in

the image. A semi-automated macros was then used to make the image binary, dilate and erode the image and then count the number of white pixels in that particular channel. Dilation and erosion help better define the borders of the object while eliminating noise from the signal for a more accurate white pixel count. This white pixel count was used as the percent coverage for either the algal and bacterial components of the biofilm for a field of view.

3.2.3 Nutrient Delivery Estimates from Salmon Carcass Decay

Salmon decay products were modelled using estimated loss rates from the Takla River (Johnston et al., 2004) and daily fish counts from the Horsefly Channel in 2009. The amount of nutrients released into the water column and available for biofilm sequestration was estimated using the same equations outlined by Johnston et al. (2004). The model outlined below, therefore, generates an estimated value for the mass of nutrients lost from salmon carcasses and delivered to the water column on a daily basis.

The total new nutrient contribution of all salmon dying on a given day, t, is estimated by:

$$Nut(t) = D(t) \times \%\ Nutrient\ (Carbon\ or\ Nitrogen) \tag{3.1}$$

where $D(t)$ is the number of dead salmon that died on day t and $\%\ Nutrient$ is the average percent composition of salmon flesh for either carbon and nitrogen. The total amount of salmon nutrients present in the stream on day t is given by:

$$Ini(t) = Nut(t) + Rem(t) \tag{3.2}$$

where $Nut(t)$ is the new arrival of nutrients on day t (equation 3.1) and the $Rem(t)$ is the total amount of nutrients remaining in the system on day t from all previous days. $Rem(t)$

accounts for the mass and nutrient loss of carcasses from previous days and is given by:

$$Rem(t) = Ini(t) - Loss(t) \tag{3.3}$$

where $Ini(t)$ is given by equation 3.2. Thus the daily mass loss of salmon (for both carbon and nitrogen; $Loss(t)$) to the water column on day t is given by:

$$Ini(t) \times (1 - e^{k}) \tag{3.4}$$

where $Ini(t)$ is calculated according to equations 3.1–3.3 and k is the constant decay rate of sockeye salmon given by Johnston et al. (2004) from Takla River. The decay rate from Johnston et al. (2004) for carbon was -0.0360 kg/day and -0.0460 kg/day for nitrogen. The downstream section of the HFC received nutrient contributions from salmon decaying in both the middle and downstream sections (See Figure 2.2). Therefore, the nutrient load received by the downstream section from decaying salmon was the sum of the middle and downstream values generated by equations 3.1–3.5.

3.2.3.1 Carcass Removal

Over the course of the experiment, some salmon were removed from the HFC system either via dead pitching or black bear (*Ursus americanus*) consumption. Dead pitching was done to reduce the number of decaying salmon down to a more natural representation of a spawning stream. If there was a net loss of fish on a given day (i.e. $D(t) - D(t-1)$ was <0), the salmon nutrients removed on that day from the stream was estimated by using the average nutrient content of salmon from the previous day and multiplying that number by the total number of fish removed from the system. Total nutrient removal is therefore estimated by:

$$Total\ nutrient\ removal = \left(\frac{Ini(t-1)}{D(t-1)}\right) * Fish\ Removed(t) \tag{3.5}$$

Dead salmon ($D(t)$) were enumerated visually by two individuals on a daily basis. In instances where the counts differed greatly (>10 salmon), the salmon were recounted until a similar count was reached. The mean nutrient content of salmon was estimated by randomly sampling four freshly dead salmon from the study reach on October 5^{th}, 2009. A small portion of somatic tissue was removed from the fish and immediately frozen. Samples were then freeze dried and shipped to an external laboratory (Pacific Centre for Isotopic and Geochemical Research, University of British Columbia). Using equations 3.1–3.5, a carbon to nitrogen molar ratio was estimated for the sampling period.

3.2.4 Assumptions

Several assumptions are made in the accounting of dead pitched and bear removed salmon carcasses. The first is that carcasses were removed randomly, such that all levels of decay have an equal chance of removal. Evidence of bear removal was seen throughout the channel not just the banks. Moreover, bears removed fish from the HFC with evidently little preference for any particular decay stage of fish. Salmon in an advanced state of decay were consumed by bears just as readily as fresh carcasses. Dead pitching was done on one day (September 26^{th}, 2009) and all dead fish were removed from the system. This indicates that fish were randomly removed from the channel and this method of accounting for salmon nutrient content is appropriate.

A second key assumption is that the calculated loss rate for each nutrient does not vary between the Takla River (Johnston et al., 2004) and the Horsefly River. Water temperature during the period of salmon decay would likely be the biggest difference between sample areas. To assess the differences, average temperature during the decay period from both streams were compared. The mean temperature in the middle section of the HFC during the post spawn period was 9.63°C (SEM=0.116). The mean temperature for Takla River was taken from Figure 3 in Johnston et al. (2004) and was calculated using Engauge Digitizer (Mitchell, 2010). The mean value of all streams for every year during the post-spawn

period was calculated to give a single value. This mean temperature was 9.88°C (SEM= 0.121). These are comparable river temperatures and this small difference indicates that using the Takla River loss rate is acceptable to use in the Horsefly system.

A final assumption is that biofilms sampled for CLSM analysis are utilizing MDNs. Biofilms used for microscopic analysis were not specific analyzed for δ^{15}N and δ^{13}C isotopes. Results presented in Chapter 2, however, indicate that biofilm growth in the HFC was driven by MDNs. Thus the assumption for this chapter is that biofilms growing on polycarbonate slides follow a similar pattern of MDN incorporation.

3.2.5 Data Analysis

3.2.5.1 Manipulations

Biofilms were sampled on four occasions while nutrient release by salmon was estimated on a daily basis. To examine the relationship between salmon carcass decay and biofilm composition, the average daily nutrient release over the biofilm sampling interval was used as a comparison against biofilm measures. For example, if biofilms were sampled on October 5^{th} and October 15^{th}, the average daily nutrient release from salmon carcasses in between those dates was used as a measure of salmon nutrient contribution to the October 15^{th} biofilm sampling date. For the downstream comparison, the decay products from both the downstream and middle sections were used as biofilms in that section had nutrient contributions from both sections.

3.2.5.2 Statistical Analysis

Mean differences in biofilm composition between each section was compared statistically using a two-way ANOVA. Three separate ANOVAs were conducted using the percent coverage of bacteria, algae and the algal:bacterial ratio as response variables. Sampling week and experimental section were used as factors. Pearson's correlation test was used

to relate estimated salmon decay products to biofilm composition. Given that salmon were only present in the middle and downstream sections, upstream composition values were excluded from this particular nutrient analysis.

An additional objective of this research was to compare CLSM to the method outlined in section 2.2.4.2. Results of that spectrophotometric method were compared to algae percent coverage measured with CLSM using Pearson's correlation test. A maximum of two days separated spectrophotometric sampling and CLSM sampling. Sampling occurred approximately every week and it is these samples which are compared with Pearson's correlation test. In addition to spectrophotometrically measured algae, ash-free dry mass (AFDM) was measured to determine the total biological material present on gravels. AFDM was compared to the total percent coverage as an additional test. All statistical analysis were conducted using R 2.11.1 (2010). All graphics were created using R 2.11.1 (2010) with the *memisc* (Elff, 2010), *ggplot2*, (Wickham, 2009) and *lattice* (Sarkar, 2008) packages.

3.3 Results

It was the initial goal of this biofilm research to collect samples for CLSM from the entire salmon disturbance regime[1]. Salmon activity, however, prevented sampling of biofilms throughout the active spawn period. Salmon redd construction moved sufficient gravel to completely bury most of the clay tiles. Therefore, the clay tiles were redeployed after salmon activity had subsided and samples were only collected in the post-spawn period. All subsequent analysis of biofilm composition change applies only to the post-spawn period of the salmon disturbance regime. This limits the inference of this particular portion of the study to the response of biofilm to in-stream carcass decay of salmon.

Designing studies that incorporate the entire salmon disturbance regime is a more accurate representation of the ecological role of salmon (See Chapter 2; Janetski et al., 2009).

[1]See section 1.1 for a complete description of the salmon disturbance regime

Four sampling dates constitutes relatively weak statistical power and some care should be taken in over-extrapolating these results. Nevertheless, many biofilm studies are conducted in the absence of any statistical and quantitative analyses (But see Lawrence et al., 1998).

3.3.1 Site Characteristics

Site characteristics are identical to those presented in section 2.2.1.2. Figure 3.2 has been truncated from Figure 2.4 to reflect the CLSM sampling period. Conditions in the HFC remained relatively stable over the course of the sampling period. The HFC experienced a slight increase in discharge at the beginning of the sampling period. This increase was due to a build-up of salmon carcasses at a downstream fence causing water to back-up, subsequently raising the water level at the staff gauge. The Horsefly region experienced relatively few high intensity storms or rain events during the sampling period. The small events shown in Figure 3.2 were not likely important in terms of biofilm composition.

3.3.2 Microscope Use and Image Analysis

For each sampling period, the CLSM was run under optimal conditions using freshly stained samples with a single operator. The microscope lens was cleaned in between samples using the manufacturer's lens cleaner and 90% ethanol. Figure 3.3 is a screenshot of the image analysis process used to quantitatively assess CLSM images.

3.3.3 Biofilm Component Patterns

Biofilm components were assessed based on the levels of coverage demonstrated by a particular parameter. The total number of pixels occupied by all objects in the corresponding channel (algae or bacteria) was divided by the total number of pixels in the field of view (512×512) to determine a percent coverage. Figure 3.4 shows the patterns of composition

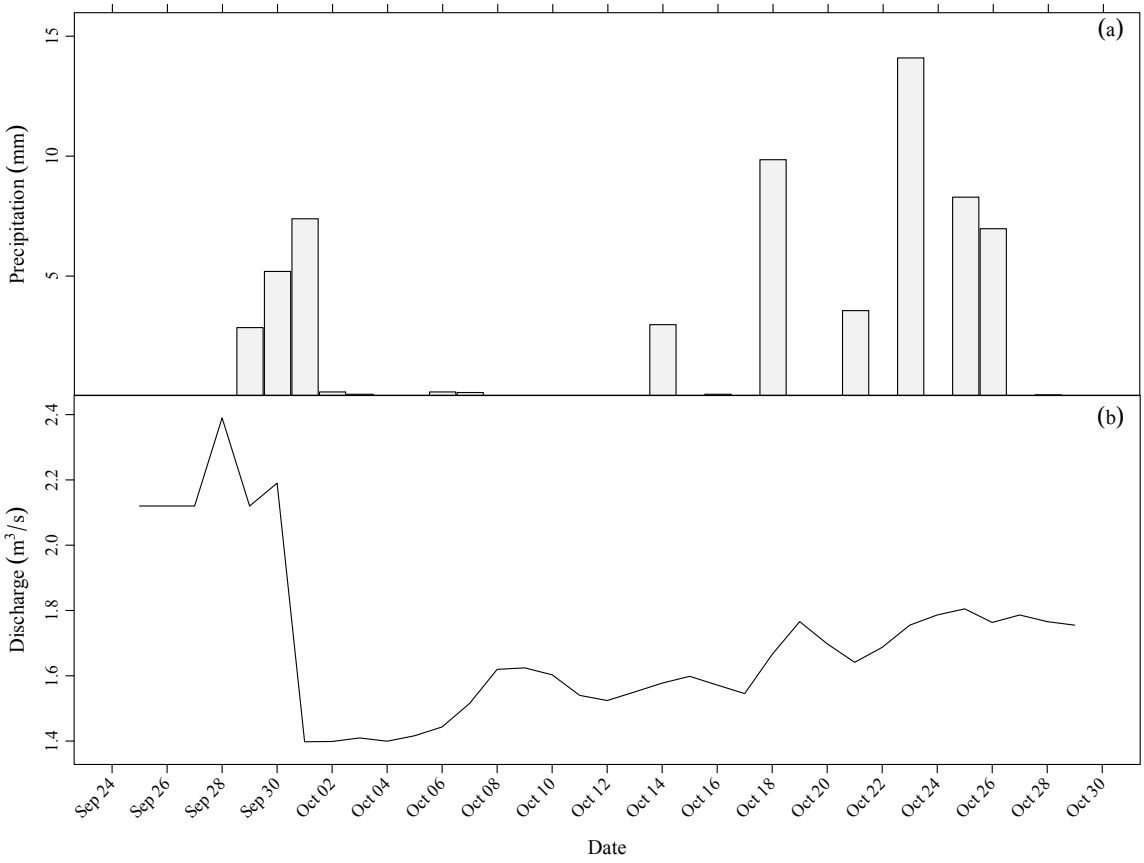

Figure 3.2: Site characteristics for the HFC over the CLSM sampling period. See section 2.2 for description of rainfall and discharge collection methods.

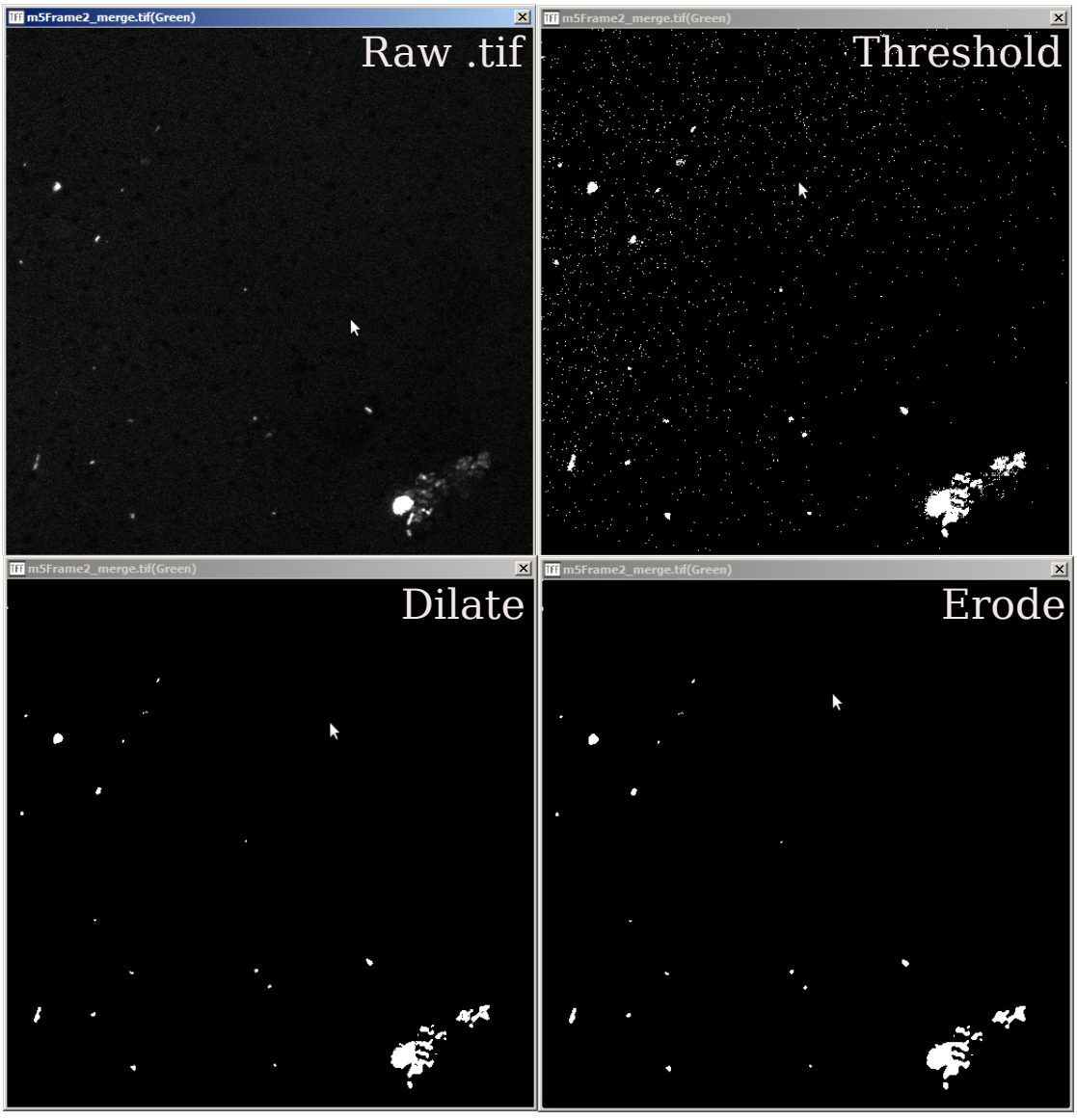

Figure 3.3: A single channel example of the image analysis process of thresholding, dilation, and eroding to determine white pixel counts. Eroding and dilation are important steps to remove noise of the CLSM image.

change over four weeks of post-spawn salmon decay.

Biofilm components were assessed statistically using a two-way ANOVA. No significant differences between sections and sampling week (with one exception) for any response variable was demonstrated over the post-spawn period (all $p<0.05$) although statistical power was weak due to low degrees of freedom and ultimately a small sample size. The lone exception in this analysis was a significant effect of time on the percent coverage of algae ($F_{1,6}=0.945$, $p=0.034$) although the effect was not significant across section. A qualitative assessment of Figure 3.4 suggests a general increase in total percent coverage of biofilm. Slides collected on October 21^{th} had a greater proportion of algae in the biofilm from samples collected in the middle section. On the subsequent sample day (October 27^{th}), there is a noticeable drop in algae coverage in the middle section but an increase in downstream bacterial coverage. This result, however, is purely qualitative.

3.3.4 Salmon Nutrient Composition

The number of salmon present (live and dead) in the HFC during the sampling period is presented in Figure 3.5. The salmon counts in Figure 3.5 were values used for $D(t)$ from equation 3.1. A subsample of fish were analyzed for elemental carbon and nitrogen (See section 2.2.3). The average carbon composition of sockeye salmon in the channel was 47.81% (SD=1.06; n=4) of the total mass. The average nitrogen composition of salmon in the channel was 14.51% (SD=0.40; n=4) of the total mass. These values were used, respectively for nitrogen and carbon, as $\%\ Nutrient$ in equation 3.1.

3.3.4.1 Nutrient Influence

Figure 3.6 represents daily salmon decay products as calculated by equations 3.1–3.5. Salmon were primarily in a die-off phase when CLSM sampling begun (Figure 3.5). There was only one significant correlation between salmon decay products and biofilm composition. This significant relationship was in the middle section between the C:N ratio and

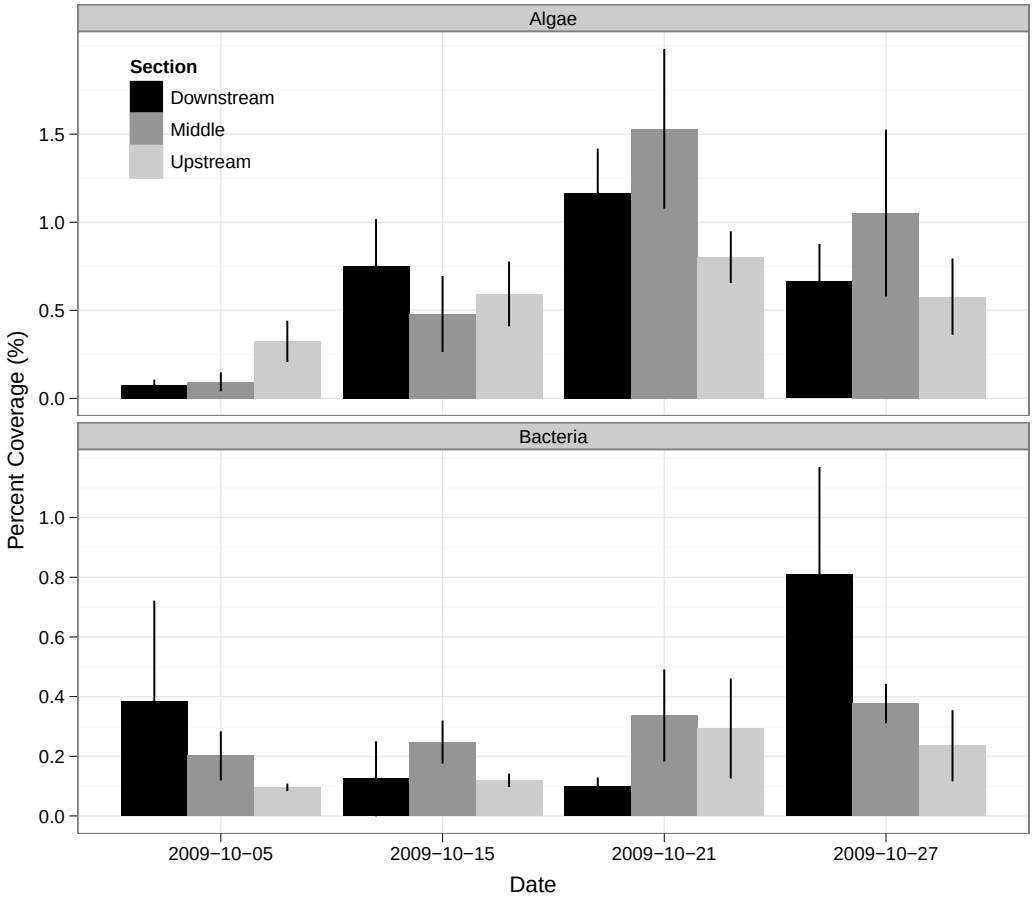

Figure 3.4: Percent coverage of biofilm components on polycarbonate strips as measured by CLSM. Components are arranged into panels according to the channel wavelength fluorescence. Error bars indicate SEM which is based on replicate sample strips from separate tiles in each section. Each strip was sub-sampled with the CLSM five times (i.e. Five fields of view) to account for spatial variability with the biofilm. These five fields of view were averaged to give a single value for each tile. Strips from five tiles were sampled for each sampling date.

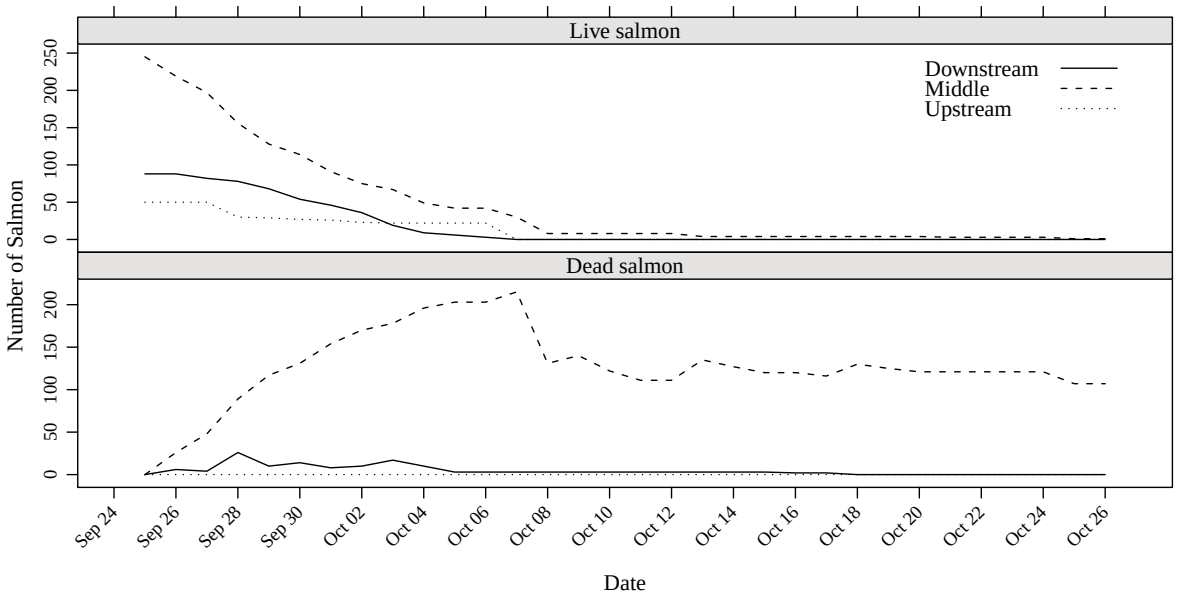

Figure 3.5: The number of salmon present, both live and dead, in the HFC during the confocal study period.

the bacterial coverage. In addition, this was a strong positive correlation. In contrast, the algal component of the growing biofilms were not significantly related to either the downstream or middle C:N ratio (Algae; Figure 3.7) nor were biofilms in the downstream section related to salmon decay products.

3.3.5 Method Comparison

In addition to biofilm composition patterns in the post-spawn period, this research also assessed differences in a) spectrophotometrically measured algae abundance and CLSM measured algae via autofluorescence and b) AFDM and total biofilm coverage as measured by CLSM. The method for spectrophotometrically measured algae abundance and AFDM is outlined in section 2.2.4.2. Neither coarse measure of biofilm (Chlorophyll *a* or AFDM) was significantly correlated to either algal or total percent coverage (Figure 3.8).

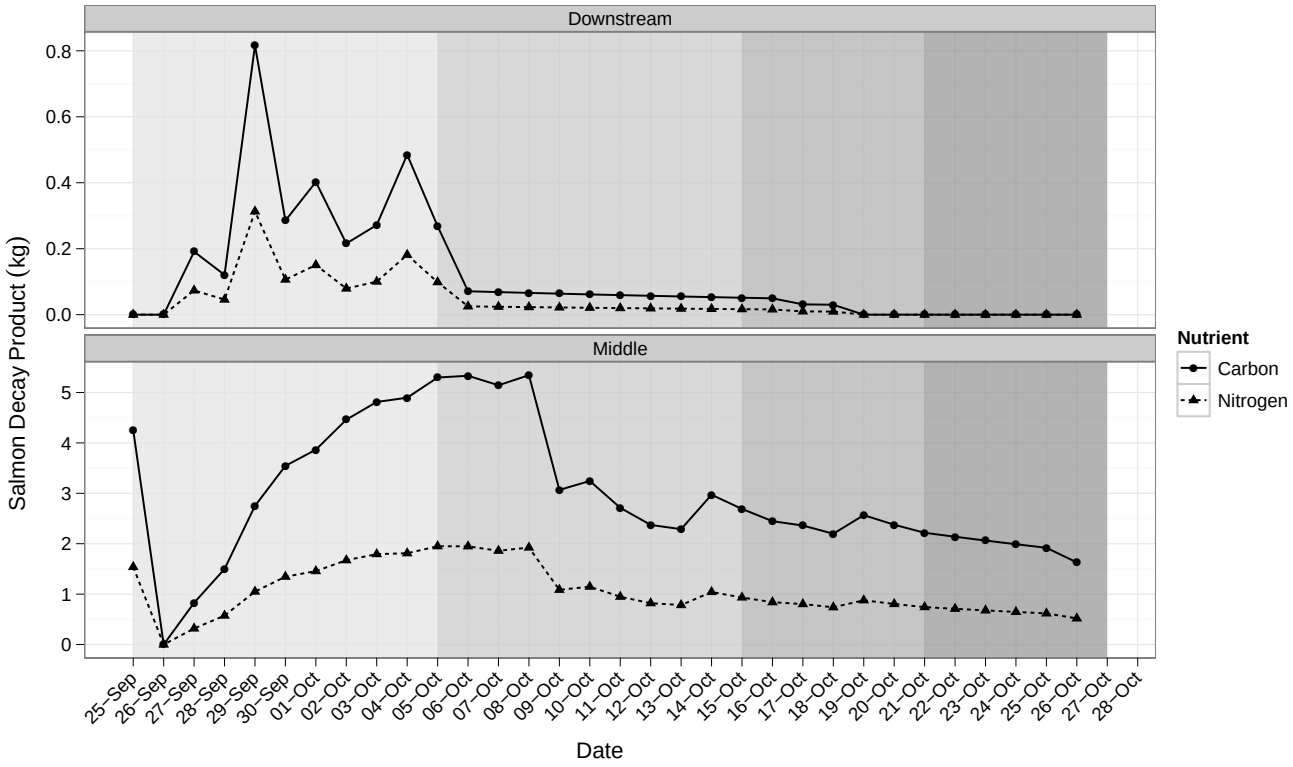

Figure 3.6: Salmon decay products as calculated from equations 3.1 - 3.5 and used for comparison in Figure 3.7. Shaded portions of this figure represent the period between CLSM sampling dates (Sampling dates also indicated in Figure 3.4).

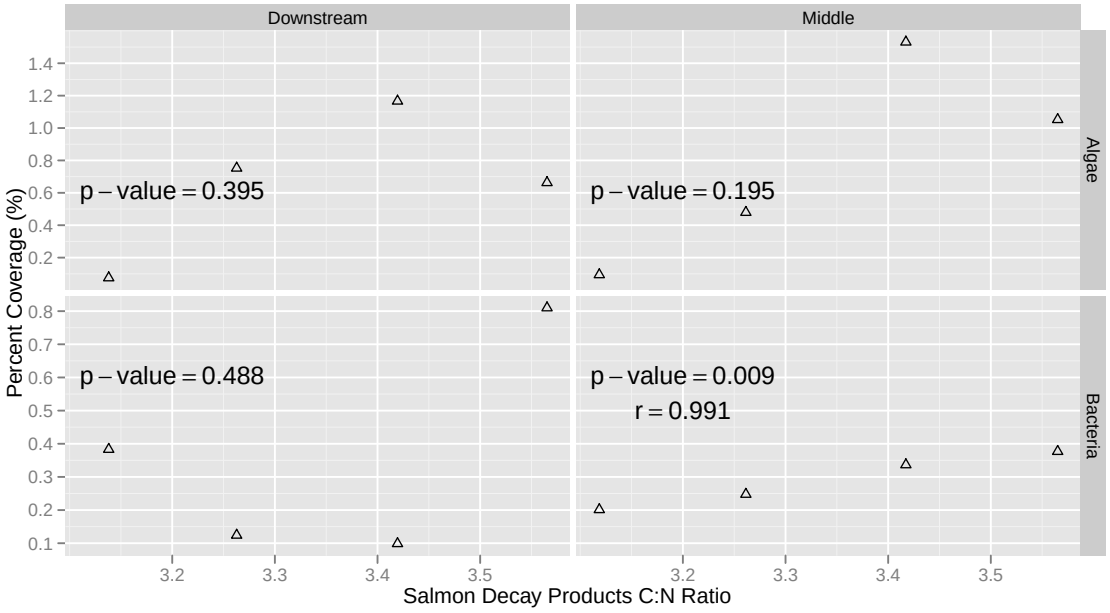

Figure 3.7: Relationship between salmon decay products C:N ratio and the percent coverage of biofilm components. Downstream decay product were calculated as the sum of the middle and downstream values. Annotations refer to results of a Pearson's Product Moment.

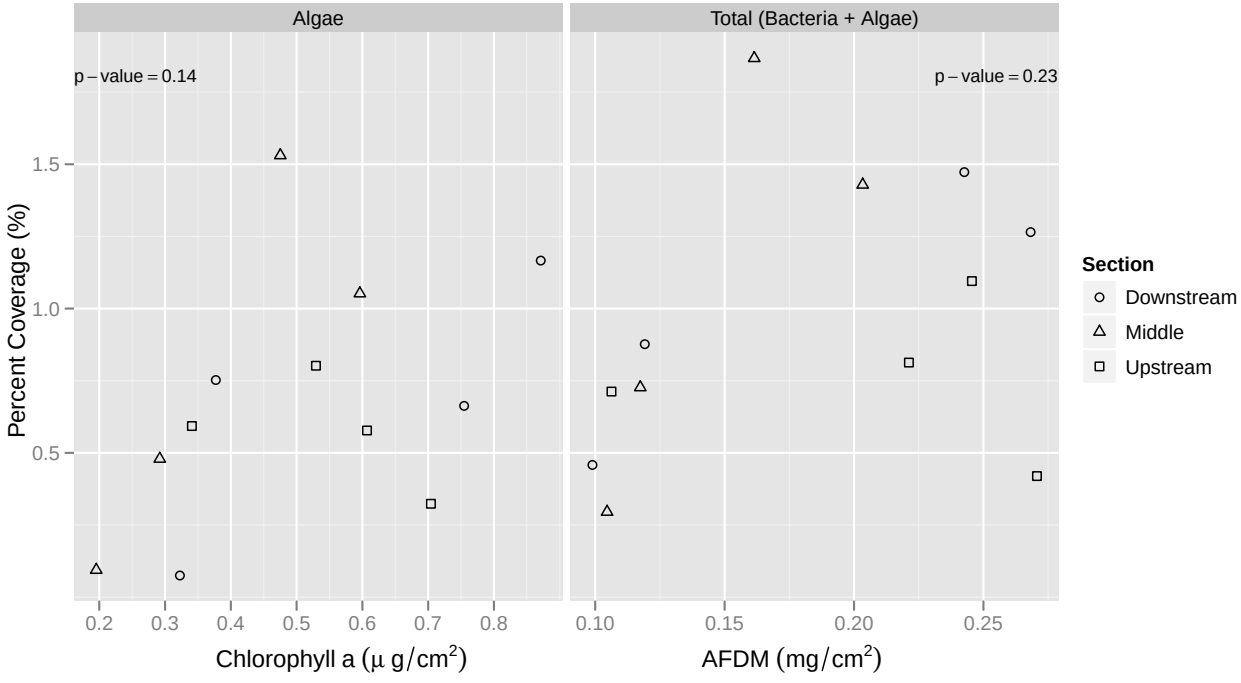

Figure 3.8: The left panel illustrated the relationship between spectrophotometrically measured chlorophyll *a* and algal coverage measured by CLSM. The right panel is the relationship between total percent coverage and AFDM

3.3.6 UNBC Confocal

The results presented here were also used to establish a protocol that will assist future users at UNBC in integrating ecologically based studies with CLSM methods. The primary difficulty encountered during this study was the distance from the sampling site to the location of the CLSM ($\approx$ 275-km). Additionally, the software required to undertake the CLSM image analysis had to be developed from scratch. Software routines and semi-automated macros were established to assist the analysis of CLSM aiding future users (See Appendix A). Future users will benefit from these software routines in addition to the protocol developed.

3.4 Discussion

Biofilms thrive in any system that has sufficient nutrient resources (Costerton et al., 1995). Elevated nutrient levels are a characteristic in spawning streams during the post-spawning period of the salmon spawning cycle (Naiman et al., 2002). Thus, biofilm growth occurs in salmon streams in the post-spawn after the fish carcasses begin to decay and release nutrients (e.g. Chaloner et al., 2007; Chapter 2). Chapter 2 demonstrated an increase in biofilm abundance after spawning and δ^{15}N values indicated that this response is likely due to salmon. The results presented here suggest that the community shift from an autotrophic (algae) dominated biofilm to a heterotrophic (bacterial) one has a functional significance for stream ecosystems opposite to pattern seen by Droppo et al. (2007). This shift would help explain the long-term biological storage of MDNs.

3.4.1 Biofilm Component Patterns

A study by Yoder et al. (2006) is the only other known published attempt to characterize microbial biofilm communities at the functional component level. Yoder et al. (2006) found increases in algae followed by increases in bacteria of biofilms during the post-

spawn period. The elevated microbial response in the presence of salmon nutrients as identified by Yoder et al. (2006) is in contrast to the results presented in Figure 3.4. Yoder et al. (2006) proposed that an initial increase in bacterial usage of MDNs. This initial colonization by bacteria provides subsequent algal colonization sites leading to a predominately autotrophic biofilm (Azam et al., 1983). The initial bacterial population bloom facilitate algal colonization by taking advantage of carbon, nitrogen and organic nutrient release from decaying carcasses (Yoder et al., 2006).

Results presented in Figure 3.4 do not demonstrate the same initial bacteria bloom. This difference may be accounted for by several reasons. The pattern seen in Figure 3.4 may simply be natural variation. An alternative explanation is that because Yoder et al. (2006) sampled on a monthly basis, in contrast to weekly sampling basis of this study, Figure 3.4 may represent a finer resolution picture of biofilm component changes.

In the context of this study, however, observed changes in biofilm composition may also reflect an important MDN sequestration pathway. Romaní and Sabater (2000) report that benthic bacterial populations use excreted algal decay product as a nutritive source. As an algal bloom begins to decline, algal exudates become a nutrient within biofilms for proximate (within the biofilm) bacteria growth (Kaplan and Bott, 1989). This pattern manifests itself as a bacterial increase (October 27^{th}) after a decrease in algae abundance (After October 21^{th}). Figure 3.4 suggests this type of pattern whereby algal exudates, themselves a product of MDN enrichment, provide microbial heterotrophic MDN storage potential. This storage potential is supported by findings that autotrophically dominated biofilm communities in aquatic systems are subject to high herbivory and decomposition and thus accumulate less carbon (Cebrián and McClelland, 1998).

Should this pattern by replicated in future studies, it may have implications for winter biofilm storage of MDNs as microbial heterotrophically dominated communities are less limited by photosynthetic activity and thus may retain MDNs over a smaller spatial scale as this study saw a downstream bacterial increases over 20-m. This result, however,

would need to be replicated with a greater sample size and further into the post-spawn period to confirm this hypothesis.

3.4.2 Nutrient Influence

The observed changes in biofilm composition presented in the above section (3.4.1) are likely being driven by changing nutrient concentrations (Lawrence et al., 1998). Mohamed et al. (1998) found variable nutrient conditions, driven by pulp mill effluent, caused changes in biofilm community composition. Neu et al. (2005) state that nutrients directly affect "the nutritive value of the biofilm for grazers and play a role in water quality", linking changes in absorbed MDNs in biofilms to foodweb level impacts. For example, Wipfli et al. (1999) found that this increase in biofilm quality resulted in higher salmonid densities. Thus, the ecosystem level impacts of biofilm enrichment appear to transfer directly back up to salmon (See Figure 1.1). Mechanisms for this enrichment, however, are still not well understood. I related the C:N ratio of salmon decay products to biofilm components to determine how that ratio affects biofilm component coverage.

Biofilm growth followed the same general development pattern in response to nutrient levels outlined by Neu and Lawrence (1997), Romaní and Sabater (2000) & Neu et al. (2005). Neu et al. (2005) found that a nitrogen addition to biofilms sampled from the South Saskatchewan River resulted in a decrease in bacterial numbers. Bacterial coverage from slides sampled from the HFC (middle section) responded to higher C:N ratio with increased coverage (Figure 3.7) suggesting a similar response as a lower C:N ratios results in less bacterial coverage. This is consistent with the general aquatic science paradigm that organic carbon limits bacterial productivity (Mohamed et al., 1998).

Relating biofilms sampled from the downstream section is complicated by the source of nutrients. Biofilms in the downstream section were subjected to upstream nutrient loads from decaying salmon in the middle section as well as decaying salmon from the downstream section (Figure 3.5). This spatial variation may explain why the relation-

ship breaks down in the downstream section. A lack of a relationship in the downstream section may indicate that advective losses were occurring in the middle section due to biofilm growth. In addition, because there were no salmon present in the downstream section late in post-spawn period, estimated nutrient contributions from decaying carcasses in the downstream section were zero, skewing already established biofilm cultures against nutrient values that would predict low biofilm coverage.

Algal coverage was not related to the presence of salmon in either section suggesting other influences on algal productivity (Figure 3.7). Neu et al. (2005) suggest that algal abundance is more limited than bacteria by specific nutrient ratios. This, however, was not a factor explicitly tested. It was not practical or desirable to isolate a single nutrient from the MDN source. An alternative explanation is that algal abundance is limited by solar radiation and that during the late fall sampling period, this was the dominating factor driving algal productivity. This lack of increasing algal abundance is in contrast to the results that are presented in Chapter 2 and are likely a consequence of the biofilm developmental stage being examined (France, 1995).

Future studies should consider measuring the nutrient ratios present in the water and of the biofilm being viewed under CLSM. If nutrients dictate biofilm composition, as Neu et al. (2005) indicate, nutrient ratios may provide useful measurements of the nutrient processing capabilities of biofilms. Identification of biofilms, beyond the level of algae and bacteria, to specific taxa (*sensu* Peterson and Grimm, 1992) will also likely be an important future research focus. Peterson and Grimm (1992) found that different taxa of algae responded differently to variable nutrient and grazer regimes. Moreover, the successional patterns of algal species after the redd construction disturbance will likely be an important determinant of nutrient processing. This assessment of community composition at the level of taxa will be crucial for future microbiological studies of biofilms in salmon streams.

3.4.3 Method Comparison

A stated goal of utilizing the CLSM was to compare conventional methods of biofilm characterization to more sophisticated CLSM methods. Figure 3.7 is the result of this comparison across all experimental sections. Figure 3.8 illustrates the comparison between a) both microscopically and spectrophotometrically measured algae and b) AFDM, a measure of total biomass, and total biological material, the sum of algae and bacterial percent coverage. Spectrophotometrically measured chlorophyll *a* and AFDM are commonly used measures of biofilm biomass in freshwater systems (Steinman and Lamberti, 1996). Neither comparison was statistically significant. Because of salmon activity, tiles had to be redeployed in the post-spawn period. Thus, biofilms measured spectrophotometrically were at a different developmental stage than biofilm examined microscopically. The difference in developmental stage explains a lack of a clear relationship between these parameters (Figure 3.8). Furthermore, this result provide evidence that different developmental stages causes different biofilm composition which in turn causes different isotope values (Staal et al., 2007) as seen in section 2.4.2. By using live/dead fluorescent probes, Neu and Lawrence (1997) demonstrated that biofilm composition changes with development, although the exact nature of the change is in itself variable.

In terms of CLSM protocol, this result highlights the temporally sensitive nature of sampling comparisons. The timing of sampling has an impact on the composition of samples. There is a clear need to have deployable CLSM slides that can withstand the rigours of the entire salmon disturbance regime. Salmon spawning disturbs the composition of streambed biofilms in an unknown way. Sampling these disturbed biofilms for CLSM would improve our understanding of the recovery of biofilms after the active-spawn period, when the potential for MDN storage is high.

3.5 Conclusions

Battin et al. (2007) noted the absence of a biofilm theoretical framework. Microbiology often still views microorganisms as single-cultures studied in isolation. Battin et al. (2007) proposed that biofilms should exist under the umbrella of landscape ecology. One of the key components of landscape ecology is the need to identify the role of disturbance in ecosystems (Urban et al., 1987). The work presented in this chapter addresses this need. The findings presented here demonstrate biofilm community changes in response to an ecological disturbance (salmon spawning) situated within an ecological framework that explicitly acknowledges the role of sediment and nutrients on biofilm storage of MDNs. Internal biofilm cycling, as evidenced by the increases in bacteria seen after a reduction algal percent coverage (Figure 3.4), identifies a potential mechanism by which MDNs are retained within a biofilm and in the stream rather than flushed immediately downstream. This mechanism has been previously recognized in the biofilm literature (Neu et al., 2005). This is, however, is the first known attempt to apply the same methodological approach to aquatic systems that receive MDN pulses. These results highlight that biofilms have a disproportionate impact on ecosystems in relation to their size and mass.

Chapter 4

Conclusions and Management Implications

4.1 Conclusions

This thesis demonstrates the importance of the salmon disturbance regime on benthic biofilm communities. More generally, this thesis contributes to the broader literature on the ecosystem effects of salmon spawning and die-off. The results presented in Chapter 2 and 3 suggest a biofilm trapping mechanism of nutrients and sediment driven by MDNs. Chapter 3 provided an initial explanation of benthic biofilm composition and storage patterns in response to MDNs. These mechanisms of MDN movement through a lotic ecosystem provide an additional perspective in which to view the watershed level benefits of salmon.

The findings in Chapter 2 support a growing body of literature that MDNs can be delivered and retained over a small downstream scale and that the driving mechanism behind this delivery and retention is flocculation. These results add a biofilm trapping component to this floc delivery process. Moore et al. (2004) demonstrated that the impact of salmon is vastly different depending on their status as a live spawner or decaying carcass. The results presented in Chapter 2 suggest that the significant temporal overlap between these two processes may be the most important determinant of the impact of salmon.

These results also suggest an absence of this biofilm trapping ability during the active-spawn period via a reduced biofilm layer. Increased sediment infiltration into the streambed during the active-spawn disturbance and a subsequent decrease in infiltration during the post-spawn fertilization period supports this trapping ability of biofilms (Chapter 2). This

relationship between biofilm growth and streambed sediment infiltration has not been previously reported.

The significant post-spawn increase of biofilm abundance and isotopic signature 20-m downstream of rotting carcasses further indicates that MDN flushing to downstream rearing lakes is limited by in-stream flocculation processes. This abundance increase is an example of the connection between salmon, a primarily marine organism, and freshwater biofilms (Lamberti et al., 2010). Salmon and biofilm form the linkage point that connects the marine and freshwater ecosystems. This is particularly true for interior Fraser River stocks of salmon and has significant implications for rearing lake productivity.

Fraser River sockeye salmon exhibit four year cyclical patterns involving one high return dominant year followed by a lower return sub-dominant year and two very low return sub-dominant years. The mechanisms behind this cyclical pattern remain unclear (Hume et al., 1996). In sub-dominant years (i.e. low salmon densities), the number of returning adult salmon directly confers a size and survival benefit to the next generation of juvenile salmon. In a dominant year, however, when there is a large number of spawners, the relationship between the number of adults and the next generation of juvenile salmon is not linear (Hyatt et al., 2004). There appears to be a threshold number of returning spawners, above which little benefit is transfered to the next generation of juvenile salmon (Hyatt et al., 2004). This is often vaguely attributed to habitat limitations and carrying capacity.

Results presented in Chapters 2 and 3, however, has identified a link between salmon spawning activity and streambed nutrient storage. At higher densities of salmon spawners, streambed nutrient storage increases the potential for the river to act as a nutrient sink; therefore, fewer nutrients being transported downstream may limit salmon-driven productivity increases in rearing lakes due to high spawning activity. This retardation of nutrient transfer, via mechanisms outlined in this thesis, may result in a reduced MDN input to the rearing lake, diminishing the capacity for a lake productivity boost from

salmon. With the river acting as a nutrient sink at high spawner densities, fewer nutrients would be transfered downstream, limiting the next generation of juvenile salmon productivity. The timing of this nutrient transfer may be limited by river flow conditions and suggests that the spring melt may be important for mobilizing stored nutrients. Thus, MDN enrichment may become particularly important at low escapements as the rearing habitat may still be operating below its carrying capacity. In this situation, MDNs would then have a significant impact.

A recent attempt to characterize the importance of various nutrient sources at the watershed level by Wipfli and Baxter (2010) highlights the magnitude of the contribution that MDNs make to the overall watershed nutrient budget. During the active-spawning period, Wipfli and Baxter (2010) estimate that approximately 50% of a stream's nutritional content is contributed by salmon. Wipfli and Baxter (2010) identify the need to focus "on the specific trophic processes and pathways that limit the productivity of riverine food webs that sustain production of salmon during their freshwater phase". The biofilm abundance increase presented in Chapter 2 presents the basal portion of one these key trophic pathways. The salmon disturbance regime structures the key trophic pathways. Wipfli et al. (2003) demonstrated this MDN mediated trophic pathway translated into faster growth of resident fish. This finding highlights the feedback nature of salmon systems presented in Chapter 1 and helps assess the magnitude of the impact presented in Chapter 2.

This substantial MDN contribution, however, may be an underestimate as Wipfli and Baxter (2010) do not explicitly account for intergravel and sediment storage mechanisms of MDNs. Intergravel and sediment storage of MDNs (via flocculation) are an important part of the nutrient cycle within salmon streams (Chapter 2; McConnachie and Petticrew, 2006; Rex and Petticrew, 2008; Petticrew and Albers, 2010). MDN storage in stream sediments (as flocculated particles) are less likely to be flushed downstream as flocs settle out of the water column faster (Droppo, 2001; Rex and Petticrew, 2008). This storage po-

tential allows for the longer term release of nutrients temporally extending the impact of salmon beyond that proposed by Wipfli and Baxter (2010). Whichever way that MDNs are processed by watersheds, the ecological value of salmon to watersheds is significant (Wipfli and Baxter, 2010).

4.2 Management Implications

Since the early eighties there has been a steady increase in the amount of sockeye returning to the Horsefly River (Figure 4.1). This increase peaked in 2001 with an escapement in excess of 1.5 million (Figure 4.1). At that time, many fisherman throughout the Fraser Basin raised concerns that spawning grounds had become saturated with salmon to the point where it was having a negative impact on overall stock health. The phenomenon was termed over-spawning[1] and was used to advocate for higher recruitment. This view can be summarized in this way (From the House of Commons Standing Committee on Fisheries and Oceans cited in Walters et al., 2004):

> "There's a high correlation between over-escapement and poor return, particularly for sockeye. Every major over-escapement event since 1956 has resulted in a near-collapse in the Skeena, in Rivers Inlet, and in the Fraser River. But our managers go on dumping more and more fish on the spawning grounds."

In 2010, after several years extremely low escapements, the Fraser River experienced the largest sockeye return in nearly a century. Soon after the total size of the Fraser River sockeye run was realized, many media outlets reported on the fear of over-spawning. Several groups, particularly those advocating for higher recruitment, proposed that fish escaping fishery pressure would over crowd spawning streams, experience high pre-spawn mortality and generally be wasted if there were not caught in a fisherman's net. After the high escapement in 2001 a report was commissioned by DFO (Walters et al., 2004) to examine

[1] Also referred to as over-escapement

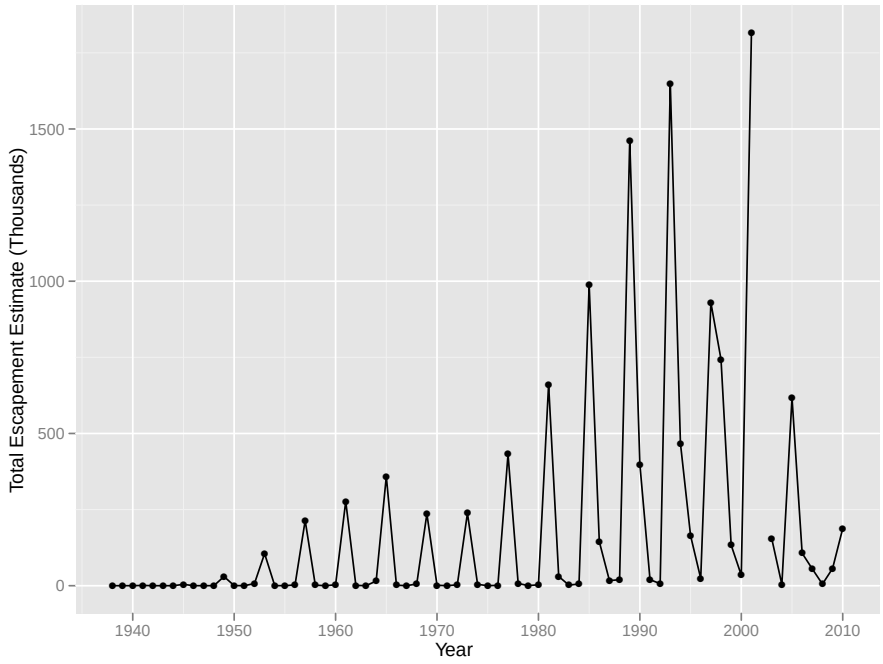

Figure 4.1: Historical Horsefly River Escapement. Stock enhancement via the HFC may have contributed to high stocks in the mid-nineties although other DFO management practices also take place within the Quesnel watershed (DFO, 2010).

if over-spawning causes stock collapses. This report found that "there is no evidence that high spawning runs place stocks at risk of collapse" (pp. 5 Walters et al., 2004).

Given the important cultural and economic legacy of salmon as a resource it is obviously crucial to strike a balance between fishery and conservation values. Traditional as well as commercial fisheries are important components of the British Columbian landscape. The concept of over-spawning, however, attempts to frame the argument in the absence of ecological values and rather portrays decaying salmon as a "waste". The results presented in this thesis demonstrate an increase in the basal portion of the foodweb that is directly due to salmon die-off. This material is recycled through the ecosystem and provides considerable ecological value (Wipfli et al., 2010). Categorizing this ecologically valuable material as "waste" overcompensates in the direction of the fishery and is indicative of an outdated single species management regime.

Bibliography

AGRAWAL, Y. C., AND H. C. POTTSMITH. 2000. Instruments for particle size and settling velocity observations in sediment transport. Marine Geology **168**: 89–114.

APHA. 1995. Standard methods for the examination of water and wastewater, 18th edition. American Public Health Association.

AZAM, F., T. FENCHEL, J. FIELD, J. GRAY, L. MEYER-REIL, AND F. THINGSTAD. 1983. The ecological role of water-column microbes in the sea. Marine Ecology Progress Series. **10**: 257–263.

BASTVIKEN, D., L. PERSSON, G. ODHAM, AND L. TRANVIK. 2004. Degradation of dissolved organic matter in oxic and anoxic lake water. Limnology and Oceanography **49**: 109–116.

BATTIN, T. J. 2000. Hydrodynamics is a major determinant of streambed biofilm activity: From the sediment to the reach scale. Limnology and Oceanography **45**: 1308–1319.

BATTIN, T. J., L. A. KAPLAN, J. D. NEWBOLD, X. H. CHENG, AND C. M. HANSEN. 2003a. Effects of current velocity on the nascent architecture of stream microbial biofilms. Applied and Environmental Microbiology **69**: 5443–5452, doi:10.1128/AEM.69.9.5443-5452.2003.

BATTIN, T. J., L. A. KAPLAN, J. D. NEWBOLD, AND C. M. HANSEN. 2003b. Contributions of microbial biofilms to ecosystem processes in stream mesocosms. Nature **426**: 439–442.

BATTIN, T. J., W. T. SLOAN, S. KJELLEBERG, H. DAIMS, I. M. HEAD, T. P. CURTIS, AND L. EBERL. 2007. Microbial landscapes: New paths to biofilm research. Nature Reviews Microbiology **5**: 76–81.

BIGGS, B. J., N. C. TUCHMAN, R. L. LOWE, AND R. J. STEVENSON. 1999. Resource stress alters hydrological disturbance effects in a stream periphyton community. Oikos **85**: 95–108.

BILBY, R. E., B. R. FRANSEN, AND P. A. BISSON. 1996. Incorporation of nitrogen and carbon from spawning coho salmon into the trophic system of small streams: Evidence from stable isotopes. Canadian Journal of Fisheries and Aquatic Sciences **53**: 164–173.

CAK, A. D., D. T. CHALONER, AND G. A. LAMBERTI. 2008. Effects of spawning salmon on dissolved nutrients and epilithon in coupled stream-estuary systems of southeastern Alaska. Aquatic Sciences **70**: 169–178, doi:10.1007/s00027-008-8090-5.

CEBRIÁN, W., AND V. MCCLELLAND. 1998. The dependence of heterotrophic consumption and C accumulation on autotrophic nutrient content in ecosystems. Ecology Letters **1**: 165–170.

CEDERHOLM, C. J., D. B. HOUSTON, D. L. COLE, AND W. J. SCARLETT. 1989. Fate of coho salmon (*Oncorhynchus kisutch*) carcasses in spawning streams. Canadian Journal of Fisheries and Aquatic Sciences **46**: 1347–1355.

CHALONER, D. T., K. M. MARTIN, M. S. WIPFLI, P. H. OSTROM, AND G. A. LAMBERTI. 2002. Marine carbon and nitrogen in southeastern Alaska stream food webs: Evidence from artificial and natural streams. Canadian Journal of Fisheries and Aquatic Science **59**: 1257–1265.

CHALONER, D. T., G. A. LAMBERTI, R. W. MERRITT, N. L. MITCHELL, P. H. OSTROM, AND M. S. WIPFLI. 2004. Variation in responses to spawning Pacific salmon among three south-eastern Alaska streams. Freshwater Biology **49**: 587–599.

CHALONER, D. T., G. A. LAMBERTI, A. D. CAK, N. L. BLAIR, AND R. T. EDWARDS. 2007. Inter-annual variation in responses of water chemistry and epilithon to Pacific salmon spawners in an Alaskan stream. Freshwater Biology **52**: 478–490.

CLAESON, S. M., J. L. LI, J. E. COMPTON, AND P. A. BISSON. 2006. Response of nutrients, biofilm and benthic insects to salmon carcass addition. Canadian Journal of Fisheries and Aquatic Sciences **63**: 1230–1241.

CONOVER, R. J. 1966. Assimilation of organic matter by zooplankton. Limnology and Oceanography **11**: 338–345.

COPE, R. S., AND J. S. MACDONALD. 1996. Responses of sockeye salmon (*Oncorhynchus nerka*) embryos to intragravel incubation environments in selected streams within the Stuart-Takla watershed, pp. 1–4. *In* Conf. Proc., Land Management Practices Affecting Aquatic Ecosystems. M.K. Brewin and D.N.A. Monita (technical co-ordinators).

COSTERTON, J. W., Z. LEWANDOWSKI, D. E. CALDWELL, D. R. KORBER, AND H. M. LAPPINSCOTT. 1995. Microbial biofilms. Annual Review of Microbiology **49**: 711–745.

CRAWLEY, M. J. 2007. The R book. John Wiley & Sons Inc.

CROSS, W. F., J. P. BENSTEAD, P. C. FROST, AND S. A. THOMAS. 2005. Ecological stoichiometry in freshwater benthic systems: Recent progress and perspectives. Freshwater Biology **50**: 1895–1912.

DEANGELIS, D. L., P. J. MULHOLLAND, J. W. ELWOOD, A. V. PALUMBO, AND A. D. STEINMAN. 1990. Biogeochemical cycling constraints on stream ecosystem recovery. Environmental Management **14**: 685–697.

DRAKE, D. C., R. J. NAIMAN, AND J. M. HELFIELD. 2002. Reconstructing salmon abundance in rivers: An initial dendrochronological evaluation. Ecology **83**: 2971–2977.

DROPPO, I. G. 2001. Rethinking what constitutes suspended sediment. Hydrological Processes **15**: 1551–1564.

DROPPO, I. G., G. G. LEPPARD, D. T. FLANNIGAN, AND S. N. LISS. 1997. The freshwater floc: A functional relationship of water and organic and inorganic floc constituents affecting suspended sediment properties. Water, Air, & Soil Pollution **99**: 43–53.

DROPPO, I. G., N. ROSS, M. SKAFEL, AND S. N. LISS. 2007. Biostabilization of cohesive sediment beds in a freshwater wave-dominated environment. Limnology and Oceanography **52**: 577–589.

ELFF, M. 2010. memisc: Tools for Management of Survey Data, Graphics, Programming, Statistics, and Simulation. `http://CRAN.R-project.org/package=memisc`. R package version 0.95-30.

FOX, J. 1997. Applied regression analysis, linear models, and related methods. Sage Publications, Inc.

FRANCE, R. 1995. Differentiation between littoral and pelagic food webs in lakes using stable carbon isotopes. Limnology and Oceanography **40**: 1310–1313.

GIBERT, J., AND L. DEHARVENG. 2002. Subterranean ecosystems: A truncated functional biodiversity. BioScience **52**: 473–481.

GRAHAM, A. A., D. J. MCCAUGHAN, AND F. S. MCKEE. 1988. Measurement of surface area of stones. Hydrobiologia **157**: 85–87.

HASSAN, M., A. GOTTESFELD, D. MONTGOMERY, J. TUNNICLIFFE, G. CLARKE, G. WYNN, H. JONES-COX, R. POIRIER, E. MACISAAC, H. HERUNTER, ET AL. 2008. Salmon-driven bed load transport and bed morphology in mountain streams. Geophysical Research Letters **35**: L04405.

HILDERBRAND, G., S. FARLEY, C. ROBBINS, T. HANLEY, K. TITUS, AND C. SERVHEEN. 1996. Use of stable isotopes to determine diets of living and extinct bears. Canadian Journal of Zoology **74**: 2080–2088.

HOCKING, M. D., AND T. E. REIMCHEN. 2002. Salmon-derived nitrogen in terrestrial invertebrates from coniferous forests of the Pacific Northwest. BMC Ecology **2:4**. `http://www.biomedcentral.com/1472-6785/2/4`.

HOOD, E., J. FELLMAN, AND R. T. EDWARDS. 2007. Salmon influences on dissolved organic matter in a coastal temperate brown-water stream: An application of fluorescence spectroscopy. Limnology and Oceanography **52**: 1580–1587.

HORN, H., AND D. C. HEMPEL. 1997. Growth and decay in an auto-/heterotrophic biofilm. Water Research **31**: 2243–2252.

HULSMAN, H., AND L. WUBBEN. 2008. Salmon spawning and sediment dynamics in the Horsefly River in British Columbia. Master's thesis, Universiteit Utrecht.

HUME, J., K. SHORTREED, AND K. MORTON. 1996. Juvenile sockeye rearing capacity of three lakes in the Fraser River system. Canadian Journal of Fisheries and Aquatic Sciences **53**: 719–733.

HUNT, A. P., AND J. D. PERRY. 1999. Algal-bacterial relationships in streams with varying DOC concentration and source, pp. 34–42. *In* C. W. Keevil, A. Godfree, D. Holt, and C. Dow [eds.], Biofilms in the Aquatic Environment. The Royal Society of Chemistry.

HYATT, K., D. MCQUEEN, K. SHORTREED, AND D. RANKIN. 2004. Sockeye salmon (*Oncorhynchus nerka*) nursery lake fertilization: Review and summary of results. Environmental Reviews **12**: 133–162.

JANETSKI, D. J., D. T. CHALONER, S. D. TIEGS, AND G. A. LAMBERTI. 2009. Pacific salmon effects on stream ecosystems: A quantitative synthesis. Oecologia **159**: 583–595.

JOHNSTON, N., J. MACDONALD, K. HALL, AND P. J. TSCHAPLINSKI. 1997. A preliminary study of the role of sockeye salmon (*Oncorhynchus nerka*) carcasses as carbon and nitrogen sources for benthic insects and fishes in the "Early Stuart" stock spawning streams, 1050 km from the ocean. Fisheries Project Report No. RD55, British Columbia Ministry of Environment, Lands and Parks, Victoria, BC `http://www.for.gov.bc.ca/hfd/library/fisheries/FPRRD55.pdf`.

JOHNSTON, N. T., E. A. MACISAAC, P. J. TSCHAPLINSKI, AND K. J. HALL. 2004. Effects of the abundance of spawning sockeye salmon (*Oncorhynchus nerka*) on nutrients and algal biomass in forested streams. Canadian Journal of Fisheries and Aquatic Sciences **61**: 384–403.

KAPLAN, L., AND T. BOTT. 1989. Diel fluctuations in bacterial activity on streambed substrata during vernal algal blooms: Effects of temperature, water chemistry, and habitat. Limnology and Oceanography **34**: 718–733.

KLINE, T. C., J. J. GOERING, O. A. MATHISEN, P. H. POE, AND P. L. PARKER. 1990. Recycling of elements transported upstream by runs of Pacific salmon: I. δ^{15}N and δ^{13}C evidence in Sashin Creek, southeastern Alaska. Canadian Journal of Fisheries and Aquatic Sciences **47**: 136–144.

KLINE, T. C., J. J. GOERING, O. A. MATHIESEN, P. H. POE, P. L. PARKER, AND R. S. SCALAN. 1993. Recycling of elements transported upstream by runs of Pacific salmon: II. δ^{15}N and δ^{13}C evidence in the Kvichak River watershed, Bristol Bay, Southwestern Alaska. Canadian Journal of Fisheries and Aquatic Sciences **50**: 2350–2365.

KONDOLF, G. M. 2000. Assessing salmonid spawning gravel quality. Transactions of the American Fisheries Society **129**: 262–281.

LAMBERTI, G. A., D. T. CHALONER, AND A. E. HERSHEY. 2010. Linkages among aquatic ecosystems. Journal of the North American Benthological Society **29**: 245–263.

LAWRENCE, D. F. 2004. The feasibility of conducting a watershed-based fish sustainability plan on the Horsefly River watershed. Master's thesis, Royal Roads University.

LAWRENCE, J., AND T. NEU. 1999. Confocal laser scanning microscopy for analysis of microbial biofilms. Methods in Enzymology **310**: 131–144.

LAWRENCE, J., D. KORBER, B. HOYLE, J. COSTERTON, AND D. CALDWELL. 1991. Optical sectioning of microbial biofilms. Journal of Bacteriology **173**: 6558–6567.

LAWRENCE, J., T. NEU, AND G. SWERHONE. 1998. Application of multiple parameter imaging for the quantification of algal, bacterial and exopolymer components of microbial biofilms. Journal of Microbiological Methods **32**: 253–261.

MANZ, W. 1999. Phylogenetic composition, spatial structure, and dynamics of lotic bacterial biofilms investigated by fluorescent in situ hybridization and confocal laser scanning microscopy. Microbial Ecology **37**: 225–237.

MCCONNACHIE, J. L., AND E. L. PETTICREW. 2006. Tracing organic matter sources in riverine suspended sediment: Implications for fine sediment transfers. Geomorphology **79**: 13–26.

MCINTYRE, P., A. FLECKER, M. VANNI, J. HOOD, B. TAYLOR, AND S. THOMAS. 2008. Fish distributions and nutrient cycling in streams: Can fish create biogeochemical hotspots? Ecology **89**: 2335–2346.

MILLS, K., AND J. BEVER. 1998. Maintenance of diversity within plant communities: Soil pathogens as agents of negative feedback. Ecology **79**: 1595–1601.

MINAKAWA, N., AND R. I. GARA. 1999. Ecological effects of a chum salmon (*Oncorhynchus keta*) spawning run in a small stream of the Pacific Northwest. Journal of Freshwater Ecology **14**: 327–335.

MINAKAWA, N., AND R. I. GARA. 2003. Effects of chum salmon redd excavation on benthic communities in a stream in the Pacific Northwest. Transactions of the American Fisheries Society **132**: 598–604.

MITCHELL, M. 2010. Engauge Digitizer - Digitizing software. `http://digitizer.sourceforge.net/`.

MITCHELL, N. L., AND G. A. LAMBERTI. 2005. Responses in dissolved nutrients and epilithon abundance to spawning salmon in southeast Alaska streams. Limnology and Oceanography **50**: 217–227.

MOERKE, A. H., AND G. A. LAMBERTI. 2003. Responses in fish community structure to restoration of two Indiana streams. North American Journal of Fisheries Management **23**: 748–759.

MOHAMED, M., J. LAWRENCE, AND R. ROBARTS. 1998. Phosphorus limitation of heterotrophic biofilms from the Fraser River, British Columbia, and the effect of pulp mill effluent. Microbial Ecology **36**: 121–130.

MONTGOMERY, D. R., J. M. BUFFINGTON, N. P. PETERSON, D. SCHUETT-HAMES, AND T. P. QUINN. 1996. Stream-bed scour, egg burial depths, and the influence of salmonid spawning on bed surface mobility and embryo survival. Canadian Journal of Fisheries and Aquatic Sciences **53**: 1061–1070.

MOORE, J. W. 2006. Animal ecosystem engineers in streams. BioScience **56**: 237–246.

MOORE, J. W., AND D. E. SCHINDLER. 2008. Biotic disturbance and benthic community dynamics in salmon-bearing streams. Journal of Animal Ecology **77**: 275–284.

MOORE, J. W., D. E. SCHINDLER, AND M. D. SCHEUERELL. 2004. Disturbance of freshwater habitats by anadromous salmon in Alaska. Oecologia **139**: 298–308.

NAIMAN, R. J., R. E. BILBY, D. E. SCHINDLER, AND J. M. HELFIELD. 2002. Pacific salmon, nutrients, and the dynamics of freshwater and riparian ecosystems. Ecosystems **5**: 399–417.

NEU, T., AND J. LAWRENCE. 2004. One-photon versus two-photon laser scanning microscopy and digital image analysis of microbial biofilms. Methods in Microbiology **34**: 89–136.

NEU, T., G. SWERHONE, AND J. LAWRENCE. 2001. Assessment of lectin-binding analysis for in situ detection of glycoconjugates in biofilm systems. Microbiology **147**: 299–313.

NEU, T., G. SWERHONE, U. BÖCKELMANN, AND J. LAWRENCE. 2005. Effect of CNP on composition and structure of lotic biofilms as detected with lectin-specific glycoconjugates. Aquatic Microbial Ecology **38**: 283–294.

NEU, T. R. 2000. Confocal laser scanning microscopy (CLSM) of biofilms, chap. 13, pp. 211–219. *In* H. Flemming, U. Szewzyk, and T. Griebe [eds.], Biofilms: Investigative Methods & Applications. CRC Press.

NEU, T. R., AND J. R. LAWRENCE. 1997. Development and structure of microbial biofilms in river water studied by confocal laser scanning microscopy. FEMS Microbiology Ecology **24**: 11–25.

NOWLIN, W. H., M. J. VANNI, AND L. H. YANG. 2008. Comparing resource pulses in aquatic and terrestrial ecosystems. Ecology **89**: 647–659.

PAULING, B., AND I. WAGNER-DÖBLER. 2006. Stream microcosm for investigating GEM impact on the indigenous bacterial community in river water and sediment. Process Biochemistry **41**: 2129–2137.

PAULY, D., V. CHRISTENSEN, J. DALSGAARD, R. FROESE, AND F. TORRES JR. 1998. Fishing down marine food webs. Science **279**: 860–863.

PAWLEY, J. [ed.]. 1995. Handbook of Biological Confocal Microscopy, 2nd ed. Springer.

PETERSON, B. J., AND B. FRY. 1987. Stable isotopes in ecosystem studies. Annual Review of Ecology and Systematics **18**: 293–320.

PETERSON, C. G. 1996. Algal ecology: Freshwater benthic ecosystems, chap. 13: Response of benthic algal communities to natural physical disturbance, pp. 375–402. Academic Press.

PETERSON, C. G., AND N. B. GRIMM. 1992. Temporal variation in enrichment effects during periphyton succession in a nitrogen-limited desert stream ecosystem. Journal of the North American Benthological Society **11**: 20–36.

PETERSON, D., AND C. FOOTE. 2000. Disturbance of small-stream habitat by spawning sockeye salmon in Alaska. Transactions of the American Fisheries Society **129**: 924–934.

PETTICREW, E., AND J. REX. 2006. The importance of temporal changes in gravel-stored fine sediment on habitat conditions in a salmon spawning stream. International Association of Hydrological Sciences Publication **306**: 434–441.

PETTICREW, E. L., AND S. J. ALBERS. 2010. Salmon as biogeomorphic agents: Temporal and spatial effects on sediment quantity and quality in a northern British Columbia spawning channel. International Association of Hydrological Sciences Publication **337**: 251–257.

PETTICREW, E. L., AND J. M. AROCENA. 2003. Organic matter composition of gravel-stored sediments from salmon-bearing streams. Hydrobiologia **494**: 17–24.

POWER, M. 1990. Resource enhancement by indirect effects of grazers: Armored catfish, algae, and sediment. Ecology **71**: 897–904.

QUINN, G., AND M. J. KEOUGH. 2002. Experimental Design and Data Analysis for Biologists. Cambridge University Press.

QUINN, T. 2005. The behavior and ecology of Pacific salmon and trout. American Fisheries Society.

R 2.11.1, R. D. C. T. 2010. R: A Language and Environment for Statistical Computing. R Foundation for Statistical Computing, Vienna, Austria. `http://www.R-project.org`. ISBN 3-900051-07-0.

RASBAND, W. S., AND IMAGEJ. 2009. ImageJ, 1.43b. National Institutes of Health, Bethesda, MD, USA. `http://rsbweb.nih.gov/ij/`.

REIMCHEN, T. 2000. Some ecological and evolutionary aspects of bear-salmon interactions in coastal British Columbia. Canadian Journal of Zoology **78**: 448–457.

REX, J., AND E. PETTICREW. 2006. Pacific salmon and sediment flocculation: Nutrient cycling and intergravel habitat quality. International Association of Hydrological Sciences Publication **306**: 1–8.

REX, J., AND E. PETTICREW. 2008. Delivery of marine-derived nutrients to streambeds by Pacific Salmon. Nature Geoscience **1**: 840–843.

REX, J. F. 2009. The flocculation feedback loop: Delivery of marine derived nutrients in Pacific salmon streams. Ph.D. thesis, University of Northern British Columbia.

ROMANÍ, A., AND S. SABATER. 2000. Influence of algal biomass on extracellular enzyme activity in river biofilms. Microbial Ecology **40**: 16–24.

ROMANÍ, A., H. GUASCH, I. MUÑOZ, J. RUANA, E. VILALTA, T. SCHWARTZ, F. EMTIAZI, AND S. SABATER. 2004. Biofilm structure and function and possible implications for riverine DOC dynamics. Microbial Ecology **47**: 316–328.

SABATER, S., H. GUASCH, A. ROMANÍ, AND I. MUÑOZ. 2002. The effect of biological factors on the efficiency of river biofilms in improving water quality. Hydrobiologia **469**: 149–156.

SABATER, S., H. GUASCH, I. MUÑOZ, AND A. ROMANÍ. 2006. Hydrology, light and the use of organic and inorganic materials as structuring factors of biological communities in Mediterranean streams. Limnetica **25**: 335–347.

SARKAR, D. 2008. Lattice: Multivariate Data Visualization with R. Springer. `http://lmdvr.r-forge.r-project.org`. ISBN 978-0-387-75968-5.

SCHEUERELL, M., P. LEVIN, R. ZABEL, J. WILLIAMS, AND B. SANDERSON. 2005. A new perspective on the importance of marine-derived nutrients to threatened stocks of Pacific salmon (Oncorhynchus spp.). Canadian Journal of Fisheries and Aquatic Sciences **62**: 961–964.

SCHINDLER, D., S. CARPENTER, J. COLE, J. KITCHELL, AND M. PACE. 1997. Influence of food web structure on carbon exchange between lakes and the atmosphere. Science **277**: 248–251.

SCHINDLER, D. E., M. D. SCHEUERELL, J. W. MOORE, S. M. GENDE, T. FRANCIS, AND W. PALEN. 2003. Pacific salmon and the ecology of coastal ecosystems. Frontiers in Ecology and the Environment **1**: 31–37.

SIEGEL, S. 1957. Nonparametric statistics. American Statistician **11**: 13–19.

STAAL, M., R. THAR, M. KÜHL, M. C. M. VAN LOOSDRECHT, G. WOLF, J. DE BROUWER, AND J. RIJSTENBIL. 2007. Different carbon isotope fractionation patterns during the development of phototrophic freshwater and marine biofilms. Biogeosciences **4**: 613–626.

STEINMAN, A. D., AND G. A. LAMBERTI. 1996. Biomass and pigments of benthic algae, chap. 17, pp. 295–313. *In* R. Hauer and G. A. Lamberti [eds.], Methods in Stream Ecology. Academic Press.

STOODLEY, P., I. DODDS, J. D. BOYLE, AND H. M. LAPPIN-SCOTT. 1999. Influence of hydrodynamics and nutrients on biofilm structure. Journal of Applied Microbiology **85**: 19–28.

STOODLEY, P., K. SAUER, D. DAVIES, AND J. COSTERTON. 2002. Biofilms as complex differentiated communities. Annual Reviews in Microbiology **56**: 187–209.

STRATHMANN, M., J. WINGENDER, AND H. FLEMMING. 2002. Application of fluorescently labelled lectins for the visualization and biochemical characterization of polysaccharides in biofilms of *Pseudomonas aeruginosa*. Journal of Microbiological Methods **50**: 237–248.

SUTHERLAND, I. W. 2001. The biofilm matrix–An immobilized but dynamic microbial environments. Trends in Microbiology **9**: 222–227.

TIEGS, S., D. CHALONER, P. LEVI, J. RÜEGG, J. TANK, AND G. LAMBERTI. 2008. Timber harvest transforms ecological roles of salmon in southeast Alaska rain forest streams. Ecological Applications: A publication of the Ecological Society of America **18**: 4–11.

TIEGS, S. D., E. Y. CAMPBELL, P. S. LEVI, J. RÜEGG, M. E. BENBOW, D. T. CHALONER, R. W. MERRITT, J. L. TANK, AND G. A. LAMBERTI. 2009. Separating physical disturbance and nutrient enrichment caused by Pacific salmon in stream ecosystems. Freshwater Biology **54**: 1864–1875, doi:{10.1111/j.1365-2427.2009.02232.x}.

TOEWS, D. A. A., AND M. J. BROWNLEE. 1981. A handbook for fish habitat protection on forest lands in British Columbia, Special Publication ed. Department of Fisheries and Oceans, Government of Canada.

URBAN, D., R. O'NEILL, AND H. SHUGART. 1987. Landscape Ecology. BioScience **37**: 119–127.

VANNOTE, R. L., G. W. MINSHALL, K. W. CUMMINS, J. R. SEDELL, AND C. CUSHING. 1980. The river continuum concept. Canadian Journal of Fisheries and Aquatic Sciences **37**: 130–137.

WALTERS, C. J., P. LEBLOND, AND B. RIDELL. 2004. Does over-escapement cause salmon stock collapse? Technical paper. Pacific Fisheries Resource Conservation Council. `http://www.fish.bc.ca/files/OverescapementReport_2004_0_Complete.pdf`.

WHITTINGHAM, M. J., P. A. STEPHENS, R. B. BRADBURY, AND R. P. FRECKLETON. 2006. Why do we still use stepwise modelling in ecology and behaviour? Journal of Animal Ecology **75**: 1182–1189.

WICKHAM, H. 2009. ggplot2: elegant graphics for data analysis. Springer New York. `http://had.co.nz/ggplot2/book`.

WILLIAMS, N. D., D. E. WALLING, AND G. J. L. LEEKS. 2007. High temporal resolution in situ measurement of the effective particle size characteristics of fluvial suspended sediment. Water Research **41**: 1081–1093.

WINEMILLER, K., A. FLECKER, AND D. HOEINGHAUS. 2010. Patch dynamics and environmental heterogeneity in lotic ecosystems. Journal of the North American Benthological Society **29**: 84–99.

WINGENDER, J., T. NEU, AND H. FLEMMING. 1999. What are bacterial extracellular polymeric substances?, Microbial Extracellular Polymeric Substances. Springer.

WIPFLI, M., AND C. BAXTER. 2010. Linking ecosystems, food webs, and fish production: Subsidies in salmonid watersheds. Fisheries **35**: 373–387.

WIPFLI, M. S., J. HUDSON, AND J. CAOUETTE. 1998. Influence of salmon carcasses on stream productivity: Response of biofilm and benthic macroinvertebrates in southeastern Alaska, USA. Canadian Journal of Fisheries and Aquatic Sciences **55**: 1503–1511.

WIPFLI, M. S., J. P. HUDSON, D. T. CHALONER, AND J. P. CAOUETTE. 1999. Influence of salmon spawner densities on stream productivity in southeast Alaska. Canadian Journal of Fisheries and Aquatic Sciences **56**: 1600–1611.

WIPFLI, M. S., J. P. HUDSON, J. P. CAOUETTE, AND D. T. CHALONER. 2003. Marine subsidies in freshwater ecosystems: salmon carcasses increase the growth rates of stream-resident salmonids. Transactions of the American Fisheries Society **132**: 371–381.

WIPFLI, M. S., J. P. HUDSON, J. P. CAOUETTE, N. L. MITCHELL, J. L. LESSARD, R. A. HEINTZ, AND D. T. CHALONER. 2010. Salmon carcasses increase stream productivity more than inorganic fertilizer pellets: A test on multiple trophic levels in streamside experimental channels. Transactions of the American Fisheries Society **139**: 824–839.

WOLFAARDT, G., J. LAWRENCE, AND D. KORBER. 1999. Function of EPS, chap. 10, pp. 171–200. *In* Microbial Extracellular Polymeric Substances: Characterization, Structure and Function. Springer.

YODER, D. M., A. VIRAMONTES, L. L. KIRK, AND L. F. HANNE. 2006. Impact of salmon spawning on microbial communities in a northern California river. Journal of Freshwater Ecology **21**: 147–155.

Appendix A

Confocal Laser Scanning Microscopy (CLSM) software scripts

A.1 Image J conversion of OIB files to stacked TIFF

```
//ver. 3.7e  1/7/2010
//Written by Glen MacDonald, Core for Communication Research
//Imaging and Microscopy Core of  Virginia Merrill Bloedel Hearing Research Center and the Cellular Morphology Core of the Center for Human Development and Disability
//Box 357923
//University of Washington
//Seattle, WA 98195-7923
//glenmac@u.washington.edu
//Requires the LOCI_tools plugin.
// On running the first macro, select a file, the dialog window displays number of channels and bit depth.
//Select merge options of "RGB", "Composite Hyperstack" or "No Merge".
//  Select a channel (0-n) for each color channel.  Error trapping: If you choose a
//channel not present, the macro exits with a message that the channel is not present.
//Placing any channel into 2 colors will create an RGB merge.
//Any channel may be assigned to more than 1 color
//This version will generate a projection image based on channels in the initial selected file
//"Save as RGB TIFF" will save stacks and projections (if selected, too) as they are created and close them.
//Batch mode will check for number of channels and z-steps.  If a file has a different number of channels from the initially selected image,
//its filename is written to the log window, but not opened, since the merge will be off.
//If projections are selected in batchmode, but a file with the same number of channels is encountered that is not a z-series,
//it will be opened, but its name will be written to the log window instead of allowing ImageJ to choke making a projection of it

var name,origformat,pType,mergeID,dir,ext,count,path,i,redc,bluc,grnc,gryc,bsizeC,create,createtype,icsext,name,prefix,bsizeZ;

// globals with initial defaults
var red="2";
var grn="1";
var blu="0";
var gry="None";
var merge="RGB";
var mip="None";
var batch=0;
var sdir="";
var destdir="";
var saveMe=false;
var closeMe=false;
var fformat="RGB";

macro "Import Channel Order [1]"{
requires("1.42d");
run("Bio-Formats Macro Extensions");
path=File.openDialog("Select a file");//path+filename
IJ.redirectErrorMessages();
dir = File.getParent(path)+"/";//path to file
name=File.getName(path);//get filename
namel=lengthOf(name);
basename=File.nameWithoutExtension;
if (name==basename)
  exit("This file name does not have an extension to indicate file type. \nPlease rename with the appropriate extension. E.g. '.tif', '.jpeg', '.ics', etc.");
basenamel=lengthOf(basename);
ext=substring(name,basenamel+1,namel);
Ext.getFormat(path, format);
origformat=format;
Ext.setId(path);
Ext.getSizeC(sizeC);//delivers the number of channels
Ext.getSizeZ(sizeZ);
Ext.getSizeT(sizeT);
cH=newArray(sizeC+1);
for (j=1;j<sizeC+1;j++)
  cH[j]=d2s(j-1,0);
cH[0] = "*None*";
Ext.getPixelType(pixelType);
pelType=pixelType;
matchPixelType(pType);
if (sizeZ>1)
  zplanes="\nThis is a Z-series with "+sizeZ+" image planes.";
else
  zplanes="";
if (sizeT>1)
  tplanes="\nThis is a timelapse series with "+sizeT+" time points.";
else
```

```
  tplanes="";
msg="Reading image file:"+name+".\nAssign "+sizeC+" channels to merged colors.\nBit Depth is "+pType+" per pixel.";
Dialog.create("Channel Merge Options 3.7e");
Dialog.addChoice("Merge Type:", newArray("RGB", "Composite", "No merge"),merge);
Dialog.addMessage(msg+zplanes+tplanes);
Dialog.addMessage("Red merged channel:");
Dialog.addChoice("Channels:", cH,red);
Dialog.addMessage("Green merged channel:");
Dialog.addChoice("Channels:", cH,grn);
Dialog.addMessage("Blue merged channel:");
Dialog.addChoice("Channels:",  cH,blu);
Dialog.addMessage("Gray merged channel:");
Dialog.addChoice("Channels:",  cH,gry);
Dialog.addChoice("Create Projection Image",newArray("None", "Average Intensity","Max Intensity", "Min Intensity",  "Sum Slices", "
     Standard Deviation", "Median"),mip);
Dialog.addCheckbox("Save opened images.",saveMe);
Dialog.addChoice("Saved image format:",newArray("TIFF-RGB", "ICS-Composite"),fformat);
Dialog.addCheckbox("Process all images in directory.",batch);
Dialog.addCheckbox("Close file on save.",closeMe);
Dialog.show();
merge=Dialog.getChoice();
red=Dialog.getChoice();
grn=Dialog.getChoice();
blu=Dialog.getChoice();
gry=Dialog.getChoice();
mip=Dialog.getChoice();
fformat=Dialog.getChoice();
saveMe=Dialog.getCheckbox();
batch=Dialog.getCheckbox();
closeMe=Dialog.getCheckbox();
if (closeMe==true&&saveMe==false)
  exit("There is no point in closing files after opening unless you select to actually save them!");
if (red !="*None*"&&grn != "*None*"&&blu != "*None*"&&gry != "*None*"&&merge=="RGB")
  exit("RGB cannot merge more than 3 channels. Switch to 'Composite' to merge 4 channels.");
if (gry != "*None*"&&merge=="RGB")
  exit("Gray is only a valid option with 'Composite' merge.");
if (mip!="None"&&sizeZ==1)
  exit("This is not a z-series, projections cannot be selected.");
format=substring(fformat,0,indexOf(fformat,"-"));
icsext=".ics";
cHs=newArray(4);//contains the vars from choices: 1.2.3,4, *None*
cHs[0]=red;
cHs[1]=grn;
cHs[2]=blu;
cHs[3]=gry;
cHsc=newArray("Red","Green","Blue","Gray"); //labels for chosen channels
if (saveMe==1)
  destdir = getDirectory("Choose Destination Directory");
if (merge=="RGB") {
  create = " ";
  if (batch!=1)
    doMerge();
  else
    batchAll();
  }
if (merge=="Composite") {
  create = "create";
  if (batch!=1)
    doMerge();
  else
    batchAll();
  }
if (merge=="No merge"){
  if (batch!=1)
    noMerge();
  else
    batchAll();
  }
}

function doMerge(){
  setBatchMode(true);
  cHsm=newArray(4); //arrange image labels in order of merger
  for ( j=0; j<cHs.length;j++){ //cHs sets channel import order for r,g,b,gy
    if (cHs[j]!='*None*'){
      cHso=(cHs[j])+1;  //convert channel numbering for import
      options="open=["+path+"] autoscale specify_range split_channels view=[Standard Image]] stack_order=Default c_begin=cHso
           c_end=cHso c_step=1";
      showStatus("opening file");
      run("Bio-Formats Importer",options);
      rename(cHsc[j]);  //name for color LUT
      cHsm[j]=cHsc[j];  // make a new array for the merging with channel LUT names and *None* in orde
      }
    else{
      cHsm[j]="*None*";
      }
    }
      createtype="red=["+cHsm[0]+"] green=["+cHsm[1]+"] blue=["+cHsm[2]+"] gray=["+cHsm[3]+"] "+create;
  run("Merge Channels...", createtype);
  prefix=substring(name,0,indexOf(name,"."));
  rename(prefix+"_merge");
  file=getTitle;
```

```
161   fileID=getImageID;
      if (mip!="None")
163     doProjection(mip);
      if (saveMe==1){
165     selectImage(fileID);
          if (format=="ICS")
167         run("Bio-Formats Exporter", "save=["+destdir+file+icsext+"]");
          else
169         saveAs(format,destdir+file);
        if (closeMe==true)
171       close();
      }
173   setBatchMode("exit and display");
}
175
function noMerge(){
177   setBatchMode(true);
      for ( j=0; j<cHs.length;j++){ //cHs selects channels to import  and order for r,g,b,gy
179     if (cHs[j]!='*None*'){
          cHso=(cHs[j])+1;  //convert channel numbering for import
181       options="open=["+path+"] autoscale specify_range split_channels view=[Standard Image]] stack_order=Default c_begin=cHso
                c_end=cHso c_step=1";
          showStatus("opening file");
183       run("Bio-Formats Importer",options);
          prefix=substring(name,0,indexOf(name,"."));
185       rename(prefix+"-Ch"+cHs[j]); //name for color LUT
          file=getTitle;
187       fileID=getImageID;
          if (mip!="None")
189         doProjection(mip);
          if (saveMe==1){
191         selectImage(fileID);
          if (format=="ICS")
193         run("Bio-Formats Exporter", "save=["+destdir+file+icsext+"]");
          else
195         saveAs(format,destdir+file);
          }
197       if (closeMe==true)
            close();
199     }
      }
201   setBatchMode("exit and display");
}
203
function batchAll(){
205   list= getFileList(dir);
      for (i=0;i<list.length;i++){
207     if(File.isDirectory(dir+list[i])!=1){
          if (endsWith(list[i], ext)){
209         Ext.setId(dir+list[i]);
            Ext.getSizeC(bsizeC);
211         Ext.getSizeZ(bsizeZ);
            if (bsizeC==sizeC){
213           path=dir+list[i];
              name=list[i];
215           if (merge!="No merge")
                doMerge();
217           else
                noMerge();
219           } //if bsizec
            else
221           print(dir+list[i]+ " contains "+bsizeC+ " channels");
            }//if endswith
223       else
            ; // skip folders and other filetypes and loop to next file
225       }//if file.is
      }//for
227 }//fxn

229 function matchPixelType(pelType){
    if (matches(pixelType,"uint8"))
231   pType = "unsigned 8-bits";
    if (matches(pixelType,"uint16"))
233   pType = "unsigned 16-bits";
    if (matches(pixelType,"uint32"))
235   pType = "unsigned 32-bits";
    if (matches(pixelType,"int8"))
237   pType = "signed 8-bits";
    if (matches(pixelType,"int16"))
239   pType = "signed 16-bits";
    if (matches(pixelType,"int32"))
241   pType = "signed 32-bits";
    if (matches(pixelType,"float"))
243   pType = "floating point 32-bits";
    if (matches(pixelType,"double"))
245   pType = "64-bits double precision";
    }
247
    macro "Composite Hyperstack to RGB [2]"{
249 run("Channels Tool...");
    run("Stack to RGB");
251 }
```

```
macro "Brightest Point Projection [3]"{
noslices=nSlices;
if (noslices==1)
  exit("This is not a stack.");
run("Z Project...", "projection=[Max Intensity]");
}

function doProjection(mip){
  if (bsizeZ==1)
    print(dir+file+ " is not a z-stack.");
  else
  {
  mergeID=getImageID();
  merge=getTitle;
  mergel=lengthOf(merge);
  end=substring(mip,0,3);
  if (endsWith(merge,"_merge")==1)
    merge=substring(file,0,namel-6);
  if (end=="Ave")
    end="_AVG";
  if (end=="Max")
    end="_MAX";
  if (end=="Min")
    end="_MIN";
  if (end=="Sum")
    end="_SUM";
  if (end=="Sta")
    end="_STD";
  if (end=="Med")
    end="_MED";
  run("Z Project...", "projection=["+mip+"]");
  rename(merge+end);
  if (saveMe==1){
    saveAs("tiff",destdir+merge+end);
    if (closeMe==1)
      close();
    }
  }
}

macro "Commands Help [4]"{
Dialog.create("Commands Help");
Dialog.addMessage("'Import Channel Order [1]' - Opens dialog window with options for file merger.\n'Composite Hyperstack to RGB [2]' - Converts an active image with 16-bits/channel into an RGB file with 8-bits/channel. Useful to convert images for Photoshop or PowerPoint. \n'Brightest Point Projection [3]' - Creates a maximum intensity projection from the active window. \n'Close All Images [7]' - Closes all open image windows (without saving anything).\nSee the Import Channel Order Macro documentation for complete information.\nSelecting a file with the wrong filename extension or a misspelled extension will result in a long Java error message in the Log Window. ");
Dialog.show();
}

macro "Channels Help [5]"{
Dialog.create("Channel Help");
Dialog.addMessage("Merge Type:\n'RGB' merges stacks at 8-bits per channel. \n'Composite' merges stacks at >8 bits per channel, and retains more metadata.\n'No Merge' opens each channel as a separate stack.\nFV-1000 channel order is 0 [shortest wavelength] to n [longest wavelength].  E.g. 0=blue, 1=green, 2=red, 3=far red. \n  Fewer channels change the numbering e.g. 2 channels 0=green, 1=red or 0=blue and 1=red.  \n Limit which image channels are opened by 'No Merge' by assigning to a color, even though they will be opened in grayscale.\n");
Dialog.show();
}

macro "Check Box Help [6]"{
Dialog.create("Checkbox Help");
Dialog.addMessage("These options are applied when opening files through the Import Channel Order macro.\n'Create Projection Image' - Select a projection method.  This requires a Z-stack!\n'Save opened images' -\n  Images and projections are saved to the destination directory. \n'Saved image format' - \n  RGB-TIFF converts images to 8-bits per channel (RGB) and saves as a TIFF. \n  ICS-Composite saves Composite merged images at native bit depth, such as 16-bits per channel. \n'Process all images in directory' -\nApplies your settings to all data files in the directory that have the same filename extension.  ALL FILES MUST HAVE THE SAME NUMBER OF CHANNELS! \n 'Close on save' - Each image is closed after it is saved.");
Dialog.show();
}

macro "Close All Images [7]"{
for (o=0;o<nImages;o++)
  close();
}
```

A.2 Scion Image macros for the analysis of stacked TIFF files

```
macro 'lectin macro[1]'

{lectin image processing macro makes it so the average is the average of the pixels that are being counted in an eroded and dilated image}
```

```
{a macro to do our typical image analysis which is for each slice in a z series get the number of white thresholded pixels above a
      certain value and the mean pixel value of the image above the threshold value}
{setting the threshold value for the stack and starting the macro}
var
          Thrvalue:integer;
          Addvalue:integer;
          i:integer;
          n,mean,mode,min,max:real;
          npx:integer;
          mn:real;
          nsl:integer;
          sln:integer;
begin      { THRESHOLD VALUE FOR LECTIN IMAGES }
          Thrvalue:=GetNumber('Threshold value for series is:',250);
          Addvalue:=255-Thrvalue;
          nsl:=nSlices;
          sln:=0;
          Measure;
          rUser1[rCount]:=11111.11111;
          rUser2[rCount]:=111.11111;
          UpdateResults;
begin
          if nslices=0 then begin
          PutMessage('This window is not a stack');
          exit;
    end;
    for i:=1 to nSlices do begin
          SelectSlice(i);
          {this is where you put in what to do for the slice}
{*****************new stuff*******}
SelectAll;
    Copy;
MakeNewWindow('temp');
SetNewSize(512,512);
Paste;
SetThreshold(Thrvalue);
MakeBinary;
Dilate;
Erode;
Copy;
Dispose;
ScaleMath(false);
Paste;
Add;
{*************************}
AddConstant(Addvalue);
{Gets mean  and puts it in user2 }
          SetUser2Label('mean');
         Measure;
          GetResults(n,mean,mode,min,max);
          mn:=Mean;

{thresholding to 255 and making binary subroutine}
          SetThreshold(255);
          MakeBinary;
{ Count White Pixels subroutine Counts the number  white pixels in the current
selection and stores the counts in the User1 columns. }
          SetUser1Label('White');
          rUser1[rCount]:=262144-histogram[255];
          rUser2[rCount]:=mn;
          UpdateResults;
          sln:=sln+1;
{comment out the next three lines if you dont want the file closed at the end}
            if sln=nsl then begin
            Dispose;
            end;
 end;
end;
end;
end;
end;

macro 'bacteria (green pixels)[b]'

{a macro to determine the area of bacteria colored green in our usual image sequence stained with SYTO 9 this macro erodes and
     dilates}
{setting the threshold value for the stack and starting the macro}
var
          Thrvalue:integer;
          Addvalue:integer;
          i:integer;
          n,mean,mode,min,max:real;
          npx:integer;
          mn:real;
          nsl:integer;
          sln:integer;
begin {  THRESHOLD VALUE FOR BACTERIA HERE }
          Thrvalue:=GetNumber('Threshold value for series is:',200);
          Addvalue:=255-Thrvalue;
          nsl:=nSlices;
          sln:=0;
```

```
            Measure;
96          rUser1[rCount]:=11111.11111;
           rUser2[rCount]:=111.11111;
98          UpdateResults;
begin
100         if nslices=0 then begin
            PutMessage('This window is not a stack');
102         exit;
    end;
104     for i:=1 to nSlices do begin
            SelectSlice(i);
106         {this is where you put in what to do for the slice}
          {thresholding to thrvalue  and making binary subroutine}
108         SetThreshold(Thrvalue);
            MakeBinary;
110       Dilate;
            Erode;
112       Measure;
{ Count White Pixels subroutine Counts the number  white pixels in the current
114 selection and stores the counts in the User1 columns. }
            SetUser1Label('White');
116         rUser1[rCount]:=262144-histogram[255];
            rUser2[rCount]:=0;
118         UpdateResults;
            sln:=sln+1;
120 {comment out the next three lines if you dont want the file closed at the end}
              if sln=nsl then begin
122           Dispose;
              end;
124  end;
end;
126 end;
end;
128 end;

130 macro 'algae (far red pixels)[a]'

132 {a macro to determine the area of bacteria colored green in our usual image sequence stained with SYTO 9 this macro erodes and
        dilates}
{setting the threshold value for the stack and starting the macro}
134 var
            Thrvalue:integer;
136         Addvalue:integer;
            i:integer;
138         n,mean,mode,min,max:real;
            npx:integer;
140         mn:real;
            nsl:integer;
142         sln:integer;
begin {  THRESHOLD VALUE FOR ALGAE HERE }
144         Thrvalue:=GetNumber('Threshold value for series is:',210);
            Addvalue:=255-Thrvalue;
146         nsl:=nSlices;
            sln:=0;
148         Measure;
            rUser1[rCount]:=11111.11111;
150        rUser2[rCount]:=111.11111;
            UpdateResults;
152 begin
            if nslices=0 then begin
154         PutMessage('This window is not a stack');
            exit;
156     end;
    158 for i:=1 to nSlices do begin
            SelectSlice(i);
160         {this is where you put in what to do for the slice}
          {thresholding to thrvalue  and making binary subroutine}
162         SetThreshold(Thrvalue);
            MakeBinary;
164       Dilate;
            Erode;
166       Measure;
{ Count White Pixels subroutine Counts the number  white pixels in the current
selection and stores the counts in the User1 columns. }
168         SetUser1Label('White');
            rUser1[rCount]:=262144-histogram[255];
170         rUser2[rCount]:=0;
            UpdateResults;
172         sln:=sln+1;
{comment out the next three lines if you dont want the file closed at the end}
174           if sln=nsl then begin
              Dispose;
176           end;
 end;
178 end;
end;
180 end;
end;
182
macro 'cyanos (red pixels)[c]'
184
```

```
{a macro to determine the area of bacteria colored green in our usual image sequence stained with SYTO 9 this macro erodes and
    dilates}
{setting the threshold value for the stack and starting the macro}
var
          Thrvalue:integer;
          Addvalue:integer;
          i:integer;
          n,mean,mode,min,max:real;
          npx:integer;
          mn:real;
          nsl:integer;
          sln:integer;
begin {  THRESHOLD VALUE FOR ALGAE HERE }
          Thrvalue:=GetNumber('Threshold value for series is:',210);
          Addvalue:=255-Thrvalue;
          nsl:=nSlices;
          sln:=0;
          Measure;
          rUser1[rCount]:=11111.11111;
         rUser2[rCount]:=111.11111;
          UpdateResults;
begin
          if nslices=0 then begin
          PutMessage('This window is not a stack');
          exit;
    end;
    for i:=1 to nSlices do begin
          SelectSlice(i);
          {this is where you put in what to do for the slice}
        {thresholding to thrvalue  and making binary subroutine}
          SetThreshold(Thrvalue);
          MakeBinary;
      Dilate;
          Erode;
      Measure;
{ Count White Pixels subroutine Counts the number  white pixels in the current
selection and stores the counts in the User1 columns. }
          SetUser1Label('White');
          rUser1[rCount]:=262144-histogram[255];
          rUser2[rCount]:=0;
          UpdateResults;
          sln:=sln+1;
{comment out the next three lines if you dont want the file closed at the end}
            if sln=nsl then begin
            Dispose;
            end;
 end;
end;
end;
end;
end;


macro 'polymer macro[p]'

{lectin image processing macro makes it so the average is the average of the pixels that are being counted in an eroded and
    dilated image}

{a macro to do our typical image analysis which is for each slice in a z series get the number of white thresholded pixels above a
     certain value and the mean pixel value of the image above the threshold value}
{setting the threshold value for the stack and starting the macro}
var
          Thrvalue:integer;
          Addvalue:integer;
          i:integer;
          n,mean,mode,min,max:real;
          npx:integer;
          mn:real;
          nsl:integer;
          sln:integer;
begin      { THRESHOLD VALUE FOR POLYMER IMAGES }
          Thrvalue:=GetNumber('Threshold value for series is:',245);
          Addvalue:=255-Thrvalue;
          nsl:=nSlices;
          sln:=0;
          Measure;
          rUser1[rCount]:=11111.11111;
         rUser2[rCount]:=111.11111;
          UpdateResults;
begin
          if nslices=0 then begin
          PutMessage('This window is not a stack');
          exit;
    end;
    for i:=1 to nSlices do begin
          SelectSlice(i);
          {this is where you put in what to do for the slice}
{****************new stuff*******}
SelectAll;
    Copy;
MakeNewWindow('temp');
SetNewSize(512,512);
```

```
Paste;
SetThreshold(Thrvalue);
MakeBinary;
Dilate;
Erode;
Copy;
Dispose;
ScaleMath(false);
Paste;
Add;
{*************************}
AddConstant(Addvalue);
{Gets mean  and puts it in user2 }
          SetUser2Label('mean');
         Measure;
         GetResults(n,mean,mode,min,max);
          mn:=Mean;

{thresholding to 255 and making binary subroutine}
          SetThreshold(255);
          MakeBinary;
{ Count White Pixels subroutine Counts the number  white pixels in the current
selection and stores the counts in the User1 columns. }
          SetUser1Label('White');
          rUser1[rCount]:=262144-histogram[255];
          rUser2[rCount]:=mn;
          UpdateResults;
          sln:=sln+1;
{comment out the next three lines if you dont want the file closed at the end}
            if sln=nsl then begin
            Dispose;
            end;
 end;
end;
end;
end;
end;
```

A.3 R script for data processing

```
#Script to process raw confocal image files that have been run using the George Swerhone macros. Written by Sam Albers on March
    14, 2010.
#CSV files can be exported from any spreadsheet program
#.csv inputted needed to have the following header format:
# Sample Frame  rep Total Count User
#Otherwise one just needs to change the names.
pro <-read.csv("filename and file path.csv",header=TRUE,sep=",")
#This is removing the separator that the macros added
pro <- pro[!(pro$Count==11111.11),]


#These aren't the actual channel names but it makes it easier to sort if we think of the channel name as what we are trying to get
     out of the channel. Order matters here so if your data is organized differently move the labels around accordingly
pro$channel=c("cyano","bacteria","algae")
pro$macro=c("bacteria","bacteria","bacteria","algae","algae","algae","cyano","cyano","cyano")

#Organizes the data so that the correct channel is being selected against the correct macro. Each macros was run three times on
    each image so we initially start with 3 times the amount of data. This command removes this part.
pro <- pro[pro$channel==pro$macro,]


#Collapse data by the frame... establishes mean white count for frames
pro.mean <- with(pro, aggregate(pro, by=list(rep, Macro=macro), mean))

#Conditional statement that adds the correct stain to the dataframe. May need to modified if the staining regime was different.
pro.mean$stain <- with(pro.mean, ifelse(rep=="1","none", ifelse(rep=="2","syto", ifelse(rep=="3","sytolec", ifelse(rep=="4", "
    sytolec", "sytolec")))))


########################################################################
#This is a bit of a roundabout process to subtract the cyanobacteria coverage which shows up in the red and far red channel from
    the algae coverage which only shows up in the far red
pro.mean <- pro.mean[order(pro.mean$rep) , ]

pro.mean$algaecyano <- unlist( lapply(split(pro.mean, pro.mean$rep),
                function(x) x$calib2 <- x$Count- x[x$Macro == "cyano",  "Count"]) )
pro.mean <- pro.mean[order(pro.mean$Macro) , ]
############################################################
#Syto Control. Subtract the control from the other values. The assumption here is that the fluroescence in the control is
    representative of the fluorescence in the entire sample.
pro.mean$sytocontrol <- unlist( lapply(split(pro.mean, pro.mean$Macro),
                function(x) x$calib <- x$Count- x[x$stain == "none",  "Count"]) )

# This gathers the data we need from the above subtraction and combines it into a column called percentcov
pro.mean$percentcov <- (c(pro.mean[pro.mean$Macro=="algae", "algaecyano"], pro.mean[pro.mean$Macro=="bacteria", "sytocontrol"],
    pro.mean[pro.mean$Macro=="cyano", "Count"])/pro.mean$Total)*100
```

```
############################################################
#Just a trim here. Just to keep only what we need.
pro.mean <- subset(pro.mean, select = c(Macro, rep, percentcov, stain))
#Comment out section labels as needed
pro.mean$section="down"
#pro.mean$section="mid"
#pro.mean$section="up"


####File can then be exported to a .csv file which can be opened by most spreadsheet software packages
write.csv(pro.mean,"filename.csv")
################################################################
pro.mean
################################################################
```